

**UNCLASSIFIED**

---

**AD 266 666**

*Reproduced  
by the*

**ARMED SERVICES TECHNICAL INFORMATION AGENCY  
ARLINGTON HALL STATION  
ARLINGTON 12, VIRGINIA**



---

**UNCLASSIFIED**

# DISCLAIMER NOTICE

THIS DOCUMENT IS THE BEST  
QUALITY AVAILABLE.

COPY FURNISHED CONTAINED  
A SIGNIFICANT NUMBER OF  
PAGES WHICH DO NOT  
REPRODUCE LEGIBLY.

**NOTICE:** When government or other drawings, specifications or other data are used for any purpose other than in connection with a definitely related government procurement operation, the U. S. Government thereby incurs no responsibility, nor any obligation whatsoever; and the fact that the Government may have formulated, furnished, or in any way supplied the said drawings, specifications, or other data is not to be regarded by implication or otherwise as in any manner licensing the holder or any other person or corporation, or conveying any rights or permission to manufacture, use or sell any patented invention that may in any way be related thereto.

AD 266 666

AFRL - 1017

Scientific Report 3

THERMALLY DRIVEN AXIALLY SYMMETRIC CIRCULATIONS OF A PLANETARY ATMOSPHERE  
A Dynamical-Numerical Experiment

by Manfred M. Helli

Contract AF 19(604)-5965

ARPA Order 26-59

CORRIGENDUM

- p 8 Line 7 - change unit vector  $\hat{i}$  to  $\hat{j}$  in 2nd term  
Eq (4) change  $-g\hat{k}$  to  $g\hat{k}$
- p 9 Eq. (5) - change sign of  $\frac{\partial \phi}{\partial t}$  to minus
- p 16 Eq. (25) - change sign of  $\nabla \cdot (\kappa \nabla)$  to minus
- p 25 Line 2 - Eq. (64) instead of Eq. (65)
- p 29 Line 4 - (65) should be (64)
- p 39 Line 7 - change  $\square_n$  to  $\square_m$
- p 40 Line 20 - change P to p
- p 41 Line 1 - change P to p
- p 42 Line 4 - meridional to meridional

XEROX

62-1-3

AFCRL-1017

Scientific Report 3

**THERMALLY DRIVEN, AXIALLY SYMMETRIC CIRCULATIONS  
OF A PLANETARY ATMOSPHERE  
A DYNAMICAL-NUMERICAL EXPERIMENT**

*Prepared for:*

GEOPHYSICS RESEARCH DIRECTORATE  
AIR FORCE CAMBRIDGE RESEARCH LABORATORIES  
BEDFORD, MASSACHUSETTS

CONTRACT AF 19(604)-5965  
ARPA ORDER 26-59

*By: Manfred M. Holl*

STANFORD RESEARCH INSTITUTE

MENLO PARK, CALIFORNIA

\*SRI



September 1961

AFCRL-1017

*Scientific Report 3*

**THERMALLY DRIVEN, AXIALLY SYMMETRIC CIRCULATIONS  
OF A PLANETARY ATMOSPHERE  
A DYNAMICAL-NUMERICAL EXPERIMENT**

*Prepared for:*


GEOPHYSICS RESEARCH DIRECTORATE  
AIR FORCE CAMBRIDGE RESEARCH LABORATORIES  
BEDFORD, MASSACHUSETTS

CONTRACT AF 19(604)-5965  
ARPA ORDER 26-59

*By: Manfred M. Holl*

SRI Project No. 2994

*Approved:*

  
.....

D. R. SCHEUCH, DIRECTOR ELECTRONICS AND RADIO SCIENCES DIVISION

Copy No. ....54

## ABSTRACT

---

A dynamical-numerical experiment is designed to evolve thermally-driven circulations, symmetric about the polar axis, in the region from equator to pole. The selection of variables and transformations of the hydrostatic equation system (primitive equations) and the development of the numerical analogue are discussed in some detail. The region is discretized into volume modules by nineteen levels in the vertical and by forty-nine equal intervals from equator to pole. The upper boundary is essentially unrestricted. Mass and absolute angular momentum are treated conservatively and in terms of fluxes across module interfaces. Heating rate distributions are prescribed in space and are stepwise introduced to disturb an atmosphere at relative rest or in balanced zonal motion. The fields are portrayed in a representative meridional plane. Pertinent numerical analyses are included and compressor-gravity oscillations are analyzed.

The first experiment, designed as a test, evolves the circulation produced by uniformly heating a narrow latitude zone at mid-latitude in a Standard Atmosphere at relative rest. Although receiving thermal energy, the heated zone locally cools due to the combined effect of the resulting circulation.

In the major experiment a heating and cooling distribution, approximating mean winter conditions, disturbs a Standard Atmosphere at relative rest. The integration evolves the initiation of a planetary circulation as frequently discussed qualitatively in elementary text books. Various applications of the model and further improvements are indicated.

## CONTENTS

---

ABSTRACT . . . . .	ii
CONTENTS . . . . .	iii
LIST OF ILLUSTRATIONS . . . . .	iv
LIST OF TABLES . . . . .	v
I INTRODUCTION . . . . .	1
II THE MATHEMATICAL-PHYSICAL SYSTEM . . . . .	7
III THE NUMERICAL ANALOGUE . . . . .	14
IV TEST INTEGRATIONS, COMPUTATIONAL STABILITY AND GRAVITY WAVES .	31
V RESULTS, ONE COLUMN OF HEATING . . . . .	42
VI RESULTS, HEMISPHERE WINTER HEATING . . . . .	51
VII RECOMMENDATIONS . . . . .	86
ACKNOWLEDGMENT . . . . .	89
REFERENCES . . . . .	90



## ILLUSTRATIONS

Fig. 1	The Arbitrary m,n Volume Module . . . . .	14
Fig. 2	The Fluxes . . . . .	18
Fig. 3	Levels and Parameters . . . . .	30
Fig. 4	One-Column Heating, $w$ at $\tau = 22$ . . . . .	
	Units: $10^{-2}$ cm sec $^{-1}$ . . . . .	43
Fig. 5	One-Column Heating, $\rho_a$ at $\tau = 22$ . . . . .	
	Units: $10^{-8}$ tons m $^{-3}$ . . . . .	44
Fig. 6	One-Column Heating, $p_a$ at $\tau = 22$ . . . . .	
	Units: $10^{-2}$ mb . . . . .	45
Fig. 7	One-Column Heating, $v$ at $\tau = 22$ . . . . .	
	Units: $10^{-2}$ m sec $^{-1}$ . . . . .	46
Fig. 8	One-Column Heating, $\omega_a$ at $\tau = 22$ . . . . .	
	Units: $10^{-10}$ radians sec $^{-1}$ . . . . .	47
Fig. 9	One-Column Heating, $T_a$ at $\tau = 22$ . . . . .	
	Units: $10^{-2}$ °C . . . . .	43
Fig. 10	One-Column Heating, Streamline Schematic at $\tau = 22$ . . . . .	49
Fig. 11	Estimate of Latent and Sensible Energy Release . . . . .	51
Fig. 12	Approximation of Mean Winter Heating . . . . .	52
Fig. 13	Winter Heating, The Evolution of Selected v Components . . . . .	55
Fig. 14	Winter Heating, $w$ at $\tau = 22$ ( $\sim 1$ hour) . . . . .	
	Units: $10^{-4}$ cm sec $^{-1}$ . . . . .	57
Fig. 15	Winter Heating, $\rho_a$ at $\tau = 22$ ( $\sim 1$ hour) . . . . .	
	Units: $10^{-8}$ tons m $^{-3}$ . . . . .	59
Fig. 16	Winter Heating, $p_a$ at $\tau = 22$ ( $\sim 1$ hour) . . . . .	
	Units: $10^{-3}$ mb . . . . .	61
Fig. 17	Winter Heating, $v$ at $\tau = 22$ ( $\sim 1$ hour) . . . . .	
	Units: $10^{-2}$ cm sec $^{-1}$ . . . . .	63

# ILLUSTRATIONS (Continued)

Fig. 18	Winter Heating, $\omega_a$ at $\tau = 22$ (~1 hour)	
	Units: $10^{-12}$ radians $\text{sec}^{-1}$	65
Fig. 19	Winter Heating, $T_a$ at $\tau = 22$ (~1 hour)	
	Units: $10^{-3}$ °C	67
Fig. 20	Winter Heating, $w$ at $\tau = 182$ (~9 hours)	
	Units: $10^{-3}$ cm $\text{sec}^{-1}$	69
Fig. 21	Winter Heating, $\rho_a$ at $\tau = 182$ (~9 hours)	
	Units: $10^{-7}$ tons $\text{m}^{-3}$	71
Fig. 22	Winter Heating, $p_a$ at $\tau = 182$ (~9 hours)	
	Units: $10^{-2}$ mb	73
Fig. 23	Winter Heating, $v$ at $\tau = 182$ (~9 hours)	
	Units: $10^{-1}$ cm $\text{sec}^{-1}$	75
Fig. 24	Winter Heating, $\omega_a$ at $\tau = 182$ (~9 hours)	
	Units: $10^{-10}$ radians $\text{sec}^{-1}$	77
Fig. 25	Winter Heating, $u$ at $\tau = 182$ (~9 hours)	
	Units: $10^{-1}$ cm $\text{sec}^{-1}$	79
Fig. 26	Winter Heating, $T_a$ at $\tau = 182$ (~9 hours)	
	Units: $10^{-2}$ °C	81
Fig. 27	Winter Heating, Streamline Schematic	
	at $\tau = 182$ (~9 hours)	83

## TABLES

Table I	The Evolution of Selected $v$ Components	
	in Units of $\text{cm sec}^{-1}$	85

## I INTRODUCTION

The addition and removal of thermal energy in the atmosphere (i.e., non-adiabatic heating) is exceedingly complex, depending as it does on radiational exchange processes, convection from the surface, and the storage and release of latent heat, and on other processes which are significant in the high atmosphere. The heating itself is for the most part strongly dependent on the evolving state of the atmosphere, on the distribution of radiating and absorbing substances, the temperature, the convective stability, the water forms, the vertical motion, etc., and on the time of day. However, before attempting to introduce any of this complexity into dynamical-numerical models, it is necessary to have some appreciation of both (1) the distributions of heating and cooling in the atmosphere in terms of magnitude and location relative to circulation systems and geography, and (2) the dynamical significance of such distributions. The present project set out to contribute to knowledge in both of these areas. Scientific Reports 1 and 2 on this contract<sup>(1,2)\*</sup> deal with the former; and this work is continuing. The present report (Scientific Report 3) pertains to the latter.

The experiments discussed herein were begun for the purpose of investigating the use of a suitable dynamical-numerical model for the incorporation of heating, and to learn about the dynamical significance of heating distributions. In these experiments the heating field is independently prescribed, by choice, in space and time--that is, the heating will not be coupled to any of the evolving parameters.

It was desired that these investigations should relate and contribute, in so far as possible, to techniques in the general comprehensive dynamical-numerical modeling of atmospheric evolutions.

---

\* References are listed at the end of the report.

In this work the attitude is to approximate the fields as continua. Restrictions which limit the continuum are imposed only in order to limit the magnitude of the task while still maintaining enough degrees of freedom for certain investigations.

The pertinent laws of physics, modified by the hydrostatic relationship, lead to the so-called primitive (or hydrostatic) equation system. The system is relatively unrestricted and provides a broad physical framework for the progressive incorporation of additional pertinent processes and influences. In the last few years it has been numerically integrated and investigated by several groups and researchers. The choice of dependent and independent variables leads to various transformations of the system. Our choice is to use density as a function of geometric height as the principal dependent variable of state. The preference for this choice and the system were discussed in an earlier (1960) work.<sup>(3)</sup> In the system the heating rate appears in Richardson's equation, which diagnostic equation specifies the field of vertical motion.

The dynamical significance of heating in the atmosphere ranges through all scales. Understanding is needed of its effectiveness in (1) creating thermally driven circulations, (2) modifying the evolution of circulation systems, and (3) triggering dynamic instabilities.

One of the major problems in the use of the hydrostatic system is the determination of initial numerical data for the principal dependent variables of density, and horizontal velocity. A smooth specification of these fields, in the scale of the discretization, is, in general, not sufficient because too much energy appears in compression-gravity waves, particularly in the shorter components. The compression-gravity mechanism plays a major role in the evolution. The problem focuses on having the correct field of dynamic imbalance, as calculated by the numerical analogue of the equation system.

In designing experiments for specific investigations the objective is a minimum amount of complication for a maximum return of knowledge within a specified task magnitude. Along this theme, certain

complications were selected and incorporated by design while other complications were tentatively set aside. Experiments can always be improved upon, especially afterwards. Later sections of this report contain criticisms and recommendations.

It was decided to forego variability in one horizontal dimension in favor of many levels in the vertical. The meridional plane is taken as the field of variability, and symmetry about the polar axis is imposed. The model extends from pole to equator with no flow across the equatorial wall. This calls for the use of spherical coordinates.

The problem of initial-data specification was simplified by limiting ourselves to cases which are initially in static (rest) or dynamic (steady) equilibrium. The equilibrium is then upset by a specified distribution of heating. The numerical analogue permits ready determination of a field of zonal motion which is in balance with an arbitrarily specified density distribution. The integration itself then leads to more general states for the study of subsequent evolutions under the influence of heating.

Frictional processes, both internal and boundary, were also set aside. Friction is not an inseparable complement to heating, but is an additional process acting in the evolution, and may be independently considered. It may be argued that without boundary friction, there is no cognizance in the model of the rotation of the underlying smooth earth. However, as designed, the model conserves total angular momentum about the polar axis at the value initially specified. In this way the rotation of the system is built into the evolution. The model is, of course, limited without the incorporation of friction.

The numerical analogue was designed in terms of volume modules, budgets, and fluxes for mass and angular momentum. In this way total mass and total angular momentum are conserved. Truncation errors in mass and angular momentum tendencies cancel internally in any sub-region. This is particularly useful in pressure-tendency calculations.<sup>(4)</sup>

The conventional "second-order-centered" method of time integration (i.e., the leap-frog method) was used with reservations, but as it

turned out, with some advantage in the study of the shortest-period compression-gravity mode.

The model is designed to evolve, with limitations, axially symmetric planetary circulations under the influence of specified non-adiabatic heating distributions which vary with latitude, altitude, and in time. For investigations of some effects of heating at high levels, such as conceived in solar-weather relationship studies, the upper boundary conditions are of special interest. They are essentially non-restrictive and complete. Thermal energy may be added to, or removed from, the upper reaches of the atmosphere in detail as limited by the discretization.<sup>(5)</sup>

For the numerical analogue, the meridional plane is discretized into volume modules by 49 equal intervals from equator to pole and by 19 selected levels with irregular spacing in the vertical. A time step of 3 minutes is used in the final integrations. The heating is specified for each of the volume modules.

In the integrations, abrupt changes in heating are avoided by introducing the changes gradually over several time steps. Only 1/32 of the change is introduced at first. It is then progressively doubled with successive time steps until the new rate is achieved. This procedure serves two purposes. It reduces the compression-gravity disturbances which would arise by the larger abrupt changes. It is also required, especially in beginning the integration from equilibrium, in order to minimize arousing the extraneous degrees of freedom which enter by use of the "second-order-centered" integrating procedure.<sup>(6)</sup> In proceeding from time zero to a steady heating rate, the full heating may be considered to have begun, effectively, after an interval of about 4-1/2 time-steps.

Only a few experiments were carried out with the model as developed and programmed for a Burroughs 220 electronic computer. More was not done because it was felt that an optimum had been reached in consideration of experimental findings, the desirability of model extensions, and the economic advantages of reprogramming for a larger computer.

The first set of experiments was designed primarily to test and study the model. Initially the atmosphere is at rest relative to the rotating earth. One column (i.e., the region between two latitude walls, not quite  $2^\circ$  apart) at mid-latitude is heated at a steady rate which, were the column confined by latitude walls so that each level expanded at constant pressure, would warm the column by  $10^\circ\text{C}$  in 24 hours. The general results bear on computational stability and the nature of the shortest-period compression-gravity mode. The particular results of the experiment showed the somewhat surprising result that, as a consequence of the thermally forced circulation, the heated column becomes colder than the unheated environment. This result is not in error and is physically consistent. It demonstrates dramatically the dangers of jumping to conclusions by qualitative reasoning.

The major experiment also was begun with an atmosphere at rest relative to the rotating earth. The motion is then forced by a steady heating and cooling distribution patterned after the winter season. The results are suitable as a demonstration of common elementary textbook discussions of the atmosphere as a heat engine and the formation of zones of easterly and westerly winds.

The circulations developed by the model must be interpreted with the realization that these circulations continue to develop without being permitted to break down into longitudinal disturbances due to dynamic instability. The zonal circulation and baroclinicity fields progress beyond thresholds of such instability.

If the temptation arises to compare results with mean winter-season meridional fields, it should be kept in mind that the real data contain the effects of longitudinal waves and eddies. Furthermore, the model is a limited dynamical-numerical approximation. Lastly, the integration has been carried out only far enough to show a few derivatives in the sense of a Taylor Series time expansion.

The model is general in the sense that it can be applied to arbitrary planets by changing dimensions, parameters, and initial values. Such integrations would give, under specified thermal forcing fields,

some preliminary notions of the planet's circulation. The regions of developing shear and baroclinicity may give some indication of cyclone belts.

Another application is that the model can be used for smaller-scale axially symmetric circulations including the convective scale. This is done by shrinking the horizontal dimension and imposing a constant Coriolis force. In this way the effects of a strong local release of thermal energy might be examined. Application is limited by the imposition of axial symmetry.



## II THE MATHEMATICAL-PHYSICAL SYSTEM

The basic physical relationships are expressed by the equation for continuity of matter,

$$\frac{\partial \rho}{\partial t} = - \nabla \cdot (\rho \mathbf{V}) \quad (1)$$

the acceleration equation,

$$\frac{\partial \mathbf{V}}{\partial t} = - \nabla \cdot \nabla \mathbf{V} - 2 \mathbf{\Omega} \times \mathbf{V} - \frac{1}{\rho} \nabla p - \nabla \Phi \quad (2)$$

and the thermodynamic equation,

$$\frac{D}{Dt} \ln (p \rho^{-\kappa}) = \frac{\rho R}{C_v p} \dot{Q} \quad (3)$$

The symbols have their usual meaning:  $\rho$  is the density,  $\mathbf{V}$  is the three-dimensional velocity vector,  $\mathbf{\Omega}$  is the earth's rotation vector,  $p$  is the pressure,  $\Phi$  is the apparent gravity potential,  $C_v$  is the specific heat of air at constant volume,  $\kappa = C_p/C_v$  where  $C_p$  is the specific heat of air at constant pressure,  $R$  is the gas constant for dry air, and  $\dot{Q}$  is the rate at which thermal energy is being added. Equation (3) also implicitly contains the perfect gas law,

$$p = \rho RT$$

where  $T$  is the absolute temperature.

As spherical coordinates, we take  $\phi$  as the latitude,  $\lambda$  the longitude, and  $r$  the radial distance from the center point. The corresponding

unit vectors are

$$\mathbf{i} \equiv r \cos \phi \nabla \lambda$$

$$\mathbf{j} \equiv r \nabla \phi$$

$$\mathbf{k} \equiv \nabla r$$

The velocity vector and the del operator, in corresponding components, are

$$\mathbf{V} \equiv u \mathbf{i} + v \mathbf{j} + w \mathbf{k}$$

$$\nabla \equiv \frac{\mathbf{i}}{r \cos \phi} \frac{\partial}{\partial \lambda} + \frac{\mathbf{j}}{r} \frac{\partial}{\partial \phi} + \mathbf{k} \frac{\partial}{\partial r}.$$

The expansion of the system into spherical coordinates is readily accomplished by first expanding the vector pair (or dyadic)  $\nabla \mathbf{V}$ , which we shall exhibit here, in matrix form, for reference:

$$\nabla \mathbf{V} = \begin{matrix} & \mathbf{i} & \mathbf{j} & \mathbf{k} \\ \begin{matrix} \mathbf{i} \\ \mathbf{j} \\ \mathbf{k} \end{matrix} & \left[ \begin{array}{ccc} \frac{1}{r \cos \phi} \frac{\partial u}{\partial \lambda} - \frac{v}{r} \tan \phi + \frac{w}{r} & \frac{1}{r \cos \phi} \frac{\partial v}{\partial \lambda} + \frac{u}{r} \tan \phi & \frac{1}{r \cos \phi} \frac{\partial w}{\partial \lambda} - \frac{u}{r} \\ \frac{1}{r} \frac{\partial u}{\partial \phi} & \frac{1}{r} \frac{\partial v}{\partial \phi} + \frac{w}{r} & \frac{1}{r} \frac{\partial w}{\partial \phi} - \frac{v}{r} \\ \frac{\partial u}{\partial r} & \frac{\partial v}{\partial r} & \frac{\partial w}{\partial r} \end{array} \right] \end{matrix}$$

The earth is taken as a perfect sphere, and, for consistency,

$$\nabla \Phi = -g \mathbf{k} \quad (4)$$

where  $g$  is taken as constant.

Only Eq. (1) and Eq. (2), in components, need be expanded at this point of the development:

$$\begin{aligned} \frac{\partial p}{\partial t} = & \frac{1}{r \cos \phi} \frac{\partial}{\partial \lambda} (\rho u) + \frac{1}{r} \frac{\partial}{\partial \phi} (\rho v) - \frac{\rho v}{r} \tan \phi \\ & + \frac{\partial}{\partial r} (\rho w) + 2 \rho \frac{w}{r} \end{aligned} \quad (5)$$

$$\begin{aligned} \frac{\partial u}{\partial t} = & -\frac{u}{r \cos \phi} \frac{\partial u}{\partial \lambda} + \frac{uv}{r} \tan \phi - \frac{v}{r} \frac{\partial u}{\partial \phi} - w \frac{\partial u}{\partial r} \\ & + 2 \Omega v \sin \phi - \frac{1}{\rho r \cos \phi} \frac{\partial p}{\partial \lambda} - 2 \Omega w \cos \phi - u \frac{w}{r} \end{aligned} \quad (6)$$

$$\begin{aligned} \frac{\partial v}{\partial t} = & -\frac{u}{r \cos \phi} \frac{\partial v}{\partial \lambda} - \frac{v}{r} \frac{\partial v}{\partial \phi} - w \frac{\partial v}{\partial r} - \frac{u^2}{r} \tan \phi \\ & - 2 \Omega u \sin \phi - \frac{1}{\rho r} \frac{\partial p}{\partial \phi} - v \frac{w}{r} \end{aligned} \quad (7)$$

$$\begin{aligned} \frac{\partial w}{\partial t} = & -\frac{u}{r \cos \phi} \frac{\partial w}{\partial \lambda} - \frac{v}{r} \frac{\partial w}{\partial \phi} - w \frac{\partial w}{\partial r} + 2 \Omega u \cos \phi \\ & + \frac{u^2 + v^2}{r} - \frac{1}{\rho} \frac{\partial p}{\partial r} - g \end{aligned} \quad (8)$$

The requirement of symmetry about the polar axis implies that all parameters must be independent of the longitude,  $\lambda$ . We also make the usual approximations which are based on the fact that the atmosphere is a thin layer on the earth; this is, incidentally, the basis for Eq. (4). The terms in  $w/r$ , which arise due to the expansion of a sphere with  $r$ , are neglected. Where  $r$  appears outside of the differentials it is replaced by  $a$ , the radius of the earth.

The Coriolis term arising from  $w$ , i.e.  $2 \Omega w \cos \phi$ , is neglected. The hydrostatic approximation is made by replacing Eq. (8) with the hydrostatic relationship.

The coordinate  $y \equiv a\phi$  is introduced where  $\phi$  is expressed in radians. The coordinate  $r$  is replaced by  $z$  (height above sea level)

in the differentials. Thus, our system, with the inclusion of Eq. (3), which is so far undeveloped, becomes

$$\frac{\partial \rho}{\partial t} = - \frac{1}{\cos \phi} \frac{\partial}{\partial y} (\rho v \cos \phi) - \frac{\partial}{\partial z} (\rho w) \quad (9)$$

$$\frac{\partial u}{\partial t} = - \frac{v}{\cos \phi} \frac{\partial}{\partial y} (u \cos \phi) - w \frac{\partial u}{\partial z} + 2 \Omega v \sin \phi \quad (10)$$

$$\begin{aligned} \frac{\partial v}{\partial t} = & - v \frac{\partial v}{\partial y} - w \frac{\partial v}{\partial z} \\ & - \left\{ u^2 \frac{\tan \phi}{a} + 2 \Omega u \sin \phi + \frac{1}{\rho} \frac{\partial p}{\partial y} \right\} \end{aligned} \quad (11)$$

$$0 = - \frac{1}{\rho} \frac{\partial p}{\partial z} - g \quad (12)$$

It is our preference to use the hydrostatic relationship, Eq. (12), in integrated form:

$$p = g \int_z^{\infty} \rho \, dz \quad (13)$$

The hydrostatic pressure-tendency equation may be obtained by differentiating Eq. (13) with respect to time, and substituting for  $\partial \rho / \partial t$  according to Eq. (9). This yields

$$\frac{\partial p}{\partial t} = - \frac{g}{\cos \phi} \int_z^{\infty} \frac{\partial}{\partial y} (\rho v \cos \phi) \, dz + g \rho w \quad (14)$$

We have yet to derive the pertinent Richardson's equation, which is now implicit in our system because of the stringency of the hydrostatic relationship. In the hydrostatic system, it falls on  $w$  to maintain

this relationship. We first expand Eq. (3):

$$\frac{1}{p} \left\{ \frac{\partial p}{\partial t} + v \frac{\partial p}{\partial y} - g \rho w \right\} - \frac{\kappa}{\rho} \left\{ \frac{\partial \rho}{\partial t} + v \frac{\partial \rho}{\partial y} + w \frac{\partial \rho}{\partial z} \right\} = \frac{\rho R}{C_v p} \dot{Q} .$$

We then substitute for  $\partial p / \partial t$  according to Eq. (14), and  $\partial \rho / \partial t$  according to Eq. (9):

$$\frac{1}{p} \left\{ - \frac{g}{\cos \phi} \int_z^\infty \frac{\partial}{\partial y} (\rho v \cos \phi) dz + v \frac{\partial p}{\partial y} \right\} - \frac{\kappa}{\rho} \left\{ - \frac{1}{\cos \phi} \frac{\partial}{\partial y} (\rho v \cos \phi) - \frac{\partial}{\partial z} (\rho w) + w \frac{\partial \rho}{\partial z} + v \frac{\partial \rho}{\partial y} \right\} = \frac{\rho R}{C_v p} \dot{Q} .$$

The latter equation is then developed into the form

$$\frac{\partial w}{\partial z} = \frac{1}{p} \left\{ \frac{g}{\kappa \cos \phi} \int_z^\infty \frac{\partial}{\partial y} (\rho v \cos \phi) dz - \frac{1}{\cos \phi} \frac{\partial}{\partial y} (\rho v \cos \phi) + \frac{R}{C_p} v \frac{\partial p}{\partial y} + \rho \frac{R}{C_p} \dot{Q} \right\} . \quad (15)$$

The inclusion of the derived Eq. (15) into our system makes a one-equation redundancy. We choose to dismiss the thermodynamic equation. This choice is discussed at length in Ref. 3. The selection in this case suggests later advantages in the design of the numerical analogue of the system. The question of resolution is not involved in this choice, since resolution has already been determined by the system as a whole.

It should be kept in mind that with the accomplishment of a complete system of equations, with boundary conditions, and based on approximated laws and more empirical relationships, the mathematical-physical system

has been wholly defined. Transformations of the equation system, including changes of dependent and independent variables are in themselves completely without consequence and are rather a means to such advantages as:

- (1) Forms which are more revealing for understanding of the physical processes
- (2) Forms which are more suitable for the introduction of modifications
- (3) Forms which are more revealing as to functional approach, including indigenous functions and power series solutions
- (4) Forms which are suggestive in leading more directly to better numerical analogues in terms of ease of calculation, error control, and the nature of the analogue.

At this point we are exhibiting our system by Eqs. (9), (10), (11), (13), and (15). One more transformation is now carried out which will take advantage of the special features of the axially symmetric mechanics.

Introduce,

$$\omega \equiv \Omega + \frac{u}{a \cos \phi} \quad (16)$$

$$\eta \equiv \rho \cos \phi \quad (17)$$

$$\nu \equiv \rho \omega \cos^3 \phi \quad (18)$$

where  $\omega$  is the absolute angular speed, and  $2\pi a\eta$  and  $2\pi a^3\nu$  are, respectively, the mass and absolute angular momentum of a zonal ring of unit meridional-plane area. With these parameters, Eq. (9) transforms directly into

$$\frac{\partial}{\partial t} \eta = - \frac{\partial}{\partial y} (v\eta) - \frac{\partial}{\partial z} (w\eta) \quad (19)$$

Equation (10), combined with Eq. (16) leads to

$$\frac{\partial}{\partial t} \nu = - \frac{\partial}{\partial y} (v \nu) - \frac{\partial}{\partial z} (w \nu) \quad (20)$$

The parameter  $\omega$  replaces  $u$  in Eq. (11):

$$\begin{aligned} \frac{\partial v}{\partial t} = & - v \frac{\partial v}{\partial y} - w \frac{\partial v}{\partial z} - \frac{1}{\rho} \frac{\partial p}{\partial y} \\ & - a \cos \phi \sin \phi (\omega^2 - \Omega^2) . \end{aligned} \quad (21)$$

These equations, Eqs. (19), (20), and (21), together with Eqs. (13) and (15), are an expression of the system.

It should also be stated that  $w = 0$  at  $z = 0$  (smooth earth) and  $v = 0$  at the pole, where  $\phi = \pi/2$ .

In these experiments we have extended the model over only one hemisphere, and imposed the artificial condition that  $v = 0$  at  $\phi = 0$ . In effect we have a wall at the equator. The upper boundary conditions require that the momentum remain bounded. The effective boundary conditions are revealed by the discretization, and by the numerical analogue.

### III THE NUMERICAL ANALOGUE

The hemisphere, as represented by distributions in a representative meridional plane, is divided by surfaces  $y = y_m$ , and  $z = z_n$ , which create zonal rings as volume modules. The  $m,n$ th volume module consists, in the meridional plane, of one corner, two sides, and its interior. All parameters referred to the  $m,n$  module are subscripted by  $m,n$ . The principal evolving parameters are located at points shown in Fig. 1.

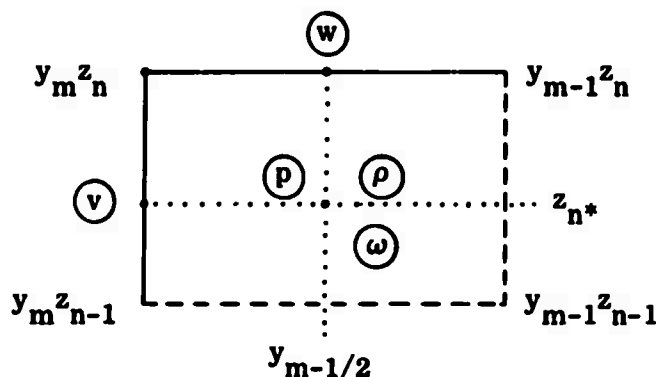


FIG. 1 THE ARBITRARY  $m,n$  VOLUME MODULE

The positioning of the parameters comes about in the design of the numerical analogue. In this way, the fields are approximated by vectors. We shall circle the components of the vectors in order to differentiate them from interim uses of the parameters in the development of the numerical analogue.

The  $y_m$  increase in regular intervals,  $\delta y = a\pi/98$ , from  $y_0 = 0$ , at the equator, to  $y_{49} = a\pi/2$ , at the pole. Levels are selected in irregular intervals, from  $z_0 = 0$  at sea level to  $z_{18} \approx 37$  km at the base of the uppermost layer of volume modules. The levels were selected according to some rather limited statistics on variability in the atmosphere. These statistics are not particularly pertinent to the present experiment.



For the formulation of upper boundary conditions, it will be seen that there is little difference between extending the upper layer of modules from  $z \approx 37$  km to  $z = \infty$ , or terminating the layer at, say,  $z = 60$  km. The difference, which comes into modeling the module dimensional constants, lies within the truncation error, and does not affect the degrees of freedom. We have labeled the top as  $z_{19} = 60$  km.

The arbitrary  $m, n$  volume module, as depicted in Fig. 1, also contains the lines  $y = y_{m-1/2}$  and  $z = z_{n*}$ . Whereas  $y_{m-1/2}$  lies midway between  $y_m$  and  $y_{m-1}$ , some statistics are brought in in selecting  $z_{n*}$ . The statistics come in the form of the N.A.C.A. Standard Atmosphere. The Standard Atmosphere values of the state parameters are denoted by the subscript  $s$ . The level,  $z_{n*}$ , is determined by the relationship

$$\int_{z_{n-1}}^{z_n} \rho_s dz = \rho_{sn*} (z_n - z_{n-1}) \quad (22)$$

The level at which  $\rho_s = \rho_{sn*}$  is the level  $z_{n*}$ , where the standard density is a mean for the layer.

With the discretization of the field established, we proceed with the design of the numerical analogue beginning with the simplest of our equations, the hydrostatic relationship, Eq. (13). The pressure is simply the weight of the column of air above. This is developed as follows:

$$\begin{aligned} \textcircled{p}_{m,n} &= g \int_{z_{n*}}^{z_{19}} \rho dz \\ &= g \left\{ \int_{z_{n*}}^{z_n} \rho dz + \sum_{r=n+1}^{19} \int_{z_{r-1}}^{z_r} \rho dz \right\} . \end{aligned}$$

Here  $r$  is used as a dummy variable for  $n$ . Thus, we make the approximation

$$\textcircled{p}_{m,n} = g \left\{ \boxed{1}_n \frac{1}{2} \textcircled{\rho}_{m,n} + \sum_{r=n+1}^{19} \boxed{1}_r \textcircled{\rho}_{m,r} \right\} \quad (23)$$

in which our first module dimensional constant is

$$\boxed{1}_n \equiv z_n - z_{n-1} \quad (24)$$

In order to conserve symbols, all module constants will be denoted by boxed numbers, subscripted according to their dependency. Further statistical refinement of the module constants is not warranted at this time, but should be considered in later developments and applications of the model.

Equations (19) and (20) are both of the form

$$\frac{\partial}{\partial t} * = \nabla \cdot (* \mathbf{V}) \quad (25)$$

in a cartesian  $y,z$  frame, where  $*$  =  $\eta$  and  $\nu$ , respectively. Analogues for these are ideally constructed by first integrating over the  $y,z$  area of the volume module, and applying Gauss's theorem:

$$\frac{d}{dt} \int_A * da = - \int_L * \mathbf{V} \cdot d\boldsymbol{\ell} \quad (26)$$

That is, the total change rate in the module is equal to the net flux rate into the module. In designing the analogues, one-to-one correspondences are imposed between the mass of the module and the density at an interior point, and between the absolute angular momentum of the module and  $\rho\omega$  at an interior point.

The mass of a volume module, omitting the factor  $2\pi a$ , is approximated by

$$\int_{z_{n-1}}^{z_n} \int_{y_{m-1}}^{y_m} \rho \cos \phi \, dy \, dz \approx (\rho)_{mn} [1]_n [2]_m \quad (27)$$

and the absolute angular momentum of a volume module, omitting the factor  $2\pi a^3$ , is approximated by

$$\int_{z_{n-1}}^{z_n} \int_{y_{m-1}}^{y_m} \rho \omega \cos^3 \phi \, dy \, dz \approx (\rho \omega)_{mn} [1]_n [3]_m \quad (28)$$

where

$$[2]_m \equiv \int_{y_{m-1}}^{y_m} \cos \phi \, dy \quad (29)$$

$$[3]_m \equiv \int_{y_{m-1}}^{y_m} \cos^3 \phi \, dy \quad (30)$$

For the fluxes through module interfaces, the speeds are suitably located. However,  $\rho$  and  $\rho \omega$  must be interpolated. Linear interpolations are used except for  $\rho$  in the vertical, for which the Standard Atmosphere is again invoked.

For  $\rho$ , at the level  $z_n$ , is used

$$[4]_n (\rho)_{m,n+1} + [5]_n (\rho)_{mn} \quad (31)$$

where

$$[4]_n \equiv \frac{z_n - z_{n*}}{z_{n+1,*} - z_{n*}} \frac{\rho_{sn}}{\rho_{s,n+1,*}} \quad (32)$$

$$[5]_n \equiv \frac{z_{n+1,*} - z_n}{z_{n+1,*} - z_{n*}} \frac{\rho_{sn}}{\rho_{sn*}} \quad (33)$$

The interpolation is such that it would be exact if the distribution were Standard Atmosphere.

The mass flux rates are represented by  $(A)_{m,n}$  and  $(B)_{m,n}$ , and the absolute-angular-momentum flux rates by  $(C)_{m,n}$  and  $(D)_{m,n}$ , as shown in Fig. 2.

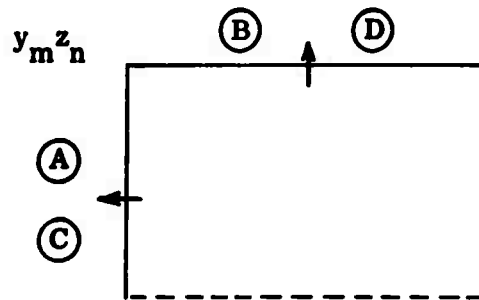


FIG. 2 THE FLUXES

In this manner, that is by first integrating over the volume module, Eqs. (19) and (20) are approximated by

$$\frac{d}{dt} (\rho)_{mn} = [6]_n [7]_m \left\{ (A)_{m-1,n} - (A)_{mn} + (B)_{m,n-1} - (B)_{mn} \right\} \quad (34)$$

$$\frac{d}{dt} (\rho \omega)_{mn} = [6]_n [8]_m \left\{ (C)_{m-1,n} - (C)_{mn} + (D)_{m,n-1} - (D)_{mn} \right\} \quad (35)$$

where  $[6]_n [7]_m$  and  $[8]_m$  are the inverses of  $[1]_n [2]_m$  and  $[3]_m$  respectively. The fluxes are calculated according to

$$A_{mn} \equiv v_{mn} \left\{ \rho_{m+1,n} + \rho_{mn} \right\} [1]_n [9]_m \quad (36)$$

$$B_{mn} \equiv w_{mn} \left\{ [4]_n \rho_{m,n+1} + [5]_n \rho_{ma} \right\} [10]_m \quad (37)$$

$$C_{mn} \equiv v_{mn} \left\{ \rho \omega_{m+1,n} + \rho \omega_{mn} \right\} [1]_n [11]_m \quad (38)$$

$$D_{mn} \equiv w_{mn} \left\{ [4]_n \rho_{m,n+1} + [5]_n \rho_{mn} \right\} \cdot \left\{ [12]_n \omega_{m,n+1} + [13]_n \omega_{mn} \right\} [14]_m \quad (39)$$

where

$$[9]_m \equiv \frac{1}{2} \cos \phi_m \quad (40)$$

$$[10]_m \equiv \cos \phi_{m-1/2} \delta y \quad (41)$$

$$[11]_m \equiv \frac{1}{2} \cos^3 \phi_m \quad (42)$$

$$[12]_n \equiv \frac{z_n - z_{n*}}{z_{n+1,*} - z_{n*}} \quad (43)$$

$$[13]_n \equiv \frac{z_{n+1,*} - z_n}{z_{n+1,*} - z_{n*}} \quad (44)$$

$$[14]_m \equiv \cos^3 \phi_{m-1/2} \delta y \quad (45)$$

All fluxes are through interior interfaces. They transport from one module into the other. It is apparent that, because the hemisphere is contained, the numerical analogue strictly conserves (except for random round-off) total mass and total absolute angular momentum:

$$\sum \Delta_n \Delta_m (\rho)_{mn} = \text{constant} \quad (46)$$

$$\sum \Delta_n \Delta_m (\rho\omega)_{mn} = \text{constant.} \quad (47)$$

The sums are taken over all modules. These sums are carried out for each time step during the integration as computational checks. It is also noteworthy that vertical mass fluxes, alone, do not change sea-level pressure.

The analogue for the Richardson's equation, Eq. (15), is also constructed by integration over the elemental  $m, n$  volume module. However, before integrating, we wish to allow for, and make explicit, some dependency of  $p$  and  $\rho$  on  $z$ , in the module. We approximate the statistics of this dependency by isothermal conditions at temperature  $T = T_{sn^*}$ :

$$p = p_{n^*} E \quad (48)$$

$$\rho = \rho_{n^*} E \quad (49)$$

where

$$E \equiv e^{\frac{-g}{RT_{sn^*}} (z - z_{n^*})} \quad (50)$$

Also, for  $z_{n-1} < z < z_n$ ,

$$\int_z^\infty \frac{\partial}{\partial y} (v \rho \cos \phi) dz = \int_z^{z_n} \frac{\partial}{\partial y} (v \rho \cos \phi) dz + S_n \quad (51)$$

where

$$S_n \equiv \sum_{r=n+1}^{19} \int_{z_{r-1}}^{z_r} \frac{\partial}{\partial y} (v \rho \cos \phi) dz. \quad (52)$$

With these substitutions, Eq. (15) becomes

$$\begin{aligned} \frac{\partial w}{\partial z} = \frac{1}{\textcircled{p}_{mn}} & \left\{ \frac{g}{\kappa \cos \phi} \left[ \frac{\partial}{\partial y} (v \rho_{n*} \cos \phi) E^{-1} \int_z^{z_n} E dz \right. \right. \\ & \left. \left. + S_n E^{-1} \right] - \frac{1}{\cos \phi} \frac{\partial}{\partial y} (v p_{n*} \cos \phi) \right. \\ & \left. + \frac{R}{C_p} v \frac{\partial}{\partial y} p_{n*} + \rho_{n*} \frac{R}{C_p} \dot{Q} \right\}. \quad (53) \end{aligned}$$

We now integrate both sides of this equation over the  $m, n$  volume module and complete the analogue:

$$\begin{aligned}
\textcircled{w}_{mn} - \textcircled{w}_{m,n-1} = \frac{1}{\delta y} \frac{1}{\textcircled{p}_{mn}} & \left\{ \textcircled{15}_m \left[ \textcircled{16}_n \left( \textcircled{A}_{mn} - \textcircled{A}_{m-1,n} \right) \right. \right. \\
& + \textcircled{17}_n \sum_{r=n+1}^{19} \left( \textcircled{A}_{mr} - \textcircled{A}_{m-1,r} \right) \\
& + \textcircled{18}_n \left[ \textcircled{18}_m \left( \textcircled{F}_{mn} - \textcircled{F}_{m-1,n} \right) \right. \\
& + \textcircled{19} \left( \textcircled{v}_{m-1,n} + \textcircled{v}_{mn} \right) \left( \textcircled{p}_{m+1,n} - \textcircled{p}_{m-1,n} \right) \\
& \left. \left. + \delta y \dot{q}_{mn} \right] \right\} . \tag{54}
\end{aligned}$$

This defines some additional parameters:

$$\textcircled{15}_m \equiv \frac{g}{\kappa \cos \phi_{m-1/2}} \tag{55}$$

$$\textcircled{16}_n \equiv \frac{R}{g} T_{sn^*} - \left( \frac{R}{g} T_{sn^*} \right)^2 \left\{ \frac{1 - e^{-\frac{g}{RT_{sn^*}} (z_n - z_{n-1})}}{z_n - z_{n-1}} \right\} \tag{56}$$

$$\textcircled{17}_n \equiv \frac{R}{g} T_{sn^*} \left[ 1 - e^{-\frac{g}{RT_{sn^*}} (z_n - z_{n-1})} \right] \tag{57}$$



$$\boxed{18}_m = \frac{1}{\cos \phi_{m-1/2}} \quad (58)$$

$$\boxed{19} = R/4 C_p \quad (59)$$

$$\dot{q}_{mn} = \frac{R}{C_p} \rho_{sn*} \dot{Q}_{mn} \quad (60)$$

In the forcing term, Eq. (60), we have made the approximation of replacing  $\odot_{m,n}$  by  $\rho_{sn*}$ .

The remaining equation for which an analogue is desired is Eq. (21). The analogue is constructed by

$$\begin{aligned} \frac{d}{dt} \odot_{mn} = & - \odot_{mn} \left( \odot_{m+1,n} - \odot_{m-1,n} \right) \frac{1}{2} \frac{1}{\delta y} \\ & - \boxed{20}_n \left( \odot_{mn} + \odot_{m+1,n} + \odot_{m+1,n-1} + \odot_{m,n-1} \right) \\ & \left( \odot_{m,n+1} - \odot_{m,n-1} \right) - \frac{\odot_{m+1,n} - \odot_{mn}}{\odot_{mn} + \odot_{m+1,n}} \frac{2}{\delta y} \\ & - \boxed{21}_m \left[ \left( \odot_{m+1,n} + \odot_{mn} \right)^2 - 4 \Omega^2 \right]. \end{aligned} \quad (61)$$

The additional parameters are

$$\boxed{20}_n = \frac{1}{4(z_{n+1,*} - z_{n-1,*})} \quad (62)$$

$$\boxed{21}_m = \frac{a \cos \phi_m \sin \phi_m}{4} \quad (63)$$

The space dependency of our mathematical-physical system is thus numerically modeled by Eqs. (23), (34), (35), (54), and (61). Also implicit in our system is the perfect gas law, which yields

$$\textcircled{T}_{mn} = \textcircled{p}_{mn} / R \textcircled{\rho}_{mn} \quad (64)$$

Some further discussion of the boundary conditions is necessary.

The lower boundary condition is

$$\textcircled{w}_{m,0} \equiv 0. \quad (65)$$

The vertical motion is thus diagnosed by progressing upward with the analogue of Richardson's equation, Eq. (54).

The upper boundary conditions essentially take the form

$$\textcircled{B}_{m,19} \equiv \textcircled{D}_{m,19} \equiv 0 \quad (66)$$

This implies that we consider  $z_{19}$  to be effectively at infinite height. Examination reveals that the heating in the upper layer of modules has little effect on the evolution via the analogue of Richardson's equation, Eq. (54). Because of Conditions (66), the calculated  $\textcircled{w}_{m,19}$  are used only in Eq. (61), in determining a mean  $w$  for the vertical advection. The influence there is rather minor.

More realistic influence of the upper layer heating may be built into the model as follows. Equation (23) yields

$$\textcircled{p}_{m,19} = g \square_{19} \left( \frac{1}{2} \textcircled{\rho}_{m,19} \right) \quad (67)$$

This, in effect, specifies the temperature there. According to Eq. (65), then,

$$\textcircled{T}_{m,19} = \frac{g}{2R} \square_{19} \quad (68)$$

By prescribing  $\square_{19}$  as a function of  $m$  and time, the heating of the upper layer may be modeled into the analogue. This requires suitable modeling considerations. In our experiments,  $\square_{19}$  was left as a constant.

The boundary conditions at the pole and at the equator are, respectively,

$$\textcircled{v}_{49,n} \equiv 0 \quad (69)$$

$$\textcircled{v}_{0,n} \equiv 0 \quad (70)$$

Additional boundary specifications are required because of the use of some double differences in Eqs. (54) and (61). In Eq. (54), in the term with the coefficient  $\square_{19}$ , appears the centered double-interval difference:

$$\textcircled{p}_{m+1,n} - \textcircled{p}_{m-1,n} \quad (71)$$

For  $m = 49$  this is replaced by the one-sided difference

$$2 \left( \textcircled{p}_{49,n} - \textcircled{p}_{48,n} \right) \quad (72)$$

and for  $m = 1$  it is replaced by the one-sided difference

$$2 \left( \textcircled{p}_{2,n} - \textcircled{p}_{1,n} \right) . \quad (73)$$

In Eq. (61), the centered double-interval difference

$$\textcircled{v}_{m,n+1} - \textcircled{v}_{m,n-1}$$

is similarly modified for  $n = 1$  and  $n = 19$ . This makes the numerical analogue system a complete system.

We have followed the procedure of first numerically modeling the space dependency of our system. It remains to discretize the time dependency and to indicate the integrating procedure. The time continuum,  $t$ , is discretized by time-increment  $\delta t$ , such that

$$t = \tau \delta t , \quad \tau = 0, 1, 2, 3 \dots \quad (74)$$

where  $\tau$  is the number of the time-step.

Initially, and at any subsequent time-step, the complete specification shall consist of the principal dependent parameters:

$$\left. \begin{array}{ll} \textcircled{\rho}_{mn} & \text{for } m = 1, 2 \dots 49 ; \quad n = 1, 2 \dots 19 \\ \textcircled{\rho\omega}_{mn} & \text{for } m = 1, 2 \dots 49 ; \quad n = 1, 2 \dots 19 \\ \textcircled{v}_{mn} & \text{for } m = 1, 2 \dots 48 ; \quad n = 1, 2 \dots 19 \end{array} \right\} \quad (75)$$

From these we may derive

$$\textcircled{\omega}_{mn} = \textcircled{\rho\omega}_{mn} / \textcircled{\rho}_{mn} \quad (76)$$

and diagnose  $\textcircled{p}_{m,n}$  according to Eq. (23) and  $\textcircled{w}_{m,n}$  according to Eq. (54).

The principal dependent parameters, (75), at  $t = \tau \delta t$ , may be represented by the vector  $\underline{V}_{\tau}$ . Equations (34), (35), and (61) give us

$$\left( \frac{d}{dt} \underline{V} \right)_{\tau} \quad (77)$$

as non-linear functions of the parameters. This derivative is approximated by the double-interval difference

$$\left( \underline{V}_{\tau+1} - \underline{V}_{\tau-1} \right) / 2 \delta t \quad (78)$$

which gives the conventional "leap-frog" integration procedure,

$$\underline{V}_{\tau+1} = \underline{V}_{\tau-1} + 2 \delta t \left( \frac{d}{dt} \underline{V} \right)_{\tau} \quad (79)$$

This completes the numerical analogue. To begin the time integration, using Eq. (79), requires that we know  $\underline{V}_{\tau}$  for two consecutive time-steps.

Stationary solutions of the numerical analogue, i.e.,  $\frac{d}{dt} \underline{V} \equiv 0$ , include the class of zonal flows

$$\textcircled{v}_{mn} \equiv 0 \quad (80)$$

with  $\textcircled{\rho}_{m,n}$  and  $\textcircled{\omega}_{m,n}$  satisfying

$$\begin{aligned} & \frac{\textcircled{p}_{m+1,n} - \textcircled{p}_{mn}}{\textcircled{\rho}_{mn} + \textcircled{\rho}_{m+1,n}} \frac{2}{\delta y} \\ & + [21]_m \left[ \left( \textcircled{\omega}_{m+1,n} + \textcircled{\omega}_{mn} \right)^2 - 4 \Omega^2 \right] \equiv 0 . \quad (81) \end{aligned}$$

Equation (81) derives from Eq. (61). Equations (80) and (81) also include the degenerate case of relative rest:

$$\textcircled{v}_{mn} \equiv 0, \quad \textcircled{\omega}_{mn} \equiv \Omega, \quad \textcircled{\rho}_{mn} = \rho_n. \quad (82)$$

In these experiments, the integration is begun by specifying a stationary solution, representing conditions both at  $\tau = 0$  and  $\tau = 1$ . The equilibrium is upset by the commencement of heating at  $\tau = 0$ . The heating is introduced in steps, as discussed in Sec. I.

The experiments discussed herein are limited to integrations begun with a Standard Atmosphere at relative rest. Heating-rate distributions, Eq. (60),

$$\dot{q}_{mn} \text{ for } m = 1, 2, \dots, 49, \quad n = 1, 2, \dots, 19$$

are specified constant in time, except that they are gradually introduced as follows:

<u>Time Interval</u>	<u>Proportional Rate</u>
0 to 2 $\delta t$	1/32
$\delta t$ to 3 $\delta t$	1/16
2 $\delta t$ to 4 $\delta t$	1/8
3 $\delta t$ to 5 $\delta t$	1/4
4 $\delta t$ to 6 $\delta t$	1/2
5 $\delta t$ to 7 $\delta t$	1
etc.	1

The levels selected and the Standard Atmosphere values for calculation of the constants are shown in Fig. 3. The values  $(p)_n$  and  $(T)_n$  correspond to the initial specification  $(\rho)_n = \rho_{sn*}$ , and are determined by Eqs. (23) and (65) respectively. Additional values required are:

$$\delta\phi = 0.03205706 \text{ radians}$$

$$a = 6,371 \text{ km}$$

$$g = 9.80665 \text{ meters secs}^{-2}$$

$$R = 287.04 \text{ kj ton}^{-1} \text{ deg}^{-1}$$

$$C_p = 1004 \text{ kj ton}^{-1} \text{ deg}^{-1} .$$

The integrations are based on the meters-tons-seconds system of units.

The computational stability of the analogue and the magnitude of the time increment,  $\delta t$ , are discussed in Sec. IV.

0 10	19	60,000.0	42,642.5	02	1.7	106	216.660	1.95004	399.85415
	18	36,592.6	33,447.0	64	10.6	6.57	216.660	6.90008	227.90024
	17	30,800.0	26,406.5	160	32.0	19.90	216.660	22.40834	243.95923
	16	22,828.2	20,016.6	96.3	87.7	54.54	216.660	57.42049	228.09980
100	15	17,595.0	15,270.3	129.6	185.6	115.42	216.660	119.93049	225.11747
	14	13,199.0	12,477.2	257.3	288.3	176.29	216.660	179.93462	217.43652
200	13	11,784.2	11,089.8	321.6	358.8	223.14	216.660	224.93998	216.40963
	12	10,363.0	9,758.6	393.5	425.2	274.28	224.729	274.94329	225.27212
300	11	9,163.9	8,344.5	457.2	504.3	338.61	233.921	339.94735	234.84443
	10	7,346.1		553.7					
400			6,180.2		646.6	460.27	247.989	464.94911	250.51126
500									
600	9	4,865.2		746.9					
			4,222.2		800.1	598.31	260.716	599.94733	261.23203
700	8	3,590.7	3,132.4	855.1	696.6	689.36	267.799	689.95012	268.02769
	7	2,681.0	2,364.6	939.4	970.1	759.60	272.789	739.93298	272.91524
800	6	2,050.3	1,801.9	1001.5	1026.7	814.70	276.448	814.95364	276.53297
	5	1,553.7	1,315.7	1052.4	1077.6	864.86	279.608	864.95145	279.63312
900	4	1,080.6	944.6	1102.9	1117.7	904.80	282.020	904.94919	282.06975
	3	806.9	670.5	1132.9	1148.1	935.26	283.802	934.95181	283.70506
	2	540.4	411.4	1162.7	1177.4	964.80	285.486	964.94160	285.51871
	1	260.6	144.0	1192.4	1208.2	996.08	287.224	996.95196	287.35495
1000	0	0.0		1225.0					
<div> <div><math>p_s</math></div> <div>(mb)</div> </div> <div> <div><math>n</math></div> <div>Level no.</div> </div> <div> <div><math>z_n</math></div> <div>(meters)</div> </div> <div> <div><math>z_{na}</math></div> <div>(meters)</div> </div> <div> <div><math>\rho_{sn}</math></div> <div>(<math>10^{-6}</math> g/m<sup>3</sup>)</div> </div> <div> <div><math>\rho_{sna}</math></div> <div>(<math>10^{-6}</math> g/m<sup>3</sup>)</div> </div> <div> <div><math>p_{sna}</math></div> <div>(mb)</div> </div> <div> <div><math>T_{sna}</math></div> <div>(°K)</div> </div> <div> <div><math>p_n</math></div> <div>(mb)</div> </div> <div> <div><math>T_n</math></div> <div>(°K)</div> </div>									

FIG. 3 LEVELS AND PARAMETERS



#### IV TEST INTEGRATIONS, COMPUTATIONAL STABILITY AND GRAVITY WAVES

The "leap-frog" method of time integration, Eq. (79), has several recognized undesirable properties which limit its usefulness. It is used here in the interests of simplicity and economy.

The centered single-difference analogue,

$$\frac{\tilde{V}_{r+1} - \tilde{V}_r}{\delta t} = \frac{d}{dt} \frac{1}{2} \left( \tilde{V}_{r+1} + \tilde{V}_r \right) \quad (83)$$

is more accurate and apparently more natural. It is implicit and may be used by reiterating each time step. The convergence condition imposes an upper limit on  $\delta t$ . The programming is more complex and the computations are lengthier than for the "leap-frog" method. For these reasons it was not used in our limited experiments.

These analogues, Eqs. (79) and (83), are readily analyzed for linear systems<sup>(7)</sup>,

$$\frac{d}{dt} \tilde{V} = \tilde{M} \tilde{V} \quad (84)$$

where the matrix  $\tilde{M}$  is an analogue of the linear operations. Such analysis is quite pertinent to non-linear systems because of the high degree of inherent linearity exhibited by evolutions and phenomena which are governed by such systems. This is especially so for gravity waves in the atmosphere, as will be demonstrated later.

Our numerical analogue was programmed for a Burroughs 220 computer having a 5000-word core memory and adequate magnetic tapes. The magnitude of our problem required a considerable amount of data transfer between tapes and cores for each time-step. As programmed, the computer running time per analogue time-step required approximately 1.25 minutes of calculations and 1.15 minutes for tape movement. In addition the

full output of the fields  $(w)$ ,  $(\rho)$ ,  $(p)$ ,  $(v)$ ,  $(\omega)$ , and  $(T)$  for a specified time-step required approximately 2.75 minutes of on-line tabulation. With output, this totals to an approximation of 5.15 minutes per time-step.

The sum checks for total mass, Eq. (46), and total absolute angular momentum, Eq. (47), are calculated for each time step.

The heating rate,  $\dot{Q}$ , has the dimensions [energy mass<sup>-1</sup> time<sup>-1</sup>], whether considered as parcel or local input. In our system the  $\dot{Q}$  field is locally specified.

A frequently encountered convention is to express heating in terms of the equivalent temperature change of a parcel at constant pressure:

$$\dot{Q} = C_p \dot{T}_E \quad (85)$$

The interpretation of this specification can be misleading if it suggests its time integration,

$$\delta Q = C_p \delta T \quad (86)$$

which is not generally meaningful in the circulating atmosphere. The full relationship for local temperature-change rate, implicit in our system, is

$$\dot{Q} = C_p \frac{\partial T}{\partial t} + \left\{ C_p \mathbf{V} \cdot \nabla T - \frac{1}{\rho} \frac{\partial p}{\partial t} - \frac{1}{\rho} \mathbf{V} \cdot \nabla p \right\} \quad (87)$$

In the case of a column whose motion is restricted to thermal expansion in the vertical, each fluid layer remains at constant pressure hydrostatically. For this evolution, Eq. (87) reduces to

$$\dot{Q} = C_p \left( \frac{\partial T}{\partial t} + w \frac{\partial T}{\partial z} \right) \quad (88)$$

and Eq. (15) reduces to

$$\frac{\partial w}{\partial z} = \frac{1}{C_p} \frac{\dot{Q}}{T} \quad (89)$$

For a sufficiently smooth temperature structure, Eq. (88) may be approximated by

$$\dot{Q} \approx C_p \frac{\partial T}{\partial t} \quad (90)$$

Since  $\dot{Q}$  is specified locally, this integrates into the approximation of local temperature change stated by Eq. (86), in which case

$$\delta T_E \approx \delta T \quad (91)$$

Our integrations, starting with an atmosphere at relative rest, commence in this fashion.

With the convention, Eq. (85), introduced into  $\dot{q}_{m,n}$ , Eq. (60), the numerical specification of the heating distribution takes the form

$$\dot{q}_{mn} \equiv R \rho_{sn} \bar{T}_E \quad mn \quad (92)$$

where  $\bar{T}_E$  is an average value for the  $m,n$  module.

As a first test experiment, the Standard Atmosphere, at relative rest, is disturbed by the heating distribution:

$$\left. \begin{aligned} \bar{T}_E &= 0 & \text{for } m \neq 25 \\ \bar{T}_E &= 10^\circ \text{C/24 hours} & \text{for } m = 25, n \end{aligned} \right\} \quad (93)$$

This experiment was designed in order to excite the smallest-scale modes, with the prospect of physically interpreting the evolution.

In order to anticipate the evolution, we should expect the following sequence of events: The heated column expands upwards. This causes an excess of pressure, over adjacent columns, at all levels above the surface. The horizontal pressure gradients so established accelerate the air out of the heated column both northward and southward. Because of this upper mass divergence, a pressure deficit first appears at the bottom of the heated column and is progressively shown by a deeper surface-based layer. This causes a lower mass convergence and the circulation pattern becomes established.

For trial run number one,  $\delta t = 1$  hour was arbitrarily selected. Computational instability was expected for so large a time increment, and the integration was carried out only to time step  $\tau = 6$ . The computational instability was violent, because the tendencies were allowed to act for  $2\delta t = 2$  hours without being checked by their consequences. The horizontal mass divergence appeared at upper levels in the heated column, at  $\tau = 3$ . By allowing it to act from  $\tau = 2$  to  $\tau = 4$ , it more than evacuated the upper three modules, producing negative density.

For trial run number two, the time increment was reduced to  $\delta t = 6$  minutes, and the integration was taken out to  $\tau = 16$ . Again we had computational instability, but the growth rate was slow enough to permit a careful analysis.

The computational instability was manifested as an oscillation of mass between even- and odd-numbered whole columns. The period of this oscillation was 4 time steps. The disturbance propagated northward and southward from the heated column at the rate of one column every two time steps.

For the disturbance growth-and-propagation mechanism, only a few terms acted in the numerical analogue. In these, where  $\rho_{m+1,n}^+$  occurred, it could be approximated by  $2\rho_{sn}^*$ . In effect the  $\rho_{m,n}$  occurred,

analogue reduced to

$$\frac{d}{dt} \textcircled{\rho}_{mn} \approx \textcircled{G}_n \textcircled{Y}_m \left\{ \textcircled{A}_{m-1,n} - \textcircled{A}_{mn} \right\} \quad (94)$$

$$\textcircled{A}_{mn} \approx \textcircled{I}_n \textcircled{Y}_m \textcircled{V}_{mn}^2 \rho_{sn}^* \quad (95)$$

$$\frac{d}{dt} \textcircled{V}_{mn} \approx \frac{-1}{\rho_{sn}^* \delta y} \left( \textcircled{P}_{m+1,n} - \textcircled{P}_{mn} \right) \quad (96)$$

and the hydrostatic pressure, Eq. (23). These four equations form a complete linear system.

Apparently, neutral compression-gravity-mode oscillations between adjacent columns had been transformed by the numerical analogue into growing modes. Since it appeared that the disturbance mechanism was essentially linear, the effect of the time-integration procedure was linearly analyzed. (7)

We analyze the effect of approximating

$$\frac{d}{dt} \underset{\sim}{V} = \underset{\sim}{M} \underset{\sim}{V} \quad (97)$$

by

$$\underset{\sim}{V}_{\tau+1} = \underset{\sim}{V}_{\tau-1} + 2 \delta t \underset{\sim}{M} \underset{\sim}{V}_{\tau} \quad (98)$$

The system of Eq. (97) has characteristic solutions (modes)

$$\underset{\sim}{V}(t) = \text{Re: } \underset{\sim}{V} e^{ict} = \text{Re: } \underset{\sim}{V} \left( e^{ic \delta t} \right)^{\tau} \quad (99)$$

Substitution in Eq. (97) yields the system of equations

$$\left[ \underset{\sim}{M} - ic \underset{\sim}{I} \right] \underset{\sim}{V} = 0 \quad (100)$$

where  $\underline{I}$  is the identity matrix. This imposes

$$|\underline{M} - ic\underline{I}| = 0 . \quad (101)$$

This characteristic polynomial has in general as many roots,  $C_j$ , as  $\underline{V}$  has components. Corresponding to each characteristic value,  $C_j$ , the system of equations in Eq. (100) yields a characteristic vector,  $\underline{V}_j$ .

The system of linear equations in Eq. (98) has characteristic solutions

$$\underline{V}_T = \text{Re: } \underline{V} \gamma^T . \quad (102)$$

Substitution in Eq. (98) yields

$$\left[ \underline{M} - \frac{\gamma^2 - 1}{2 \delta t \gamma} \underline{I} \right] \underline{V} = 0 . \quad (103)$$

In comparing Eq. (103) with Eq. (100), we see that they have the same characteristic vectors,  $\underline{V}_j$ , and that corresponding to the characteristic value,  $C_j$ , we have

$$\frac{\gamma_j^2 - 1}{2 \delta t \gamma_j} = i C_j . \quad (104)$$

This quadratic has the two roots

$$\gamma_j = i \delta t C_j \pm \sqrt{1 - (\delta t C_j)^2} . \quad (105)$$

The positive root approximates the proper modes, while the negative root yields extraneous modes admitted by the "leap-frog" method.

Consider a neutral mode with characteristic value  $C_j$  (i.e.,  $C_j$  real) and a time increment such that

$$\delta t C_j > 1 . \quad (106)$$

The proper mode of the "leap-frog" method yields the characteristic value

$$\gamma_j = i \left\{ \delta t C_j + \sqrt{(\delta t C_j)^2 - 1} \right\} \equiv i\mu \quad (107)$$

where  $\mu$  is real and greater than one. Thus, the neutral mode is transformed into an amplifying mode which satisfies

$$\tilde{V}_{j, \tau+2} / \tilde{V}_{j, \tau} = -\mu^2 . \quad (108)$$

This explains the evidenced growth cycle of four time steps.

All neutral modes for which

$$C_j > 1/\delta t \quad (109)$$

are transformed into amplifying modes, and the greater  $C_j$ , the greater is the resulting growth rate. This is what we assumed has happened in our integration.

Equation (108) provides us with a test which we can apply to trial integration number two. For the component  $V = \textcircled{v}_{25,19}$  it turns out that

$$V_9/V_7 = -3.328$$

$$V_{10}/V_8 = -3.329$$

$$V_{11}/V_9 = -3.493$$

$$V_{12}/V_{10} = -3.488$$

$$V_{13}/V_{11} = -3.512$$

$$V_{14}/V_{12} = -3.504$$

$$V_{15}/V_{13} = -3.482$$

$$V_{16}/V_{14} = -3.226$$

The component  $V = \textcircled{v}_{25,15}$  was also tried:

$$V_{15}/V_{13} = -3.626$$

$$V_{16}/V_{14} = -3.616$$

These ratios are remarkably steady.

Since the oscillations occur between adjacent whole columns, and we have 49 columns, there must be a whole family of modes with oscillation periods spread over a narrow range. This spread should arise because of the  $m$ -dependency of the module constants. The ratios above may reflect mode predominance because of the manner in which the motion was initially excited.

As a reasonable upper limit on the ratios we select

$$\mu^2 = 4$$

This yields

$$\delta t C_j = 1.25$$

and

$$C_j \approx 0.21 \text{ radian per minute} \quad (110)$$



This corresponds to the period of oscillation

$$\frac{2\pi}{C_j} \approx 1810 \text{ seconds} \quad (111)$$

Another method of approximately determining this characteristic period is by the following somewhat crude analysis of a simplified model. Consider the compression-gravity oscillation between two adjacent volume modules. Equations (94), (95), (96), and (23) yield:

$$\frac{d}{dt} (\rho)_2 = -\frac{d}{dt} (\rho)_1 = [6]_n [7]_n (A)$$

$$(A) = [1]_n [9]_m^2 \rho_{sn} (v)$$

$$\frac{d}{dt} (v) = -\left| (p)_2 - (p)_1 \right| / \rho_{sn} \delta y$$

$$(p)_1 = g [1]_n \frac{1}{2} (\rho)_1$$

$$(p)_2 = g [1]_n \frac{1}{2} (\rho)_2$$

From these equations we derive

$$\frac{d^2}{dt^2} (v) = -k^2 (v)$$

where

$$k^2 = \frac{2g}{\delta y} [1]_n^2 [6]_n [7]_m [9]_m$$

$$k \approx \sqrt{g \delta z} / \delta y \quad (112)$$

This further shows that the spread in periods which this family of modes has in our model due to  $n$ -dependency is probably rather slight. As an upper-bound estimate we put  $\delta z = 25$  km . This yields

$$k \approx 0.15 \text{ radian per minute}$$

which is somewhat lower than our over-all estimated upper bound, Eq. (110).

The preceding analysis implies that this form of computational instability should be eliminated by choosing a time increment

$$\delta t < 1/C_{\text{max}} .$$

We have estimated  $C_{\text{max}}$  at 0.21 radian per minute. Thus, the upper limit on  $\delta t$  is

$$\approx 4.8 \text{ minutes} .$$

In all subsequent integrations we use

$$\delta t = 3 \text{ minutes} .$$

This means that, as programmed for the Burroughs 220, the integration progresses at about real time.

At this point in the experiments the computer program was specified to tabulate a set of outputs at intervals of 20 time steps. Such a set of outputs consists of complete tabulations of each of the six fields,  $P$  ,  $T$  ,  $w$  ,  $\rho$  ,  $\omega$  , and  $v$  . The purpose in having two successive values in time is to inspect for stability and smoothness of the evolution, in particular, to determine the growth of extraneous behavior admitted by the "leap-frog" method. The availability of the fields in high-speed memory favored the output:

Fields  $P, T, w$ , for  $\tau = 1, 2; 21, 22; 41, 42$ ; etc.

Fields  $\rho, \omega, v$ , for  $\tau = 2, 3; 22, 23; 42, 43$ ; etc. (113)

Thus, we have all six fields for  $\tau = 2, 22, 42, 62$ , etc. In addition, the sum checks for mass and absolute angular momentum were tabulated for every time step.

It should also be mentioned that the computations are carried out in "floating point" arithmetic with approximately eight decimal digits carried throughout.

## V RESULTS, ONE COLUMN OF HEATING

A Standard Atmosphere at relative rest is disturbed by the steady heating field prescribed by Eqs. (93). This heating is limited to the region between two latitudes (Column 25 in the representative meridional plane) at mid-latitude. The equivalent temperature rate, Eq. (85), of the heating is uniform ( $10^{\circ}\text{C}/24$  hours) at all levels in the region. The heating is commenced in steps, as discussed in earlier sections.

Following the trial runs that were analyzed in Sec. IV, the experiment was repeated using the time increment of 3 minutes. The integration was carried out to  $\tau = 23$  (approximately two periods of the shortest mode in our model). No computational instability was discernible.

Although this experiment was designed primarily as a test of the model, the results appear to be sufficiently interesting for inclusion in this report. The circulation established at  $\tau = 22$  is shown in Figs. 4 to 10. These figures show that section of the representative meridional plane over which the disturbance has spread appreciably. The vertical height scale is linear in terms of Standard Pressure, except for the upper two module layers where this scale is magnified by a factor of ten (see Fig. 3). Because of this change in scale, the isoline analyses are not carried to these upper layers. The equator is at  $y_0$  and the pole at  $y_{49}$ .

Attention is drawn to the fact that Figs. 5, 6, 8, and 9 show anomaly, or change from the initial values. This is indicated by the subscript "a." In the case of Fig. 8,

$$\omega_a \equiv \omega - \Omega = u/a \cos \phi . \quad (114)$$

These figures speak well enough for themselves. Of particular interest is the somewhat surprising phenomenon of local cooling in the one column which is receiving thermal energy. This is due to the

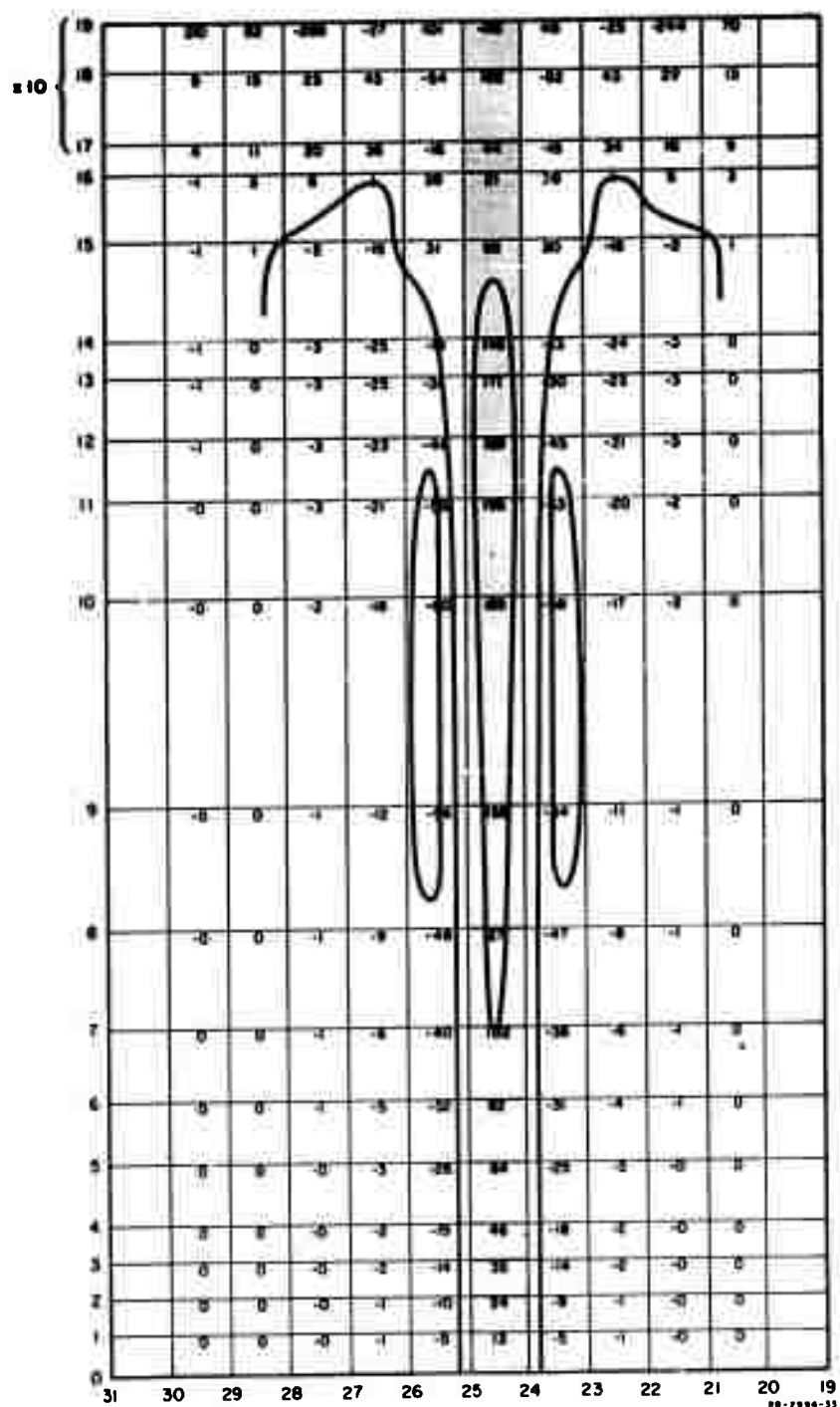


FIG. 4 ONE-COLUMN HEATING,  $w$  at  $\tau = 22$   
Units:  $10^{-2} \text{ cm sec}^{-1}$

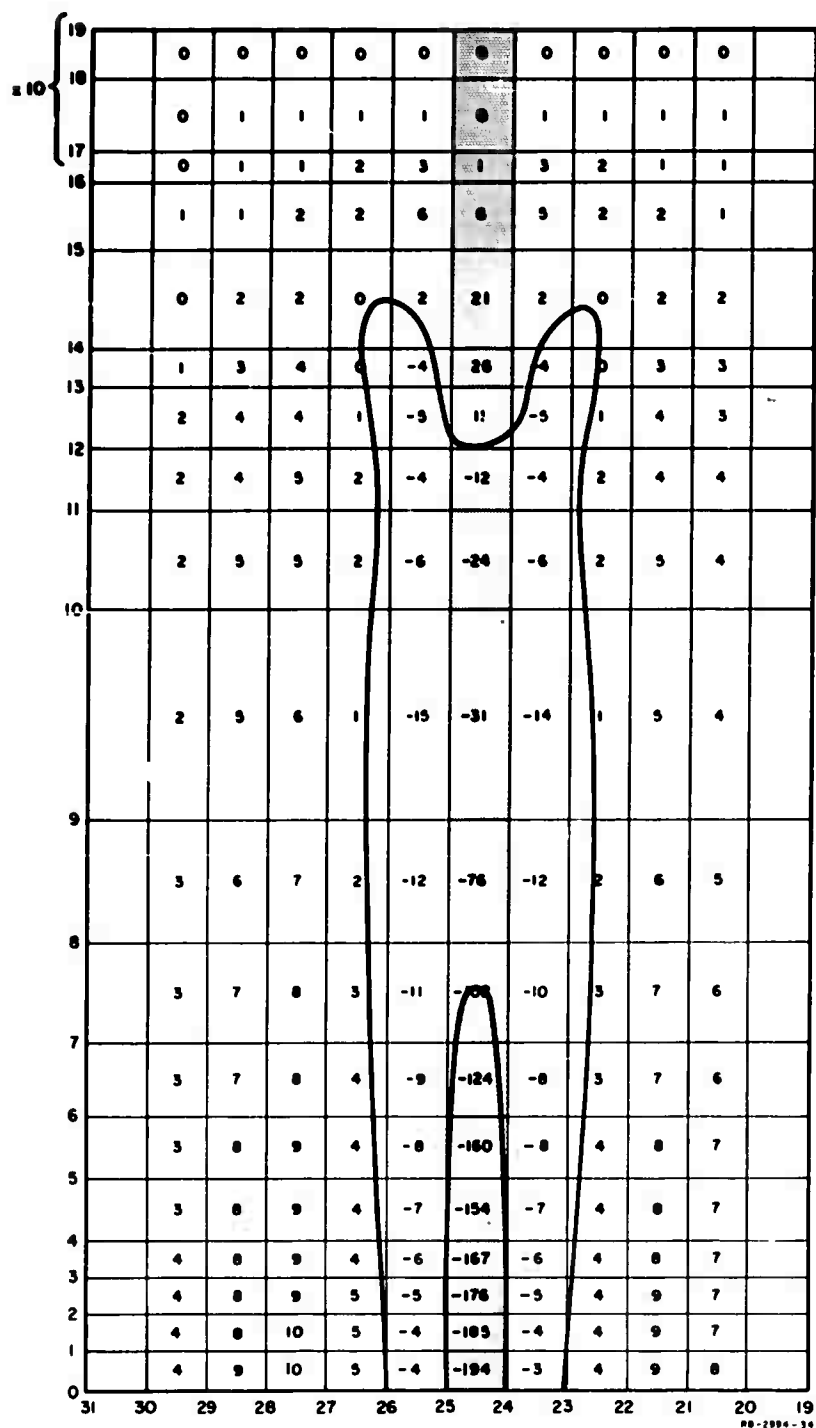


FIG. 5 ONE-COLUMN HEATING,  $\rho_a$  at  $\tau = 22$   
Units:  $10^{-8}$  tons  $m^{-3}$

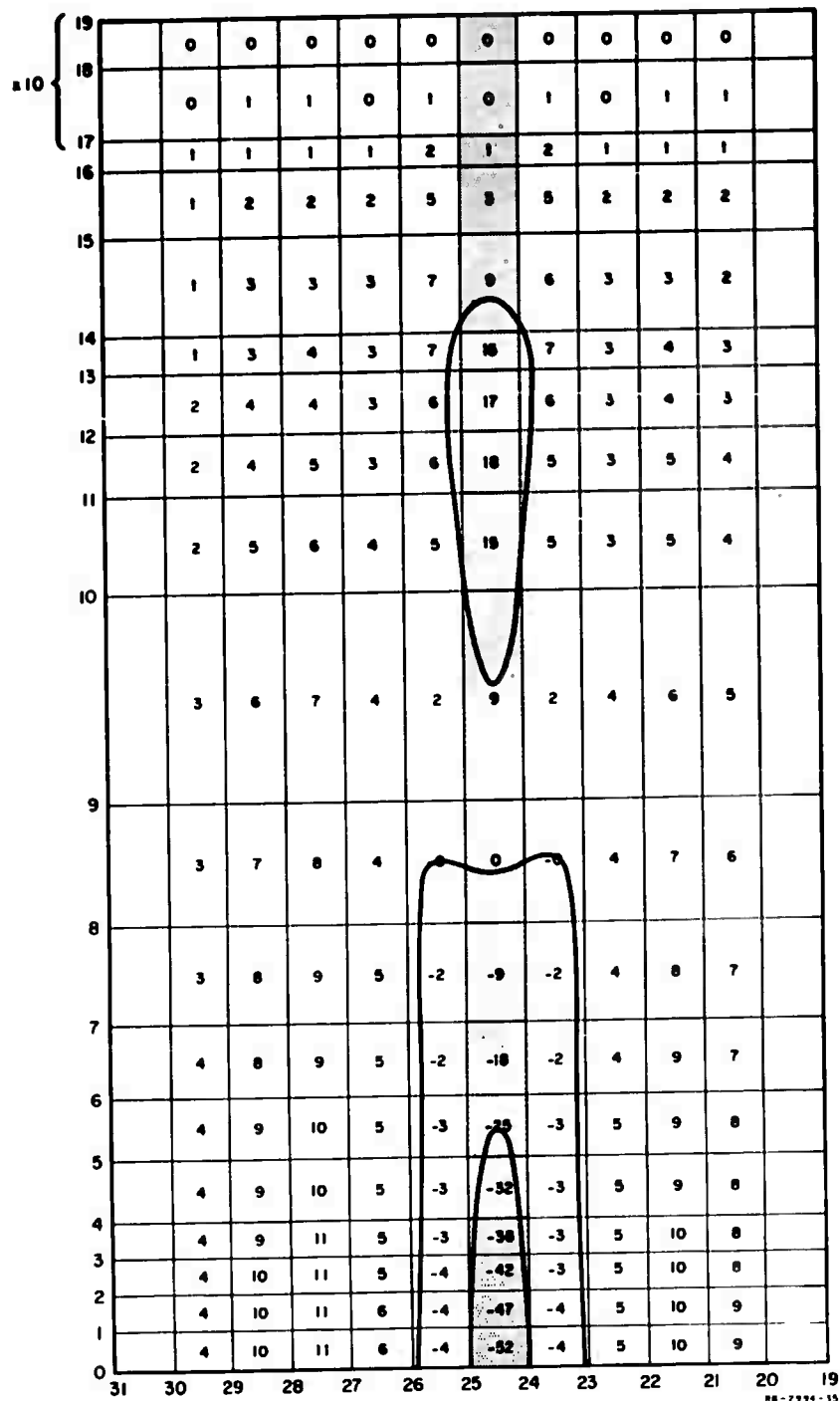
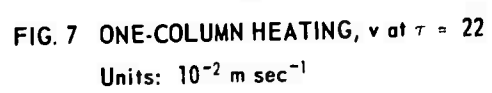


FIG. 6 ONE-COLUMN HEATING,  $p_0$  at  $\tau = 22$   
Units:  $10^{-2}$  mb





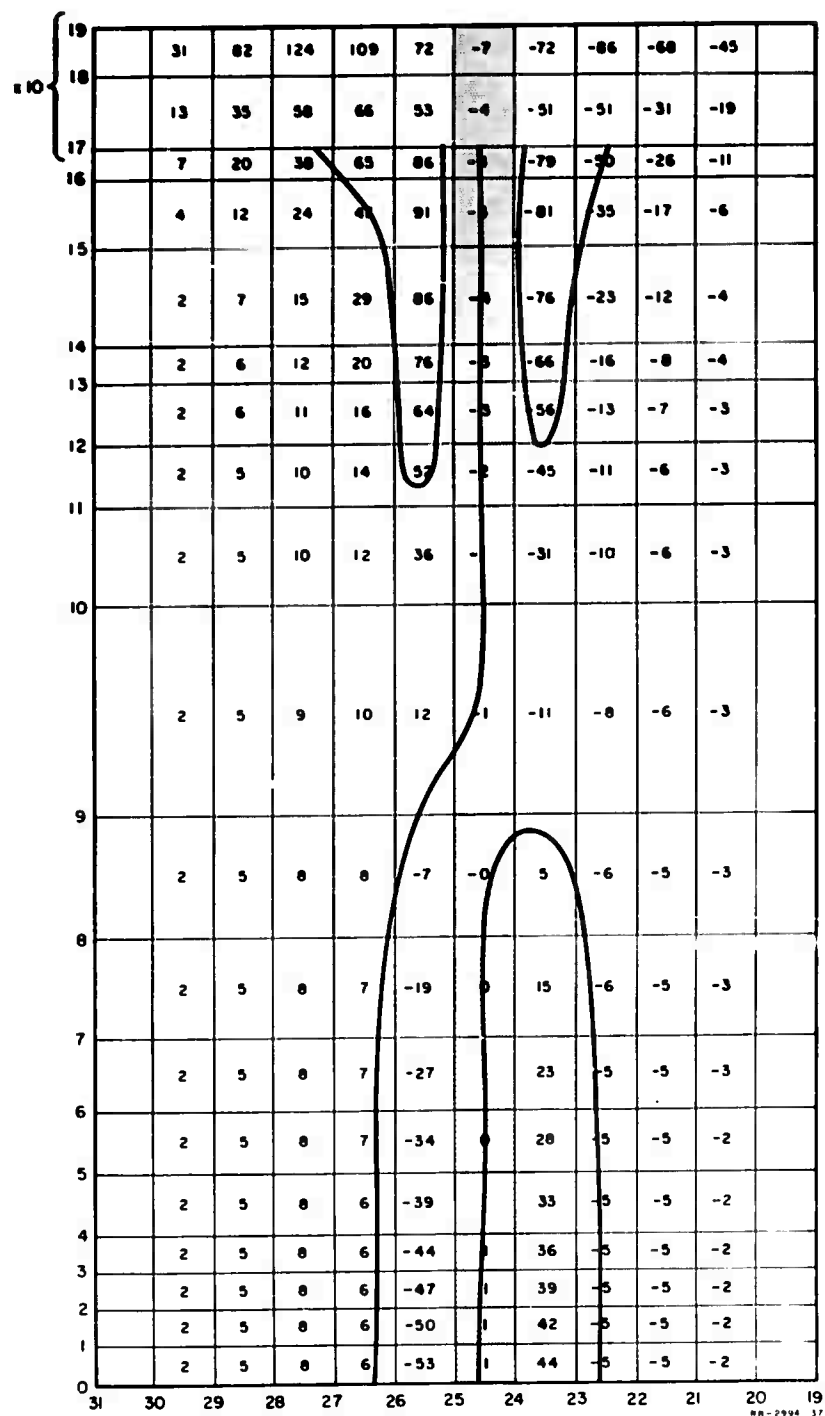


FIG. 8 ONE-COLUMN HEATING,  $\omega_0$  at  $\tau = 22$   
Units:  $10^{-10}$  radians  $\text{sec}^{-1}$

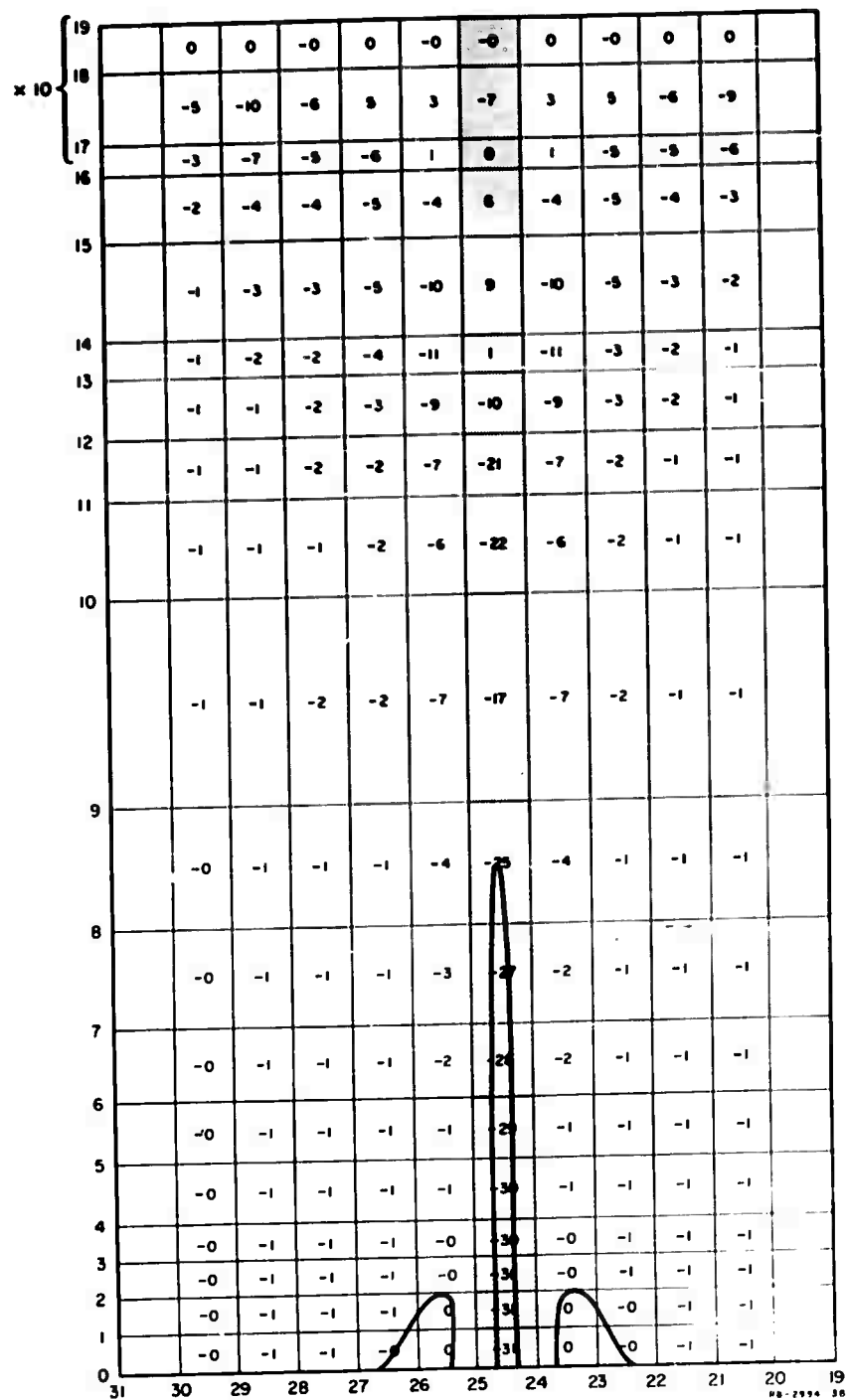


FIG. 9 ONE-COLUMN HEATING,  $T_0$  at  $\tau = 22$   
Units:  $10^{-2} \text{ } ^\circ\text{C}$

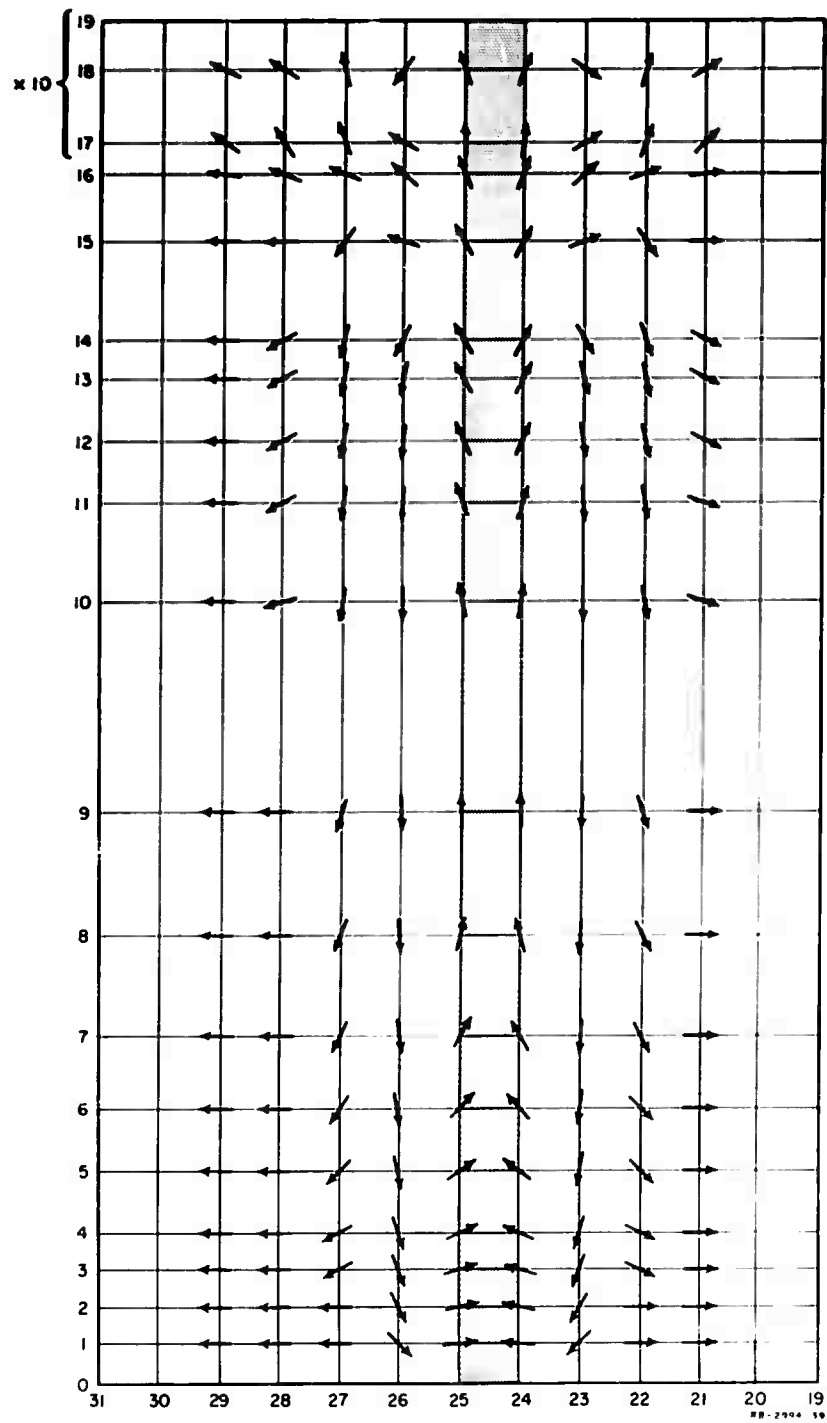


FIG. 10 ONE-COLUMN HEATING, STREAMLINE SCHEMATIC AT  $\tau = 22$

established circulation which brings mass into the column below and out of the column above. The associated ascent and adiabatic cooling apparently is sufficient to overcome the heating, in local influence.

Figure 10 is a streamline schematic. The vectors show the streamline slope, with an exaggeration of 100 in the  $W$  to  $V$  ratio.

## VI RESULTS, HEMISPHERE WINTER HEATING

For our major experiment, a heating rate, designed to approximate mean winter conditions, was used as the forcing field.

For the net radiative contribution of the heating we used the distribution of Coulson<sup>(1)</sup>. To this was added an estimate of the contribution of latent and sensible heat carried into the atmosphere from the surface layer, Fig. 11. For the latter, an equivalent temperature rate was calculated on the basis that this energy goes into uniform heating of Coulson's<sup>(1)</sup> model of the troposphere at each latitude. The total heating field in terms of equivalent temperature rate,  $\dot{T}_E$ , is given in Fig. 12. This distribution was used as the forcing field.

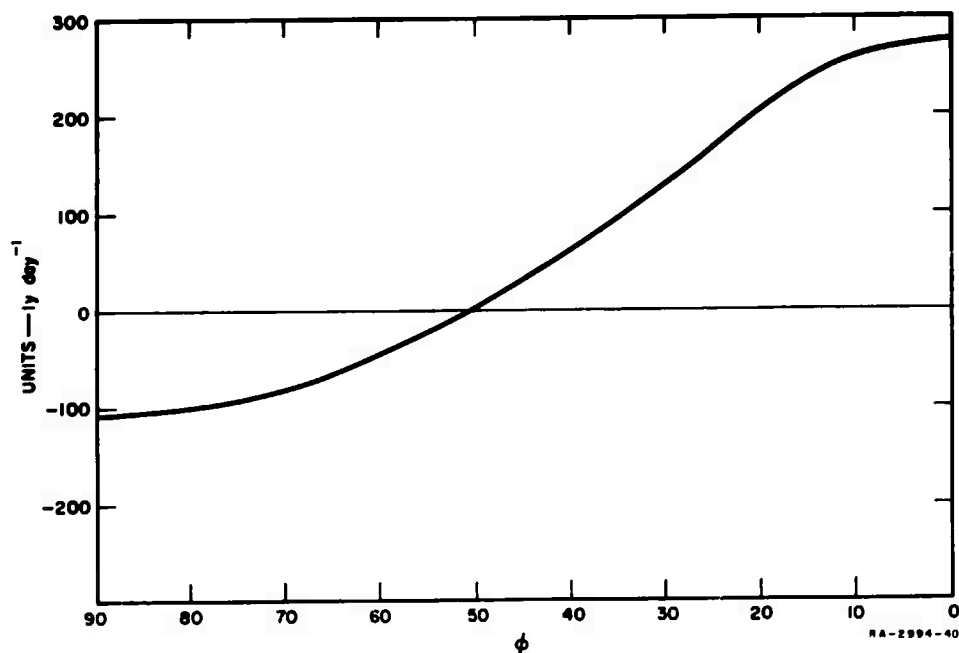
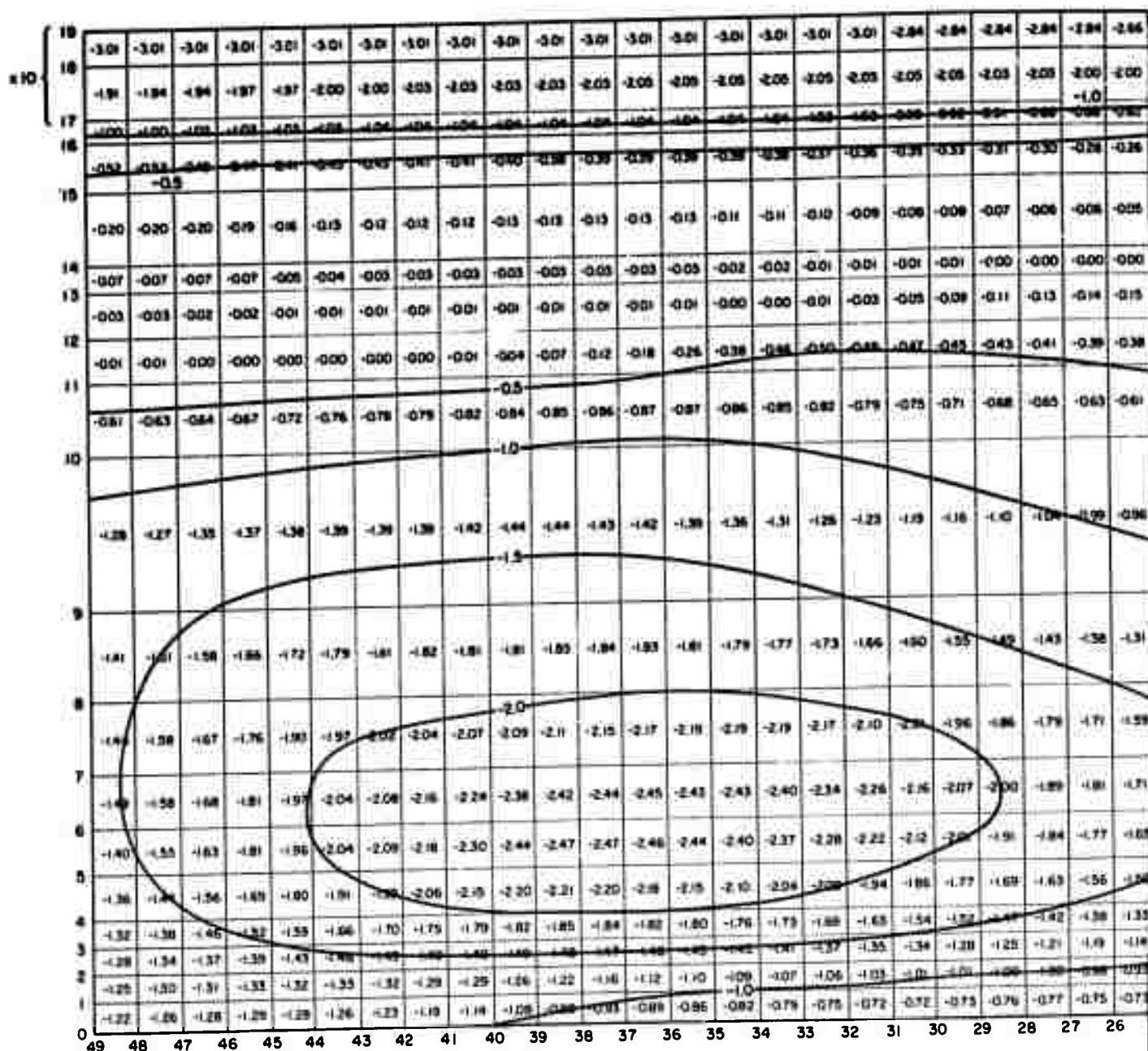


FIG. 11 ESTIMATE OF LATENT AND SENSIBLE ENERGY RELEASE



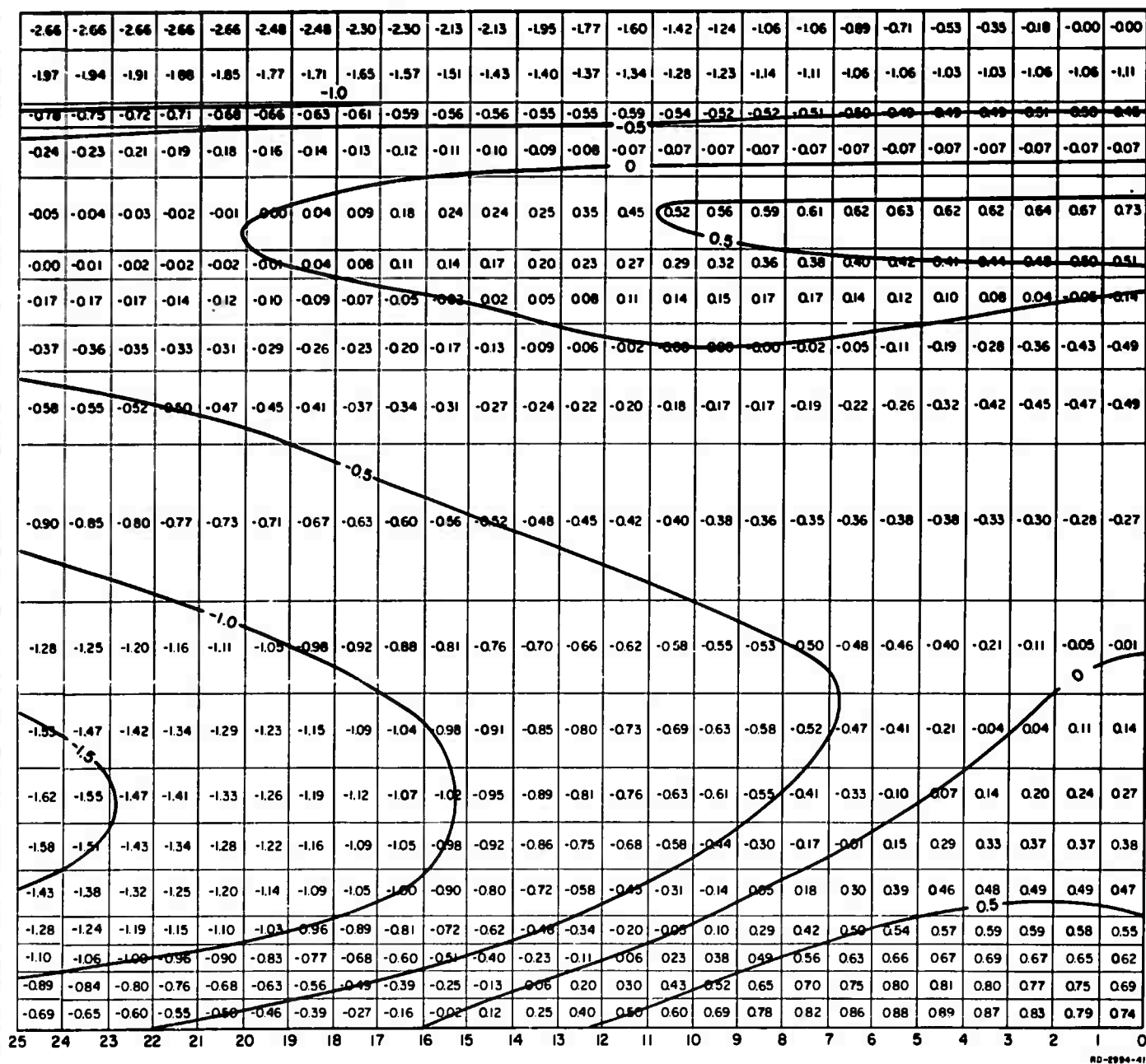


FIG. 12 APPROXIMATION OF MEAN WINTER HEATING

This approximation of mean winter heating was introduced in steps to disturb a Standard Atmosphere at relative rest. A time increment of 3 minutes was used. The integration was carried to  $\tau = 183$ . The output was as specified by Eq. (113).

The resulting evolution was smooth, as shown by selected  $v$  components given in Table I and graphed in Fig. 13. Careful analysis of successive values in Table I shows that very little extraneous behavior has been admitted by the "leap-frog" method.

Figures 14 to 19 show the distributions of  $w$ ,  $\rho_a$ ,  $p_a$ ,  $v$ ,  $\omega_a$  and  $T_a$  respectively, at time step  $\tau = 22$  (approximately Hour 1). The subscript "a" indicates anomaly, or change from the initial values.

The remaining figures, Figs. 20 to 27, refer to  $\tau = 182$  (approximately Hour 9). Figure 25 is obtained from Fig. 24 according to Eq. (114)

$$u = a \cos \phi \ \omega_a \quad (115)$$

Figure 27 is a streamline schematic. The vectors show the streamline slope, with an exaggeration of 100 in the  $w$  to  $v$  ratio.

The evolution is quite amenable to physical reasoning. The atmosphere shrinks by cooling, which is stronger northward. This shrinking results in a northward pressure gradient and northward motion at higher levels. As this flow progresses, carrying mass northward, a southward pressure gradient and southward motion develop at lower levels. A major single cell meridional motion develops with minor superimposed cells. By Hour 9, a core of westerly current has developed at about  $50^\circ$  North and a height of about 10 km.

The sum checks for mass and absolute angular momentum remain steady except for minor round-off which appears to be quite random.

As shown by Fig. 13, the evolution is in a stage of continuing development at Hour 9. The main cell seems to be shifting and



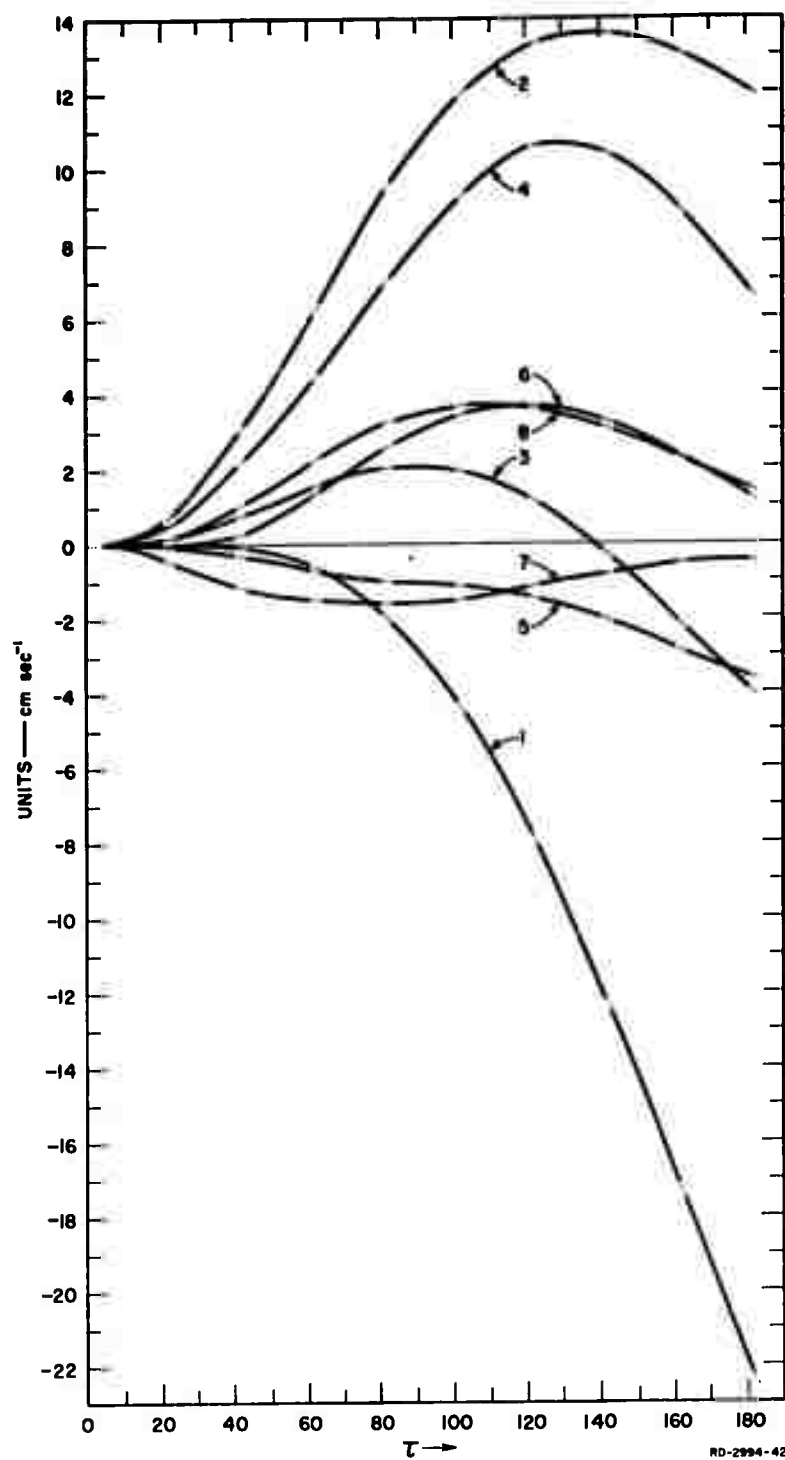
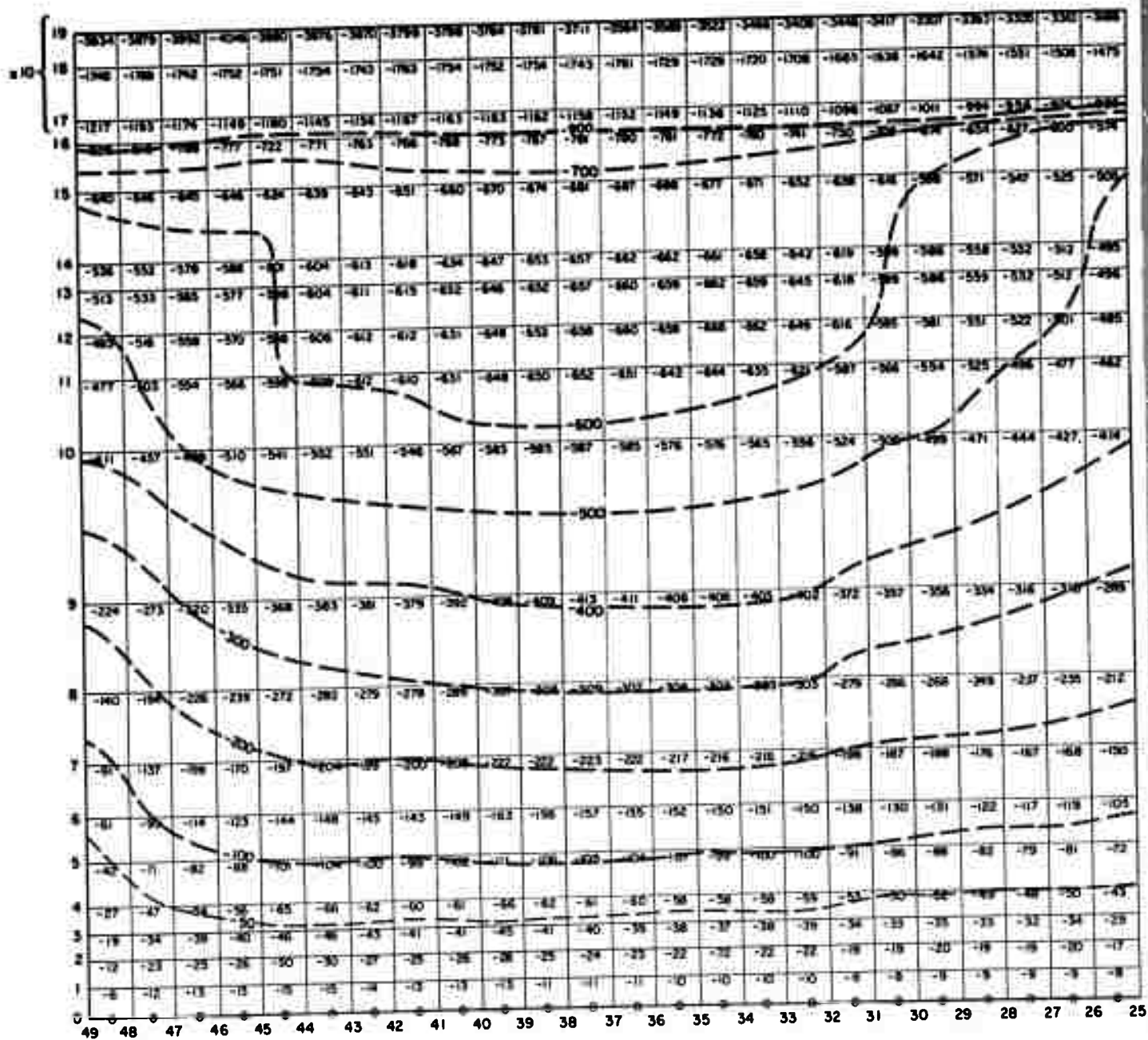


FIG. 13 WINTER HEATING, THE EVOLUTION  
OF SELECTED  $\nu$  COMPONENTS



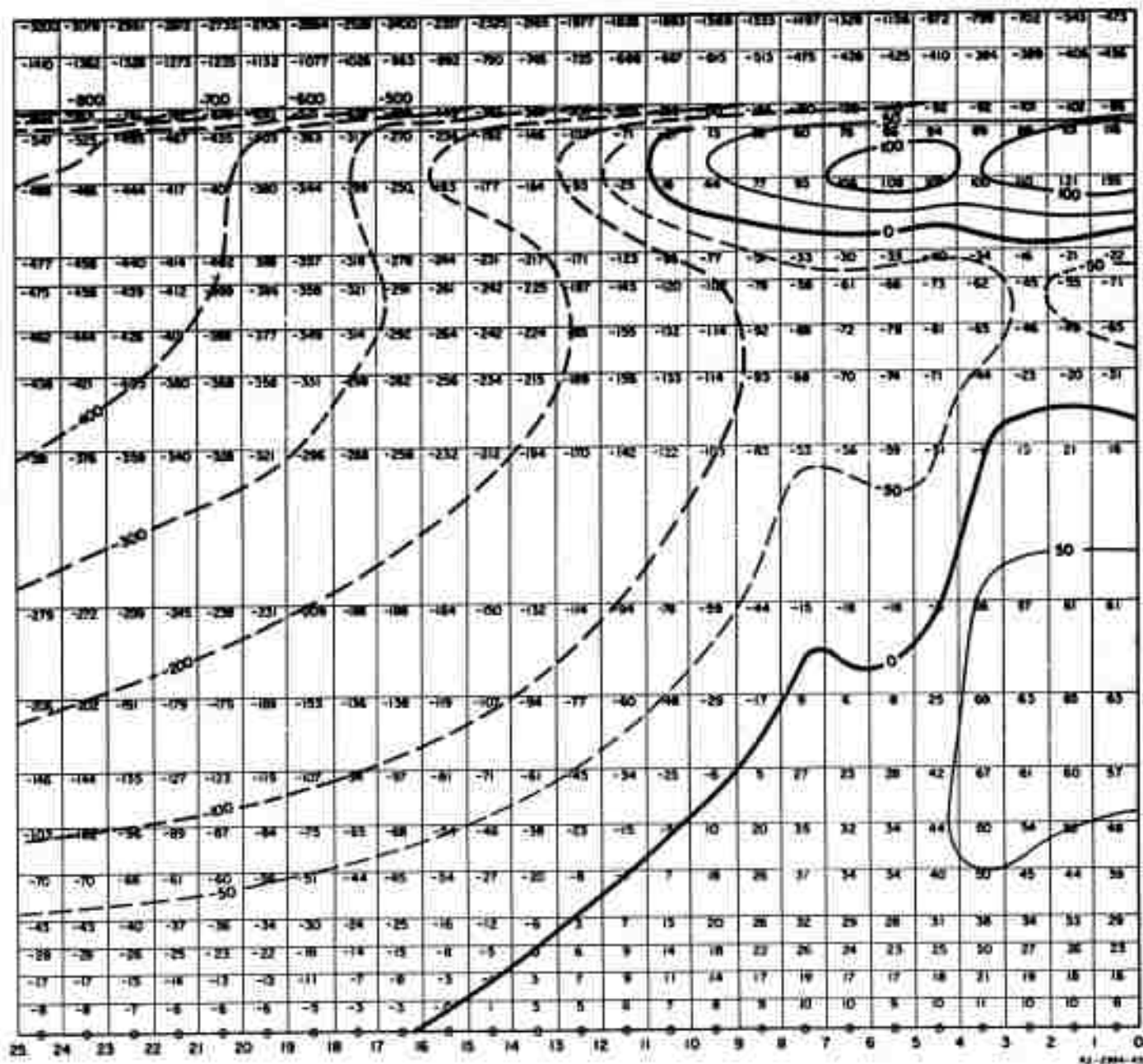
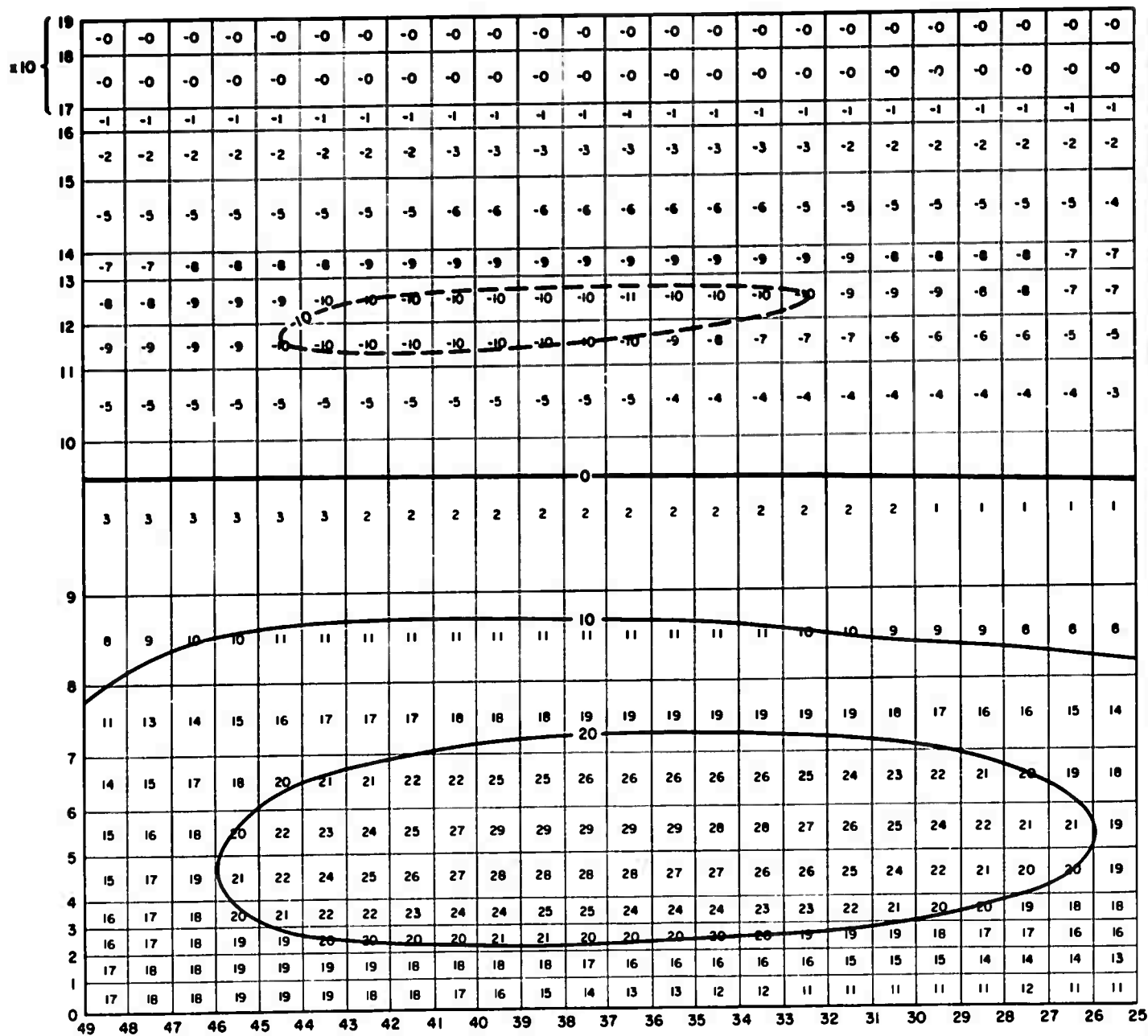


FIG. 14 WINTER HEATING, w at  $\tau = 22$  (~1 hour)  
Units:  $10^{-4} \text{ cm sec}^{-1}$



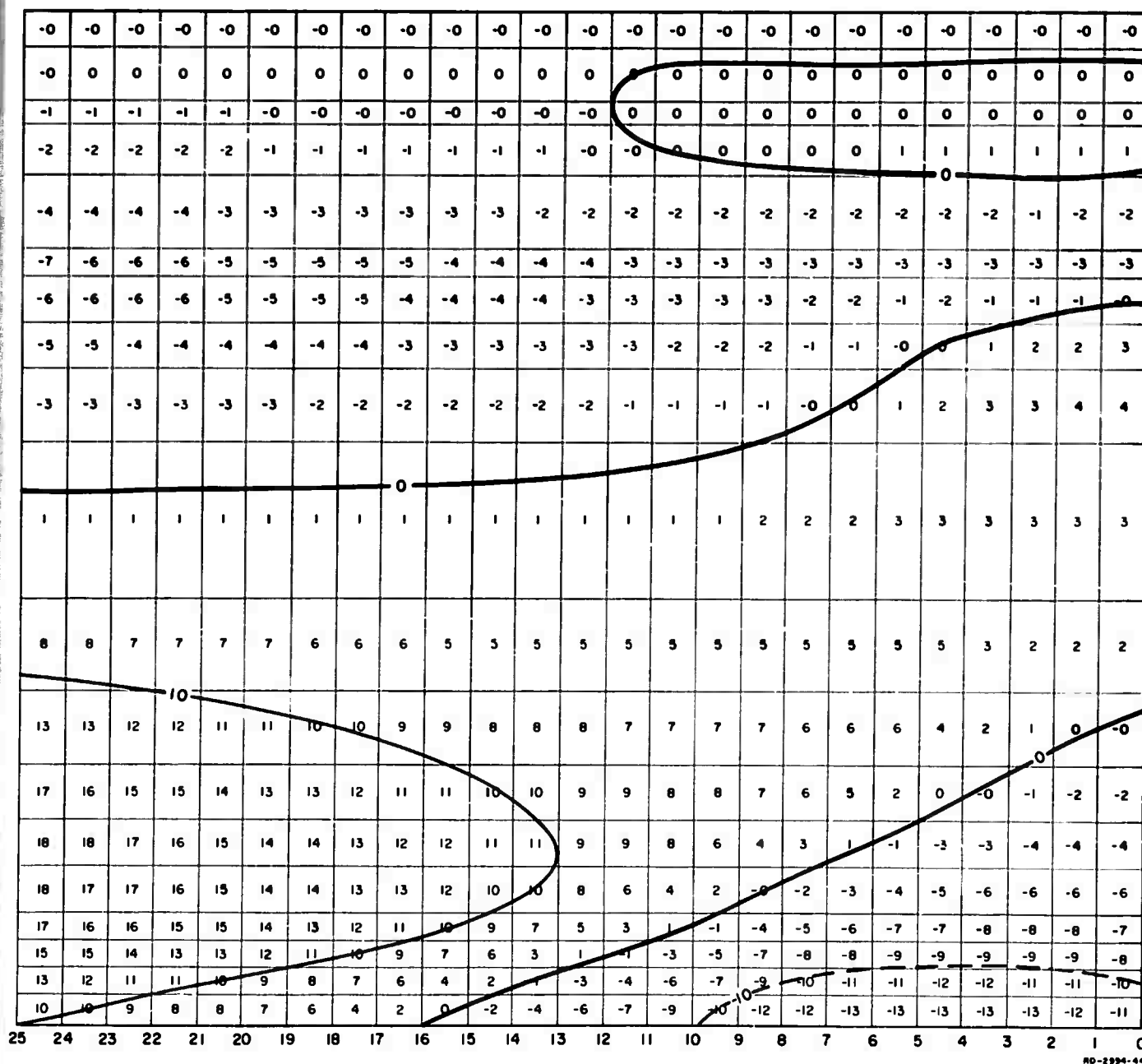
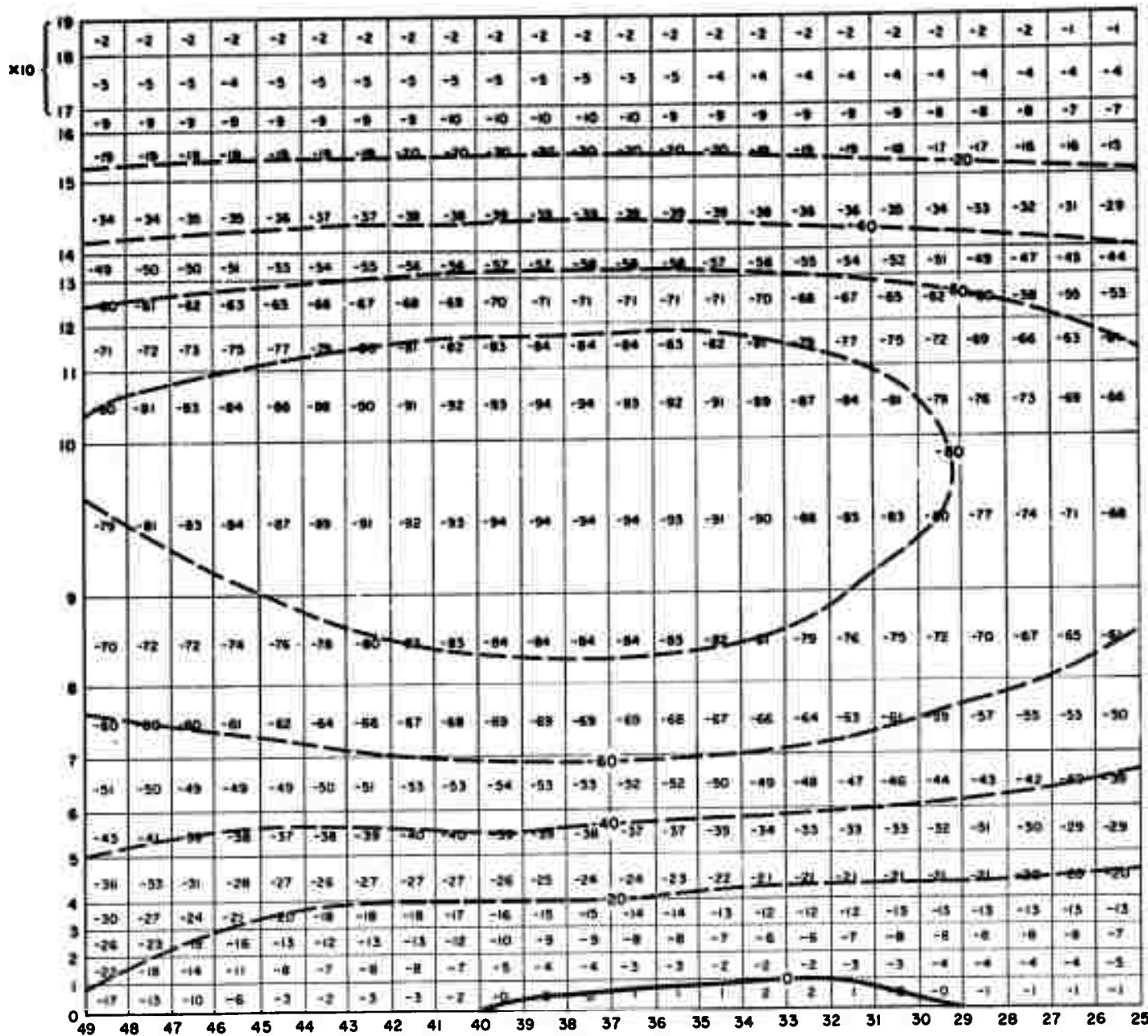


FIG. 15 WINTER HEATING,  $\rho_a$  at  $\tau = 22$  (~1 hour)  
Units:  $10^{-8}$  tons  $m^{-3}$



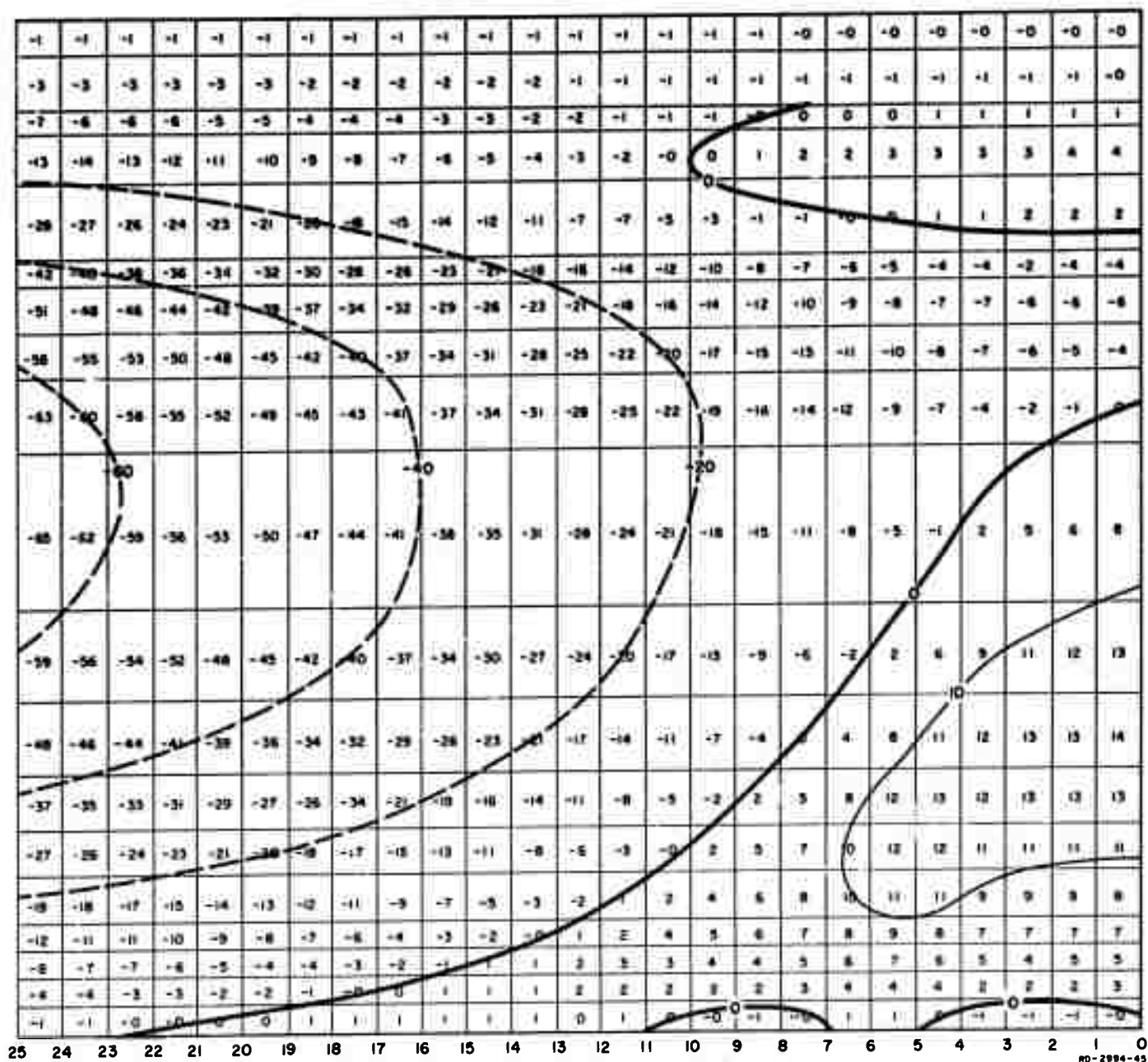
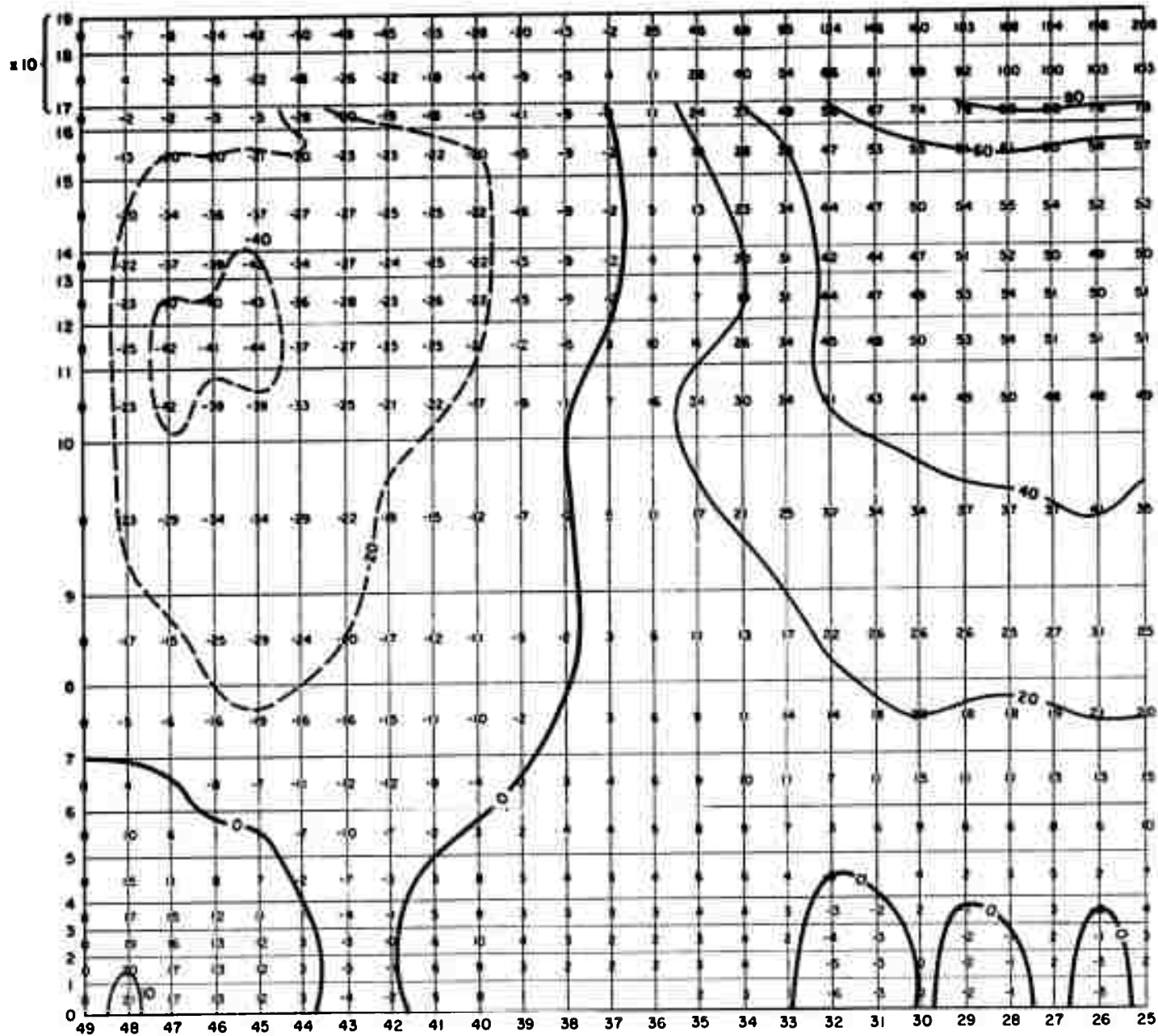


FIG. 16 WINTER HEATING,  $p_0$  at  $\tau = 22$  (~1 hour)  
Units:  $10^{-3}$  mb







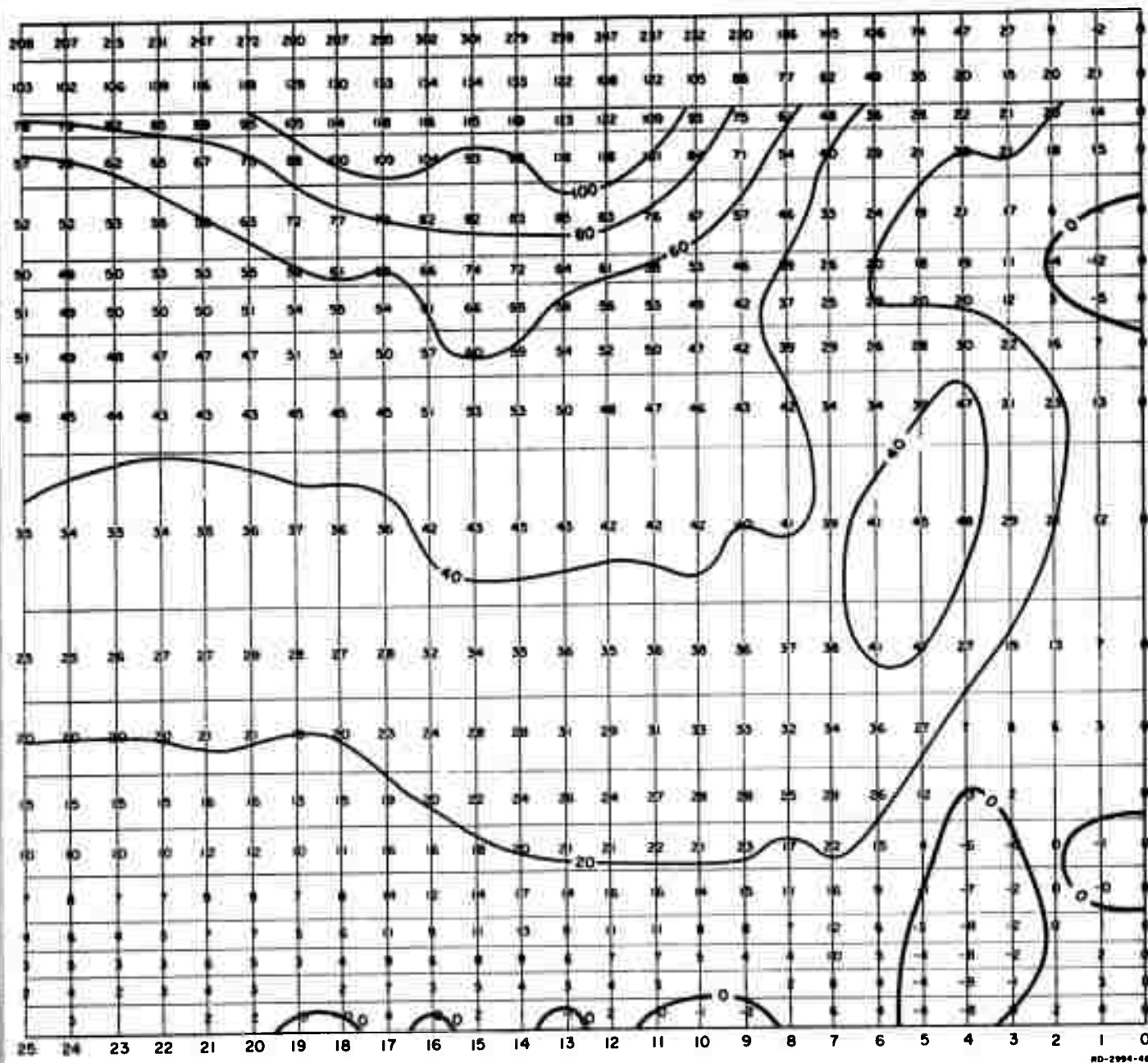
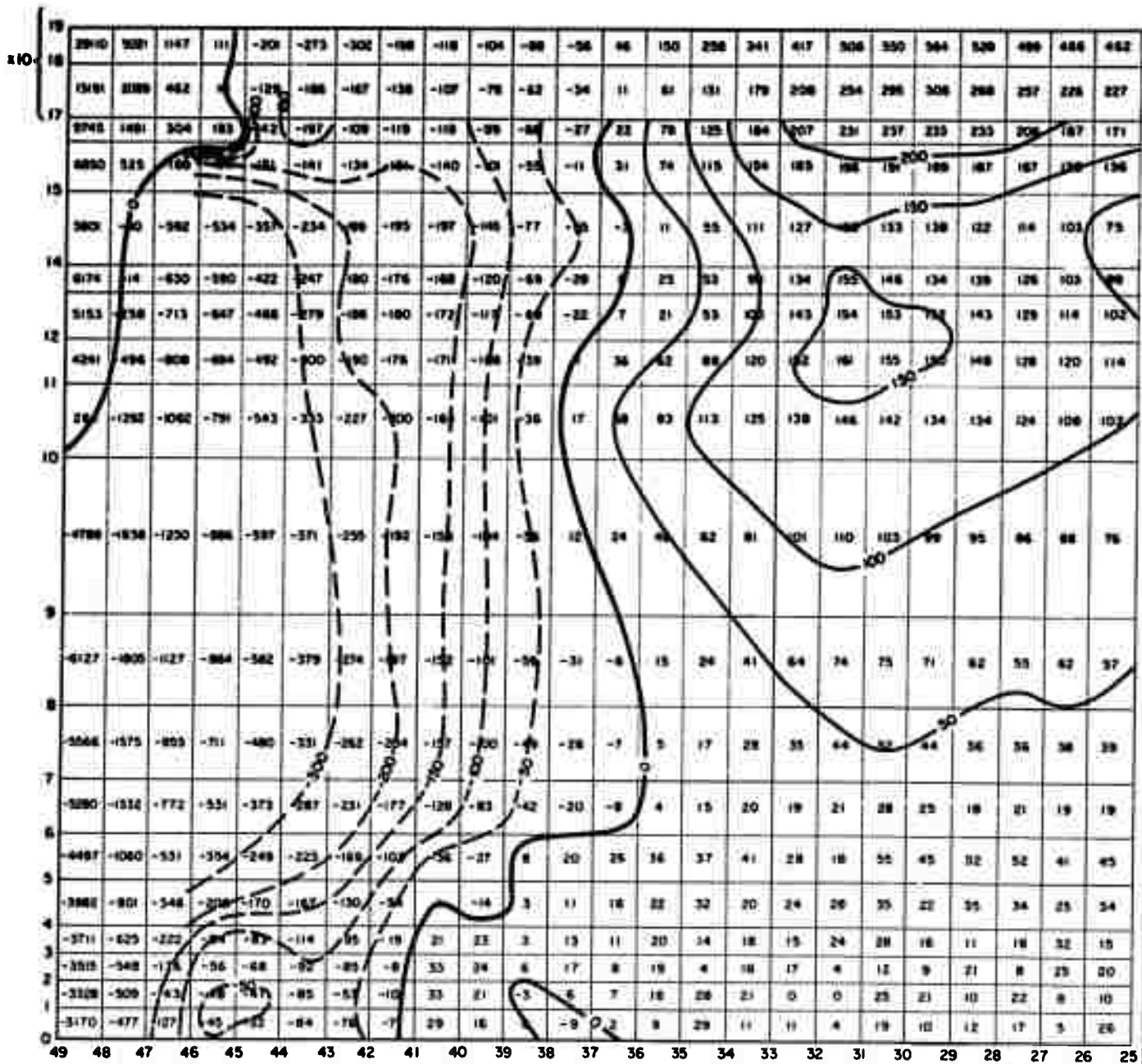


FIG. 17 WINTER HEATING,  $v$  at  $\tau = 22$  (~1 hour)  
Units:  $10^{-2} \text{ cm sec}^{-1}$



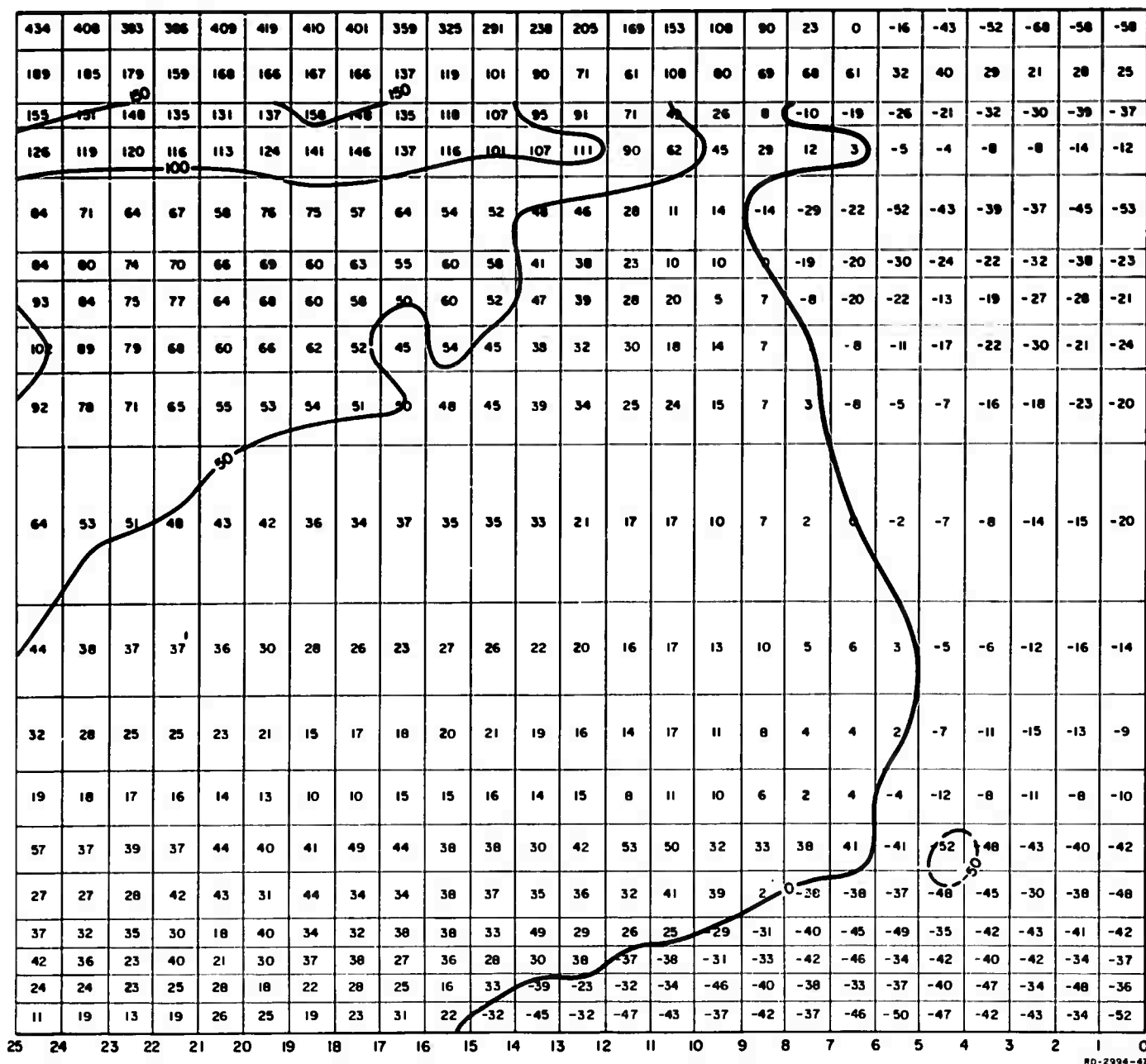
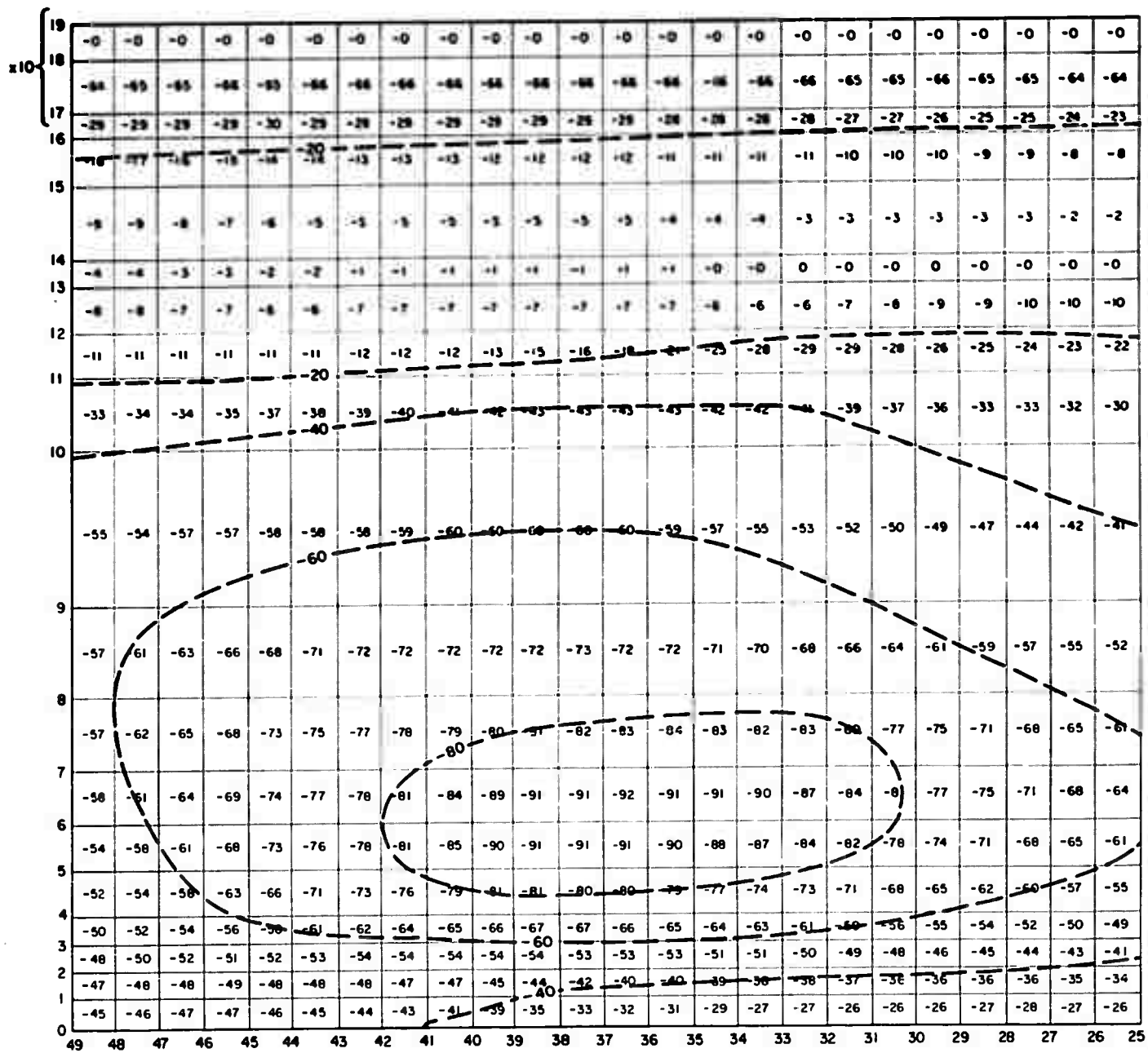


FIG. 18 WINTER HEATING,  $\omega_0$  at  $\tau = 22$  (~1 hour)  
Units:  $10^{-12}$  rodions  $\text{sec}^{-1}$



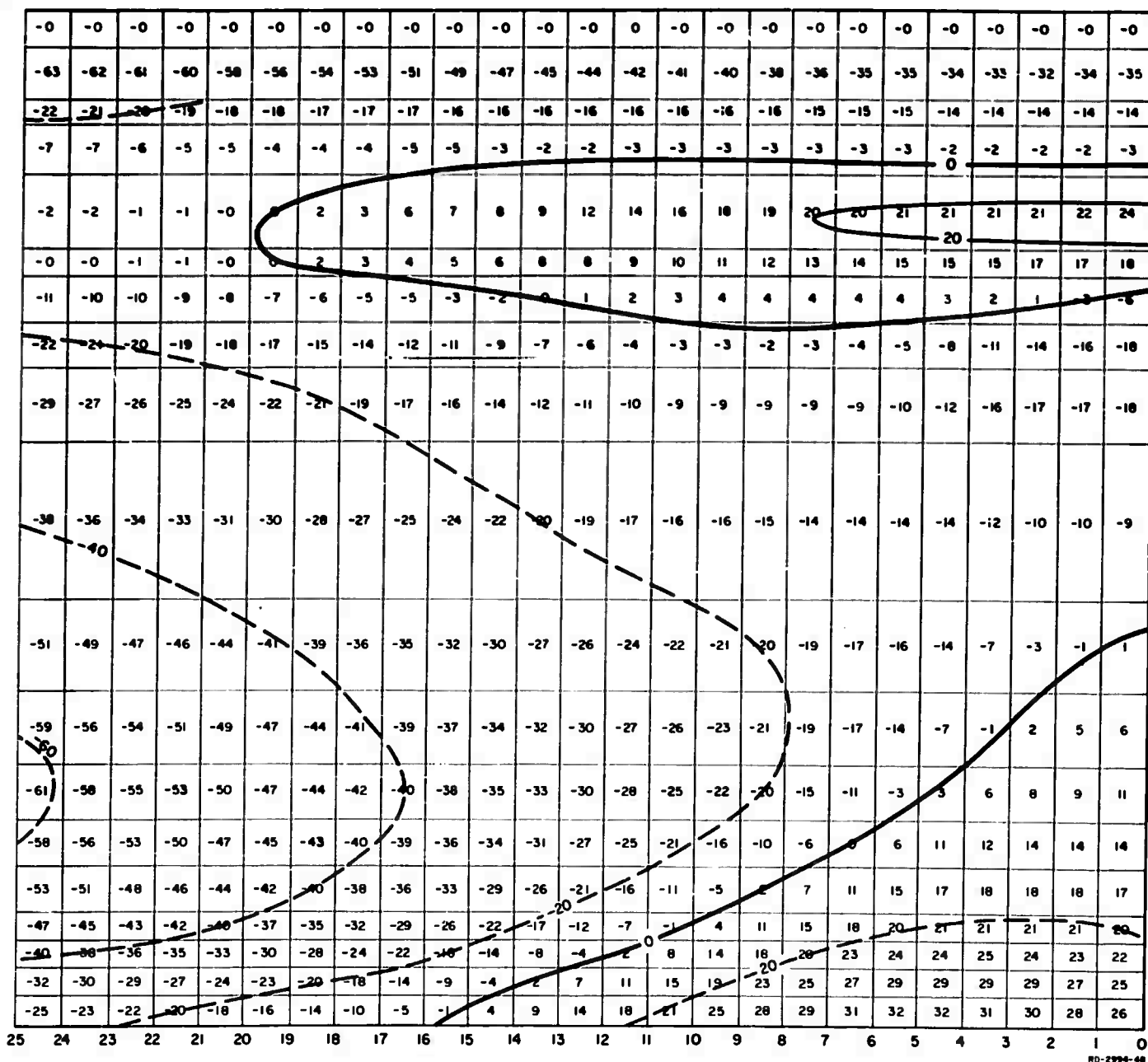
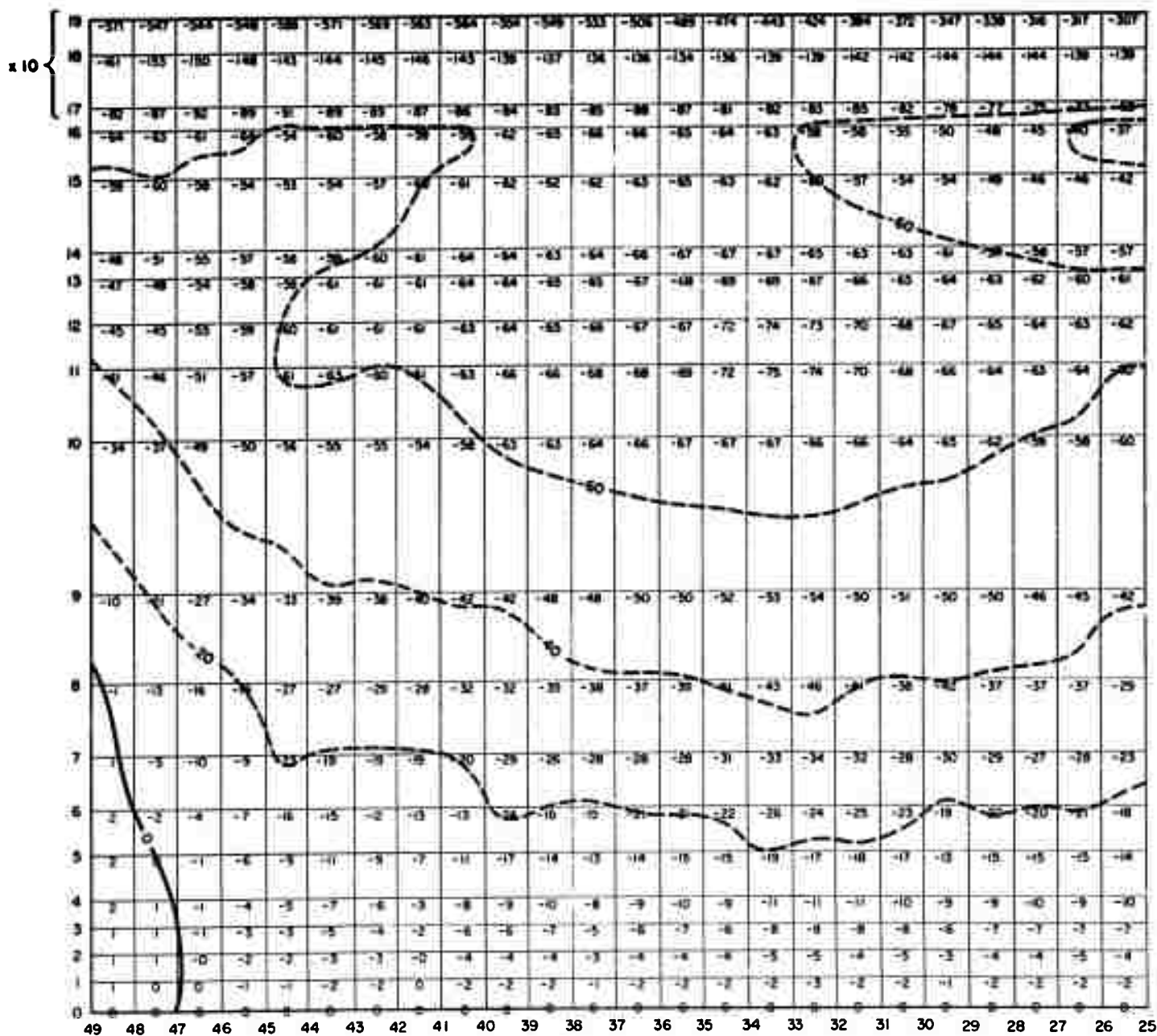


FIG. 19 WINTER HEATING,  $T_0$  at  $\tau = 22$  (~1 hour)  
Units:  $10^{-3} \text{ } ^\circ\text{C}$



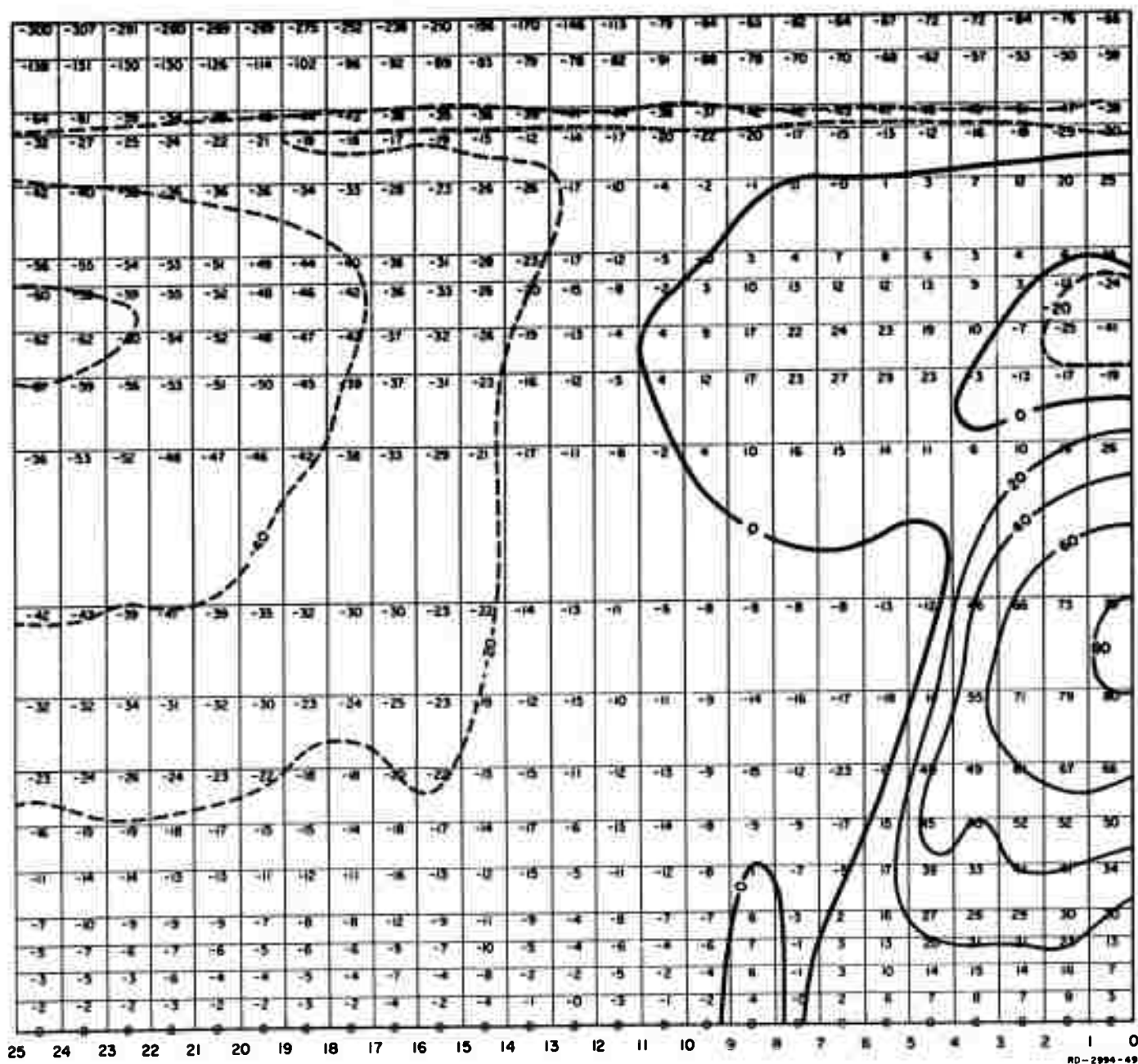


FIG. 20 WINTER HEATING,  $w$  at  $\tau = 182$  (~9 hours)  
Units:  $10^{-3} \text{ cm sec}^{-1}$







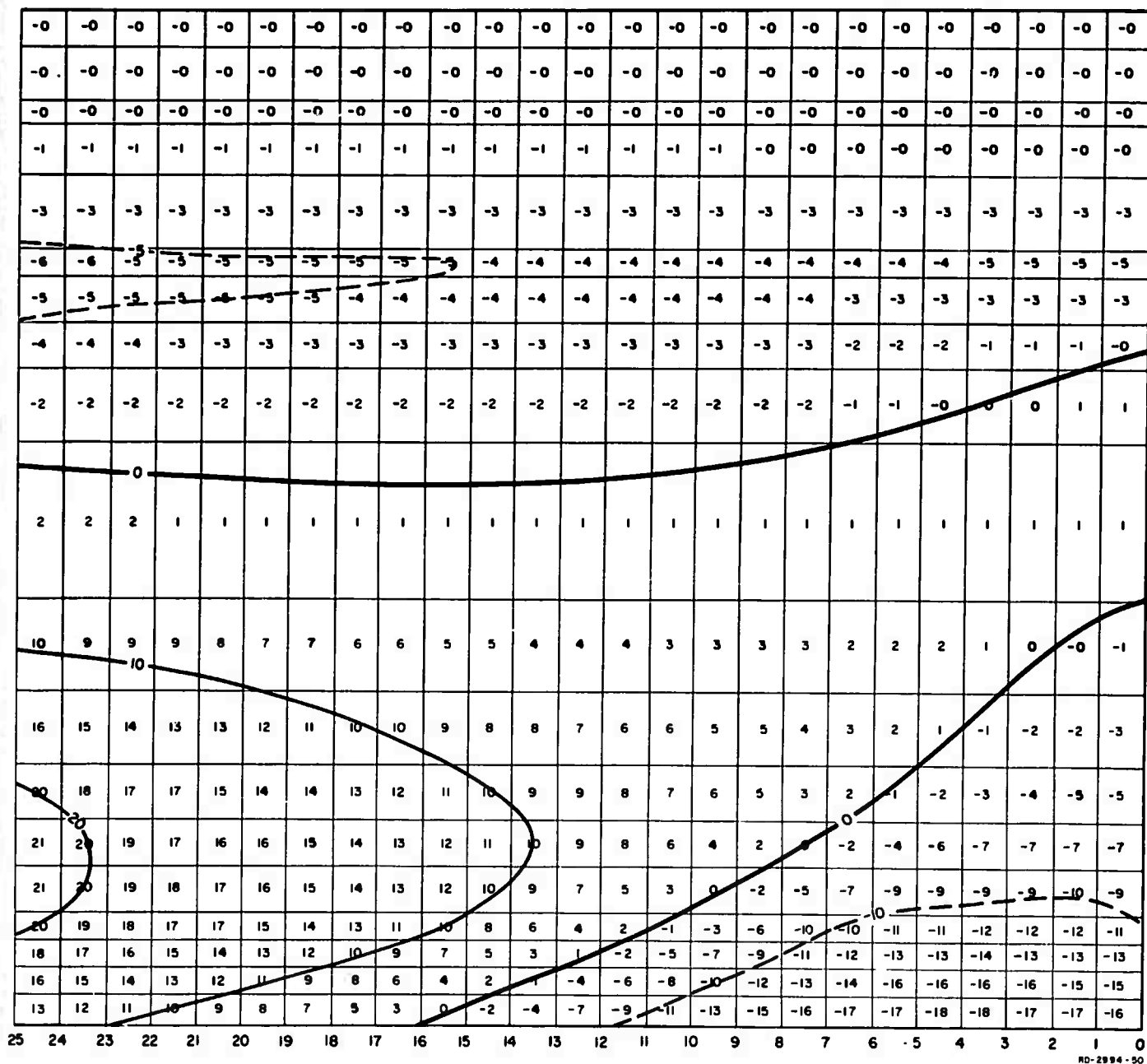
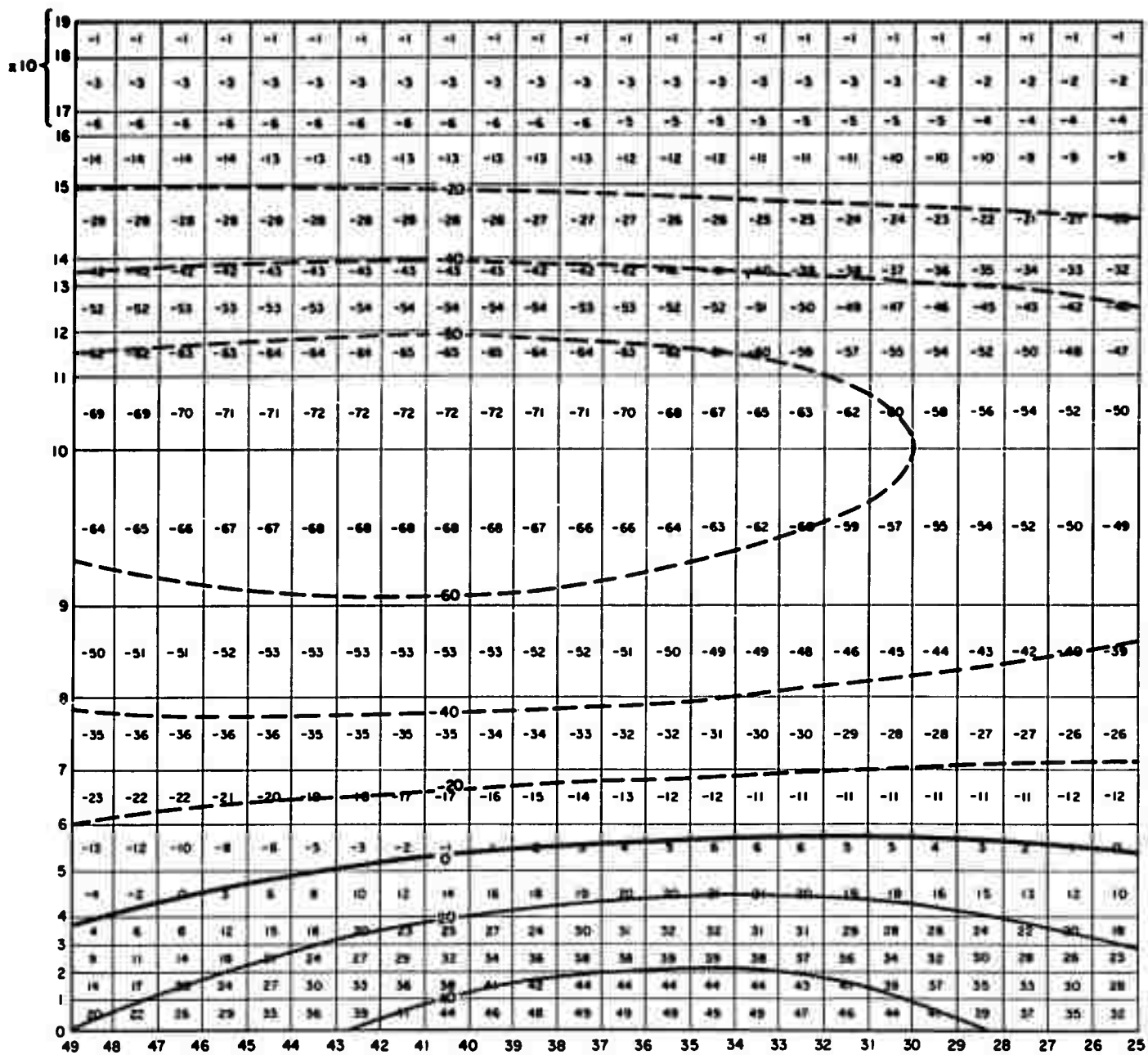


FIG. 21 WINTER HEATING,  $\rho_0$  at  $\tau = 182$  (~9 hours)  
Units:  $10^{-7}$  tons  $m^{-3}$



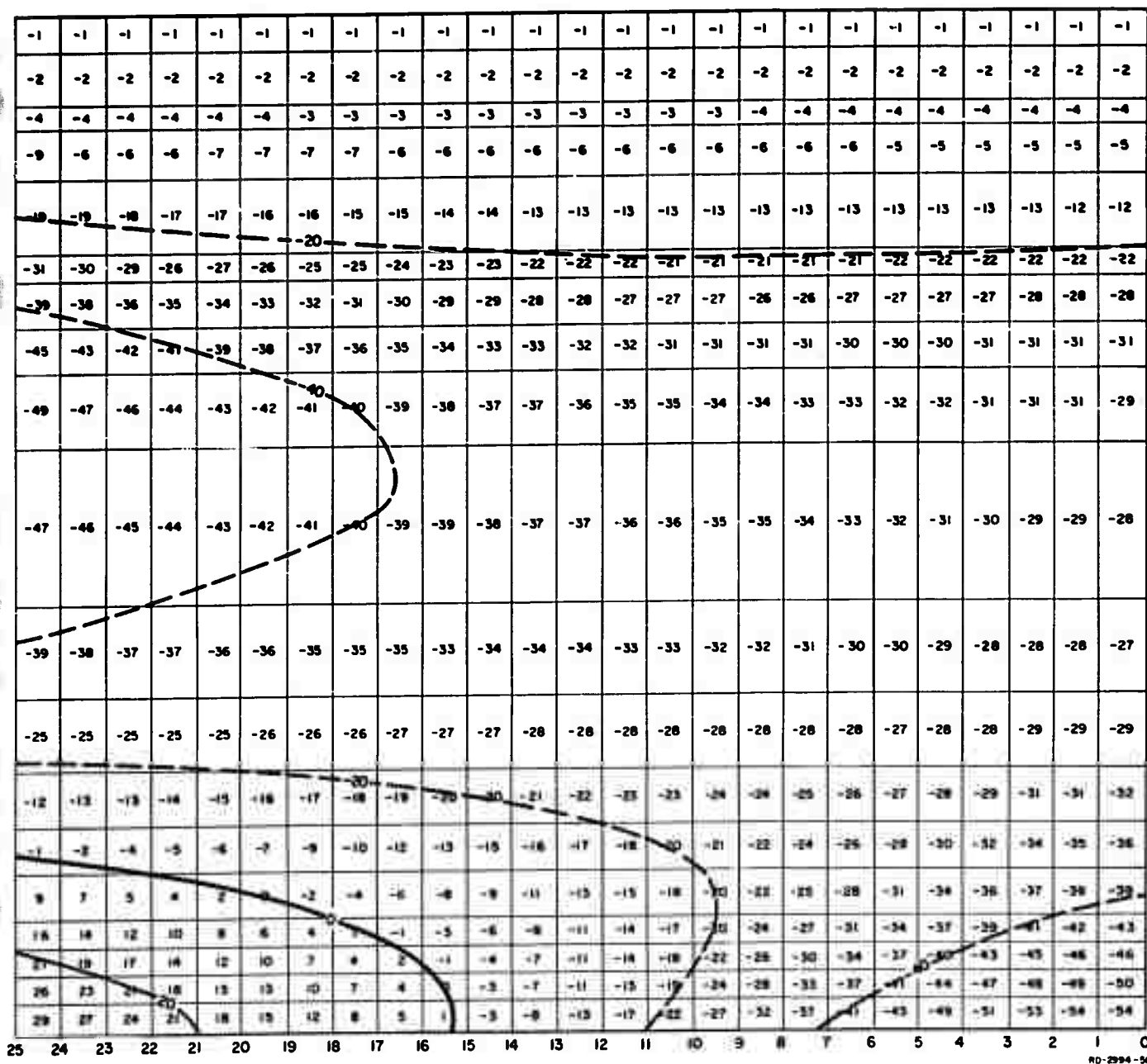
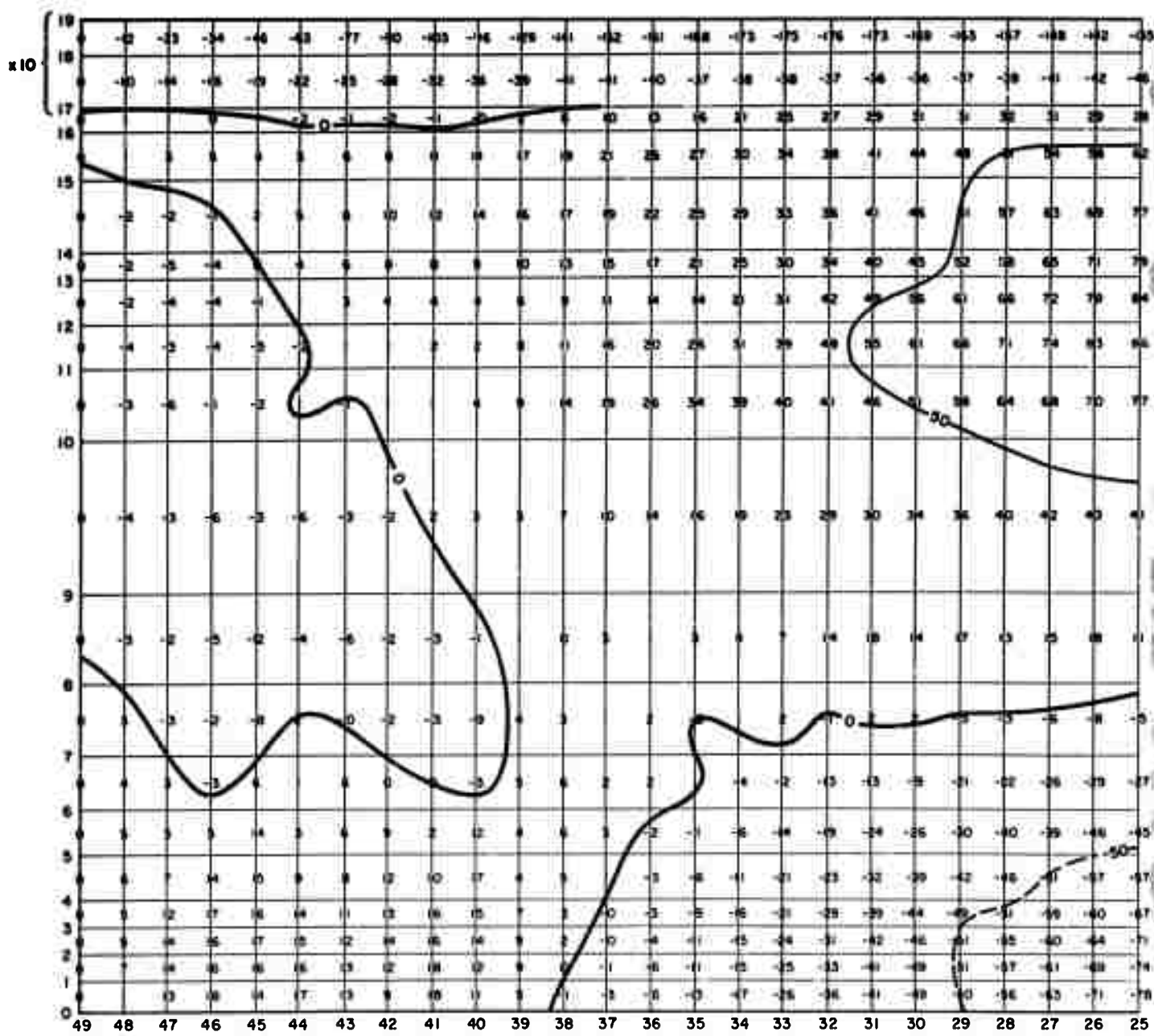


FIG. 22 WINTER HEATING,  $p_0$  at  $\tau = 182$  (~9 hours)  
Units:  $10^{-2}$  mb



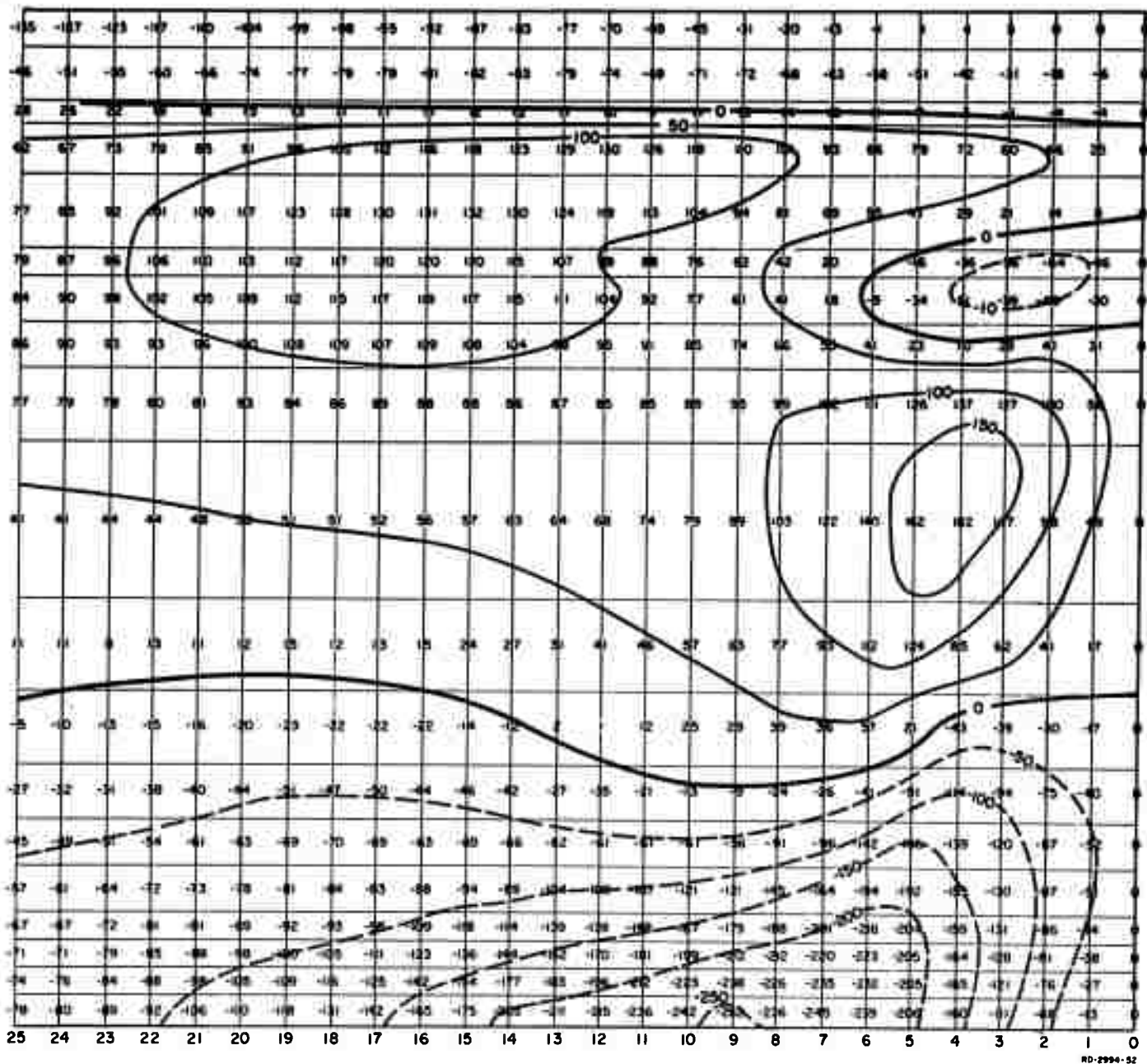
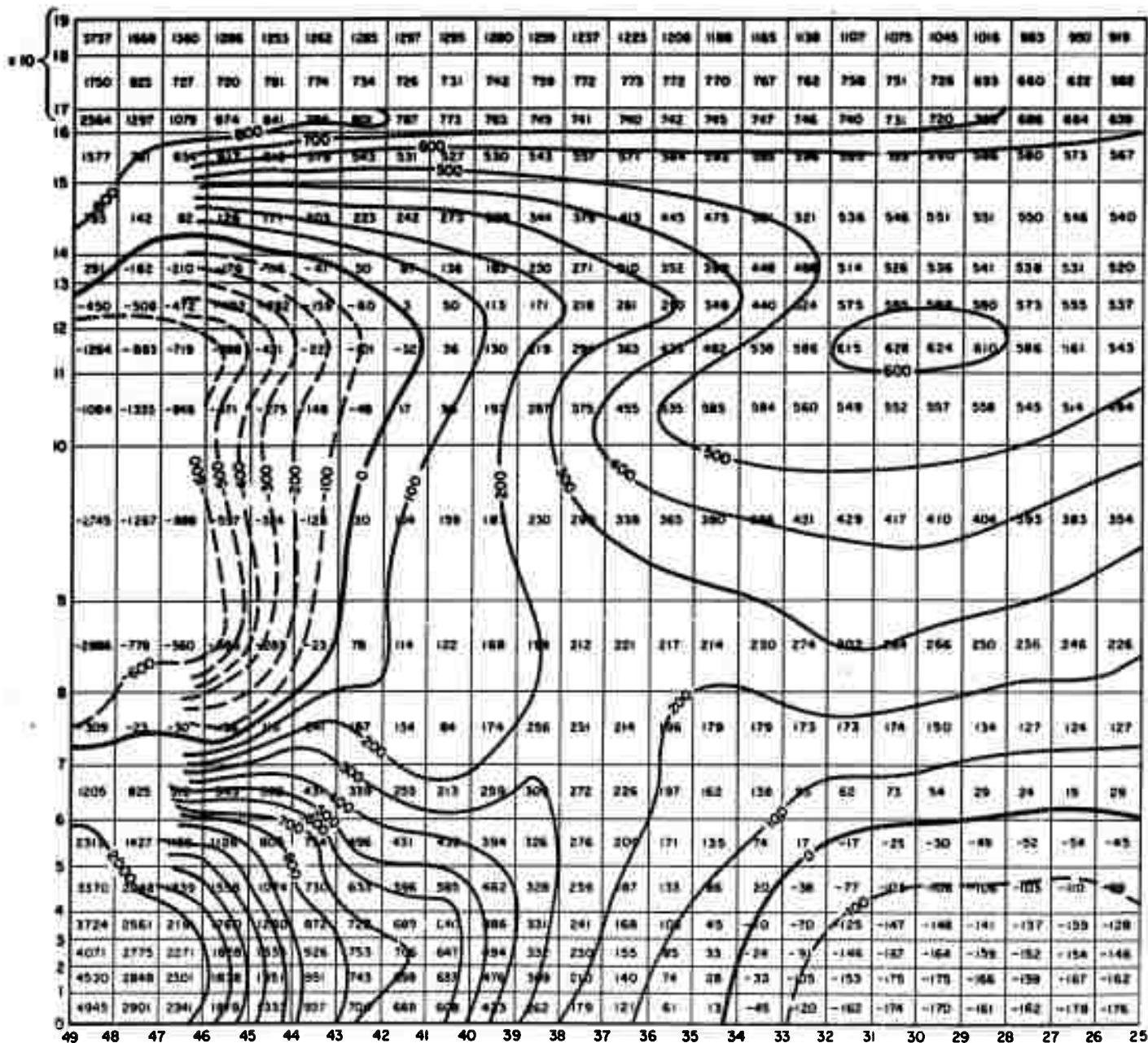


FIG. 23 WINTER HEATING,  $v$  at  $\tau = 182$  ( $\sim 9$  hours)  
Units:  $10^{-1} \text{ cm sec}^{-1}$



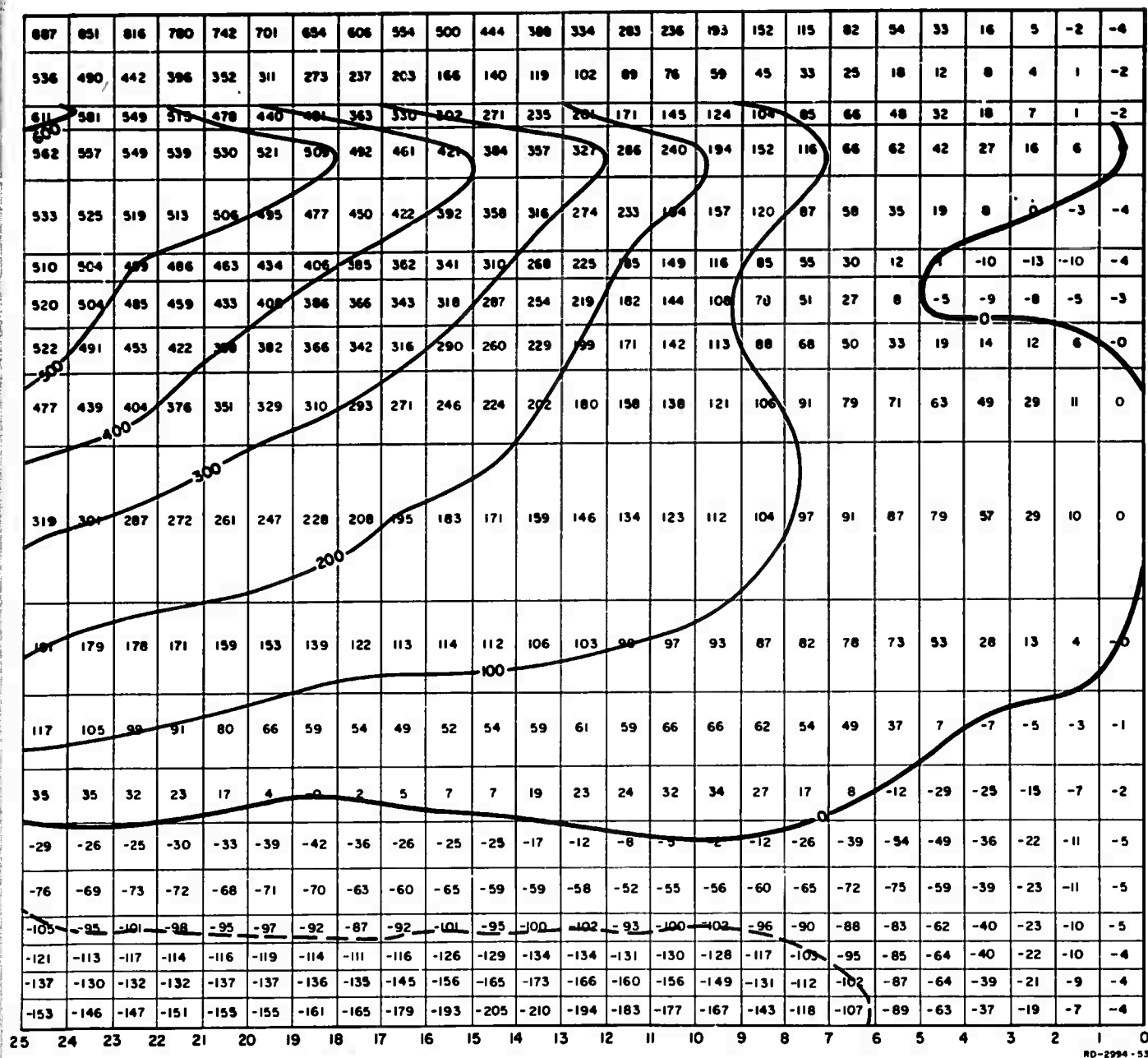
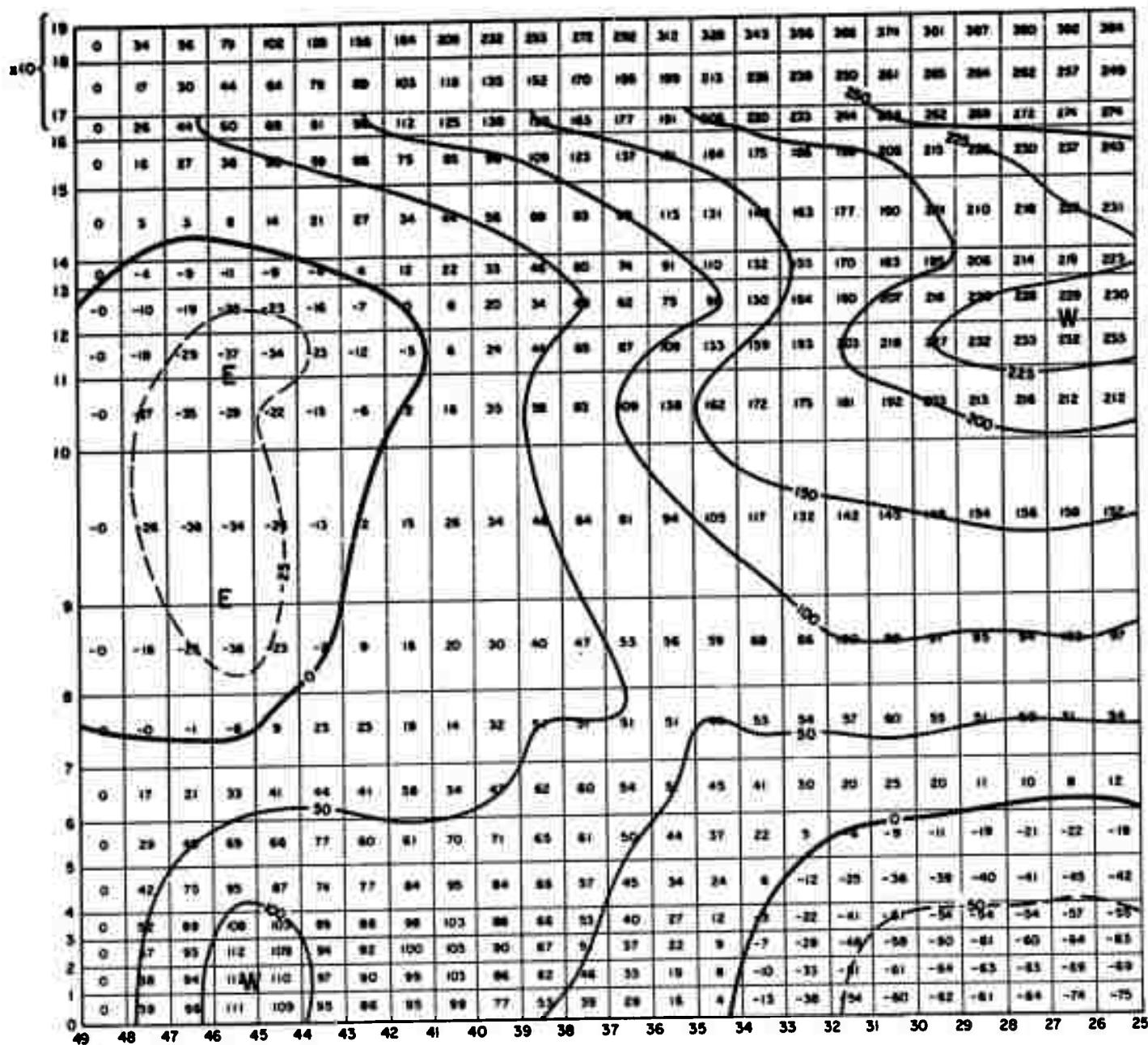


FIG. 24 WINTER HEATING,  $\omega_0$  at  $\tau = 182$  (~9 hours)  
Units:  $10^{-10}$  radians  $\text{sec}^{-1}$







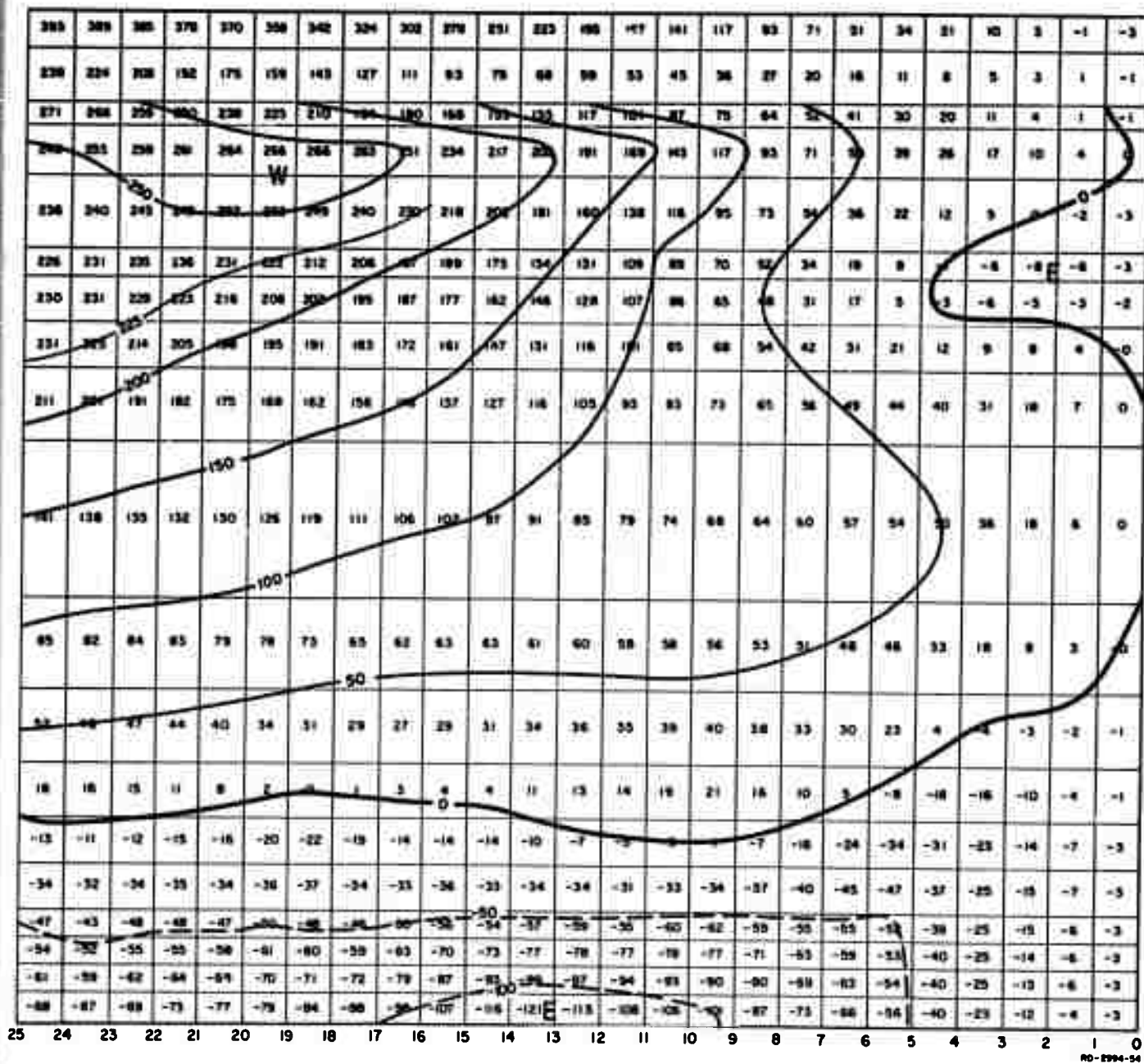
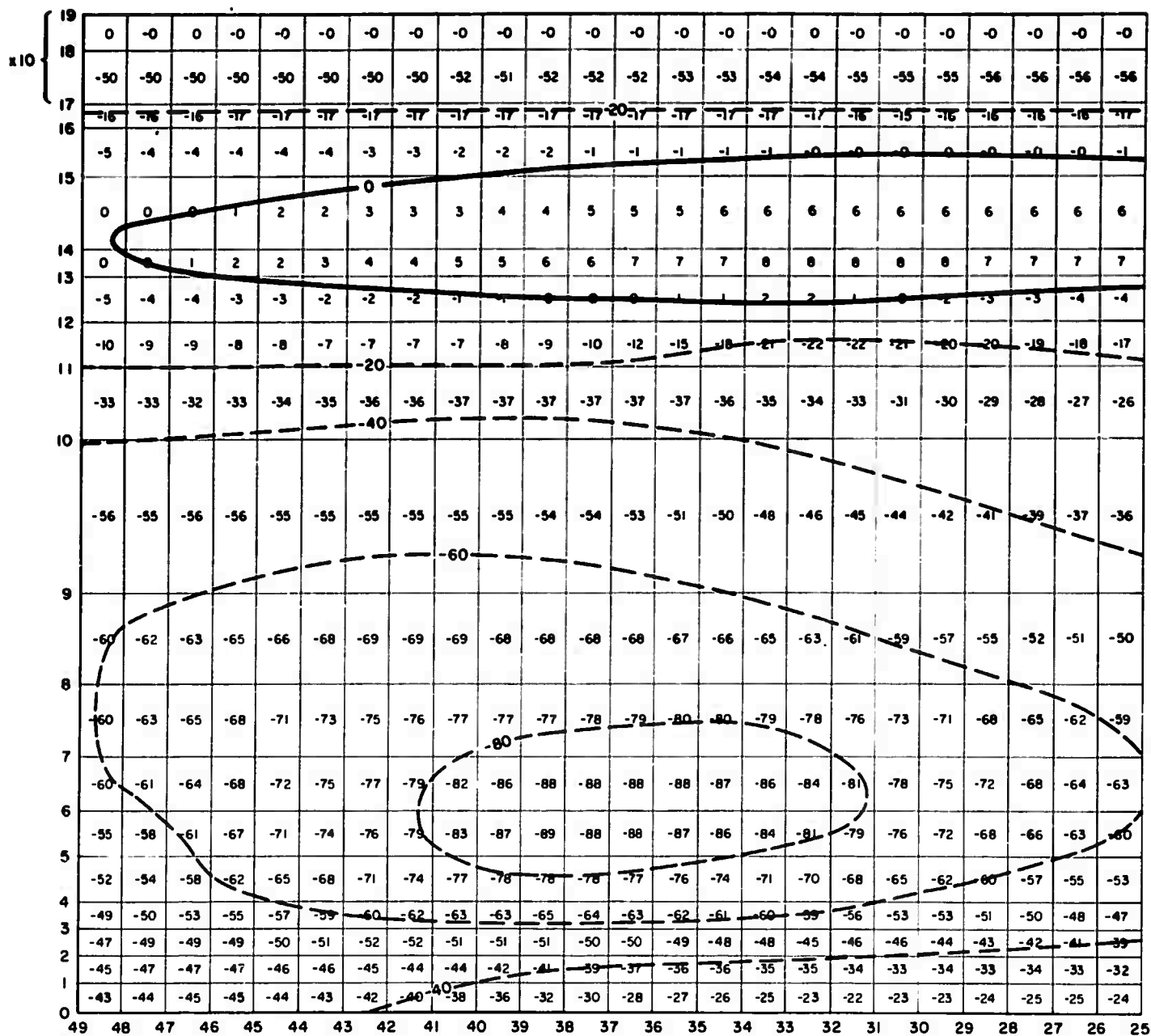


FIG. 25 WINTER HEATING,  $u$  at  $\tau = 182$  (~9 hours)  
Units:  $10^{-1} \text{ cm sec}^{-1}$



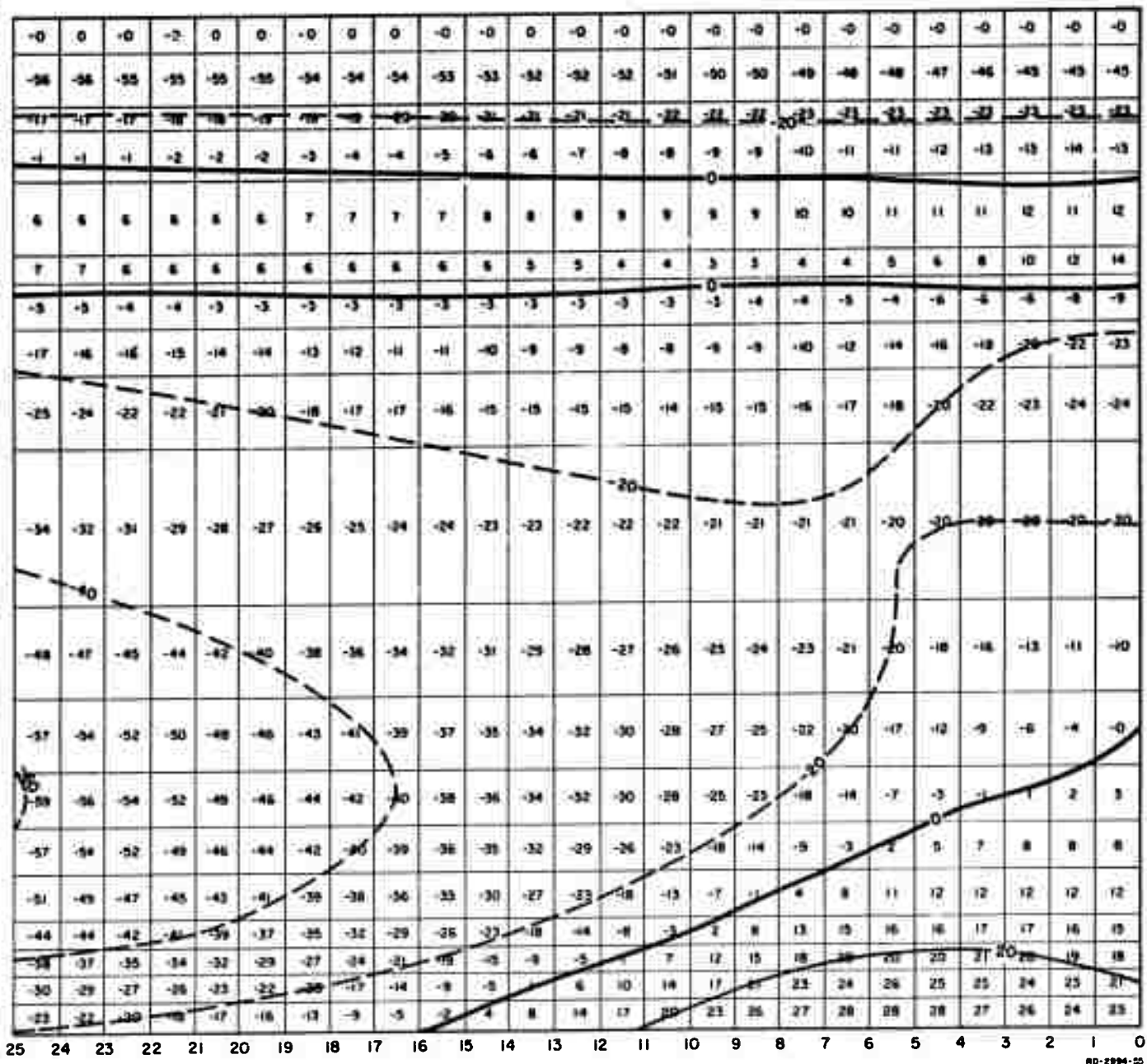
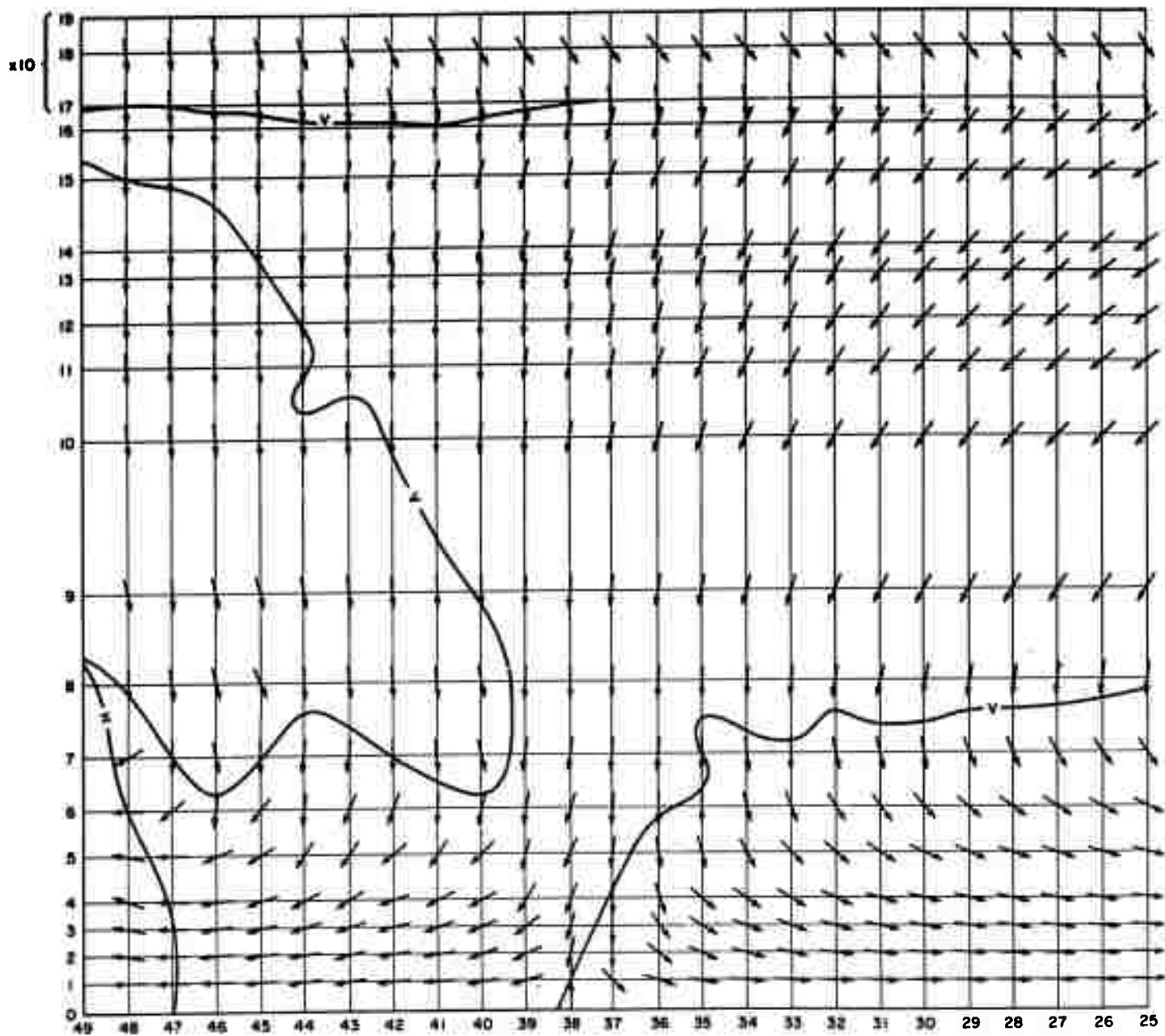


FIG. 26 WINTER HEATING,  $T_0$  at  $\tau = 182$  (~9 hours)  
Units:  $10^{-2} \text{ }^{\circ}\text{C}$



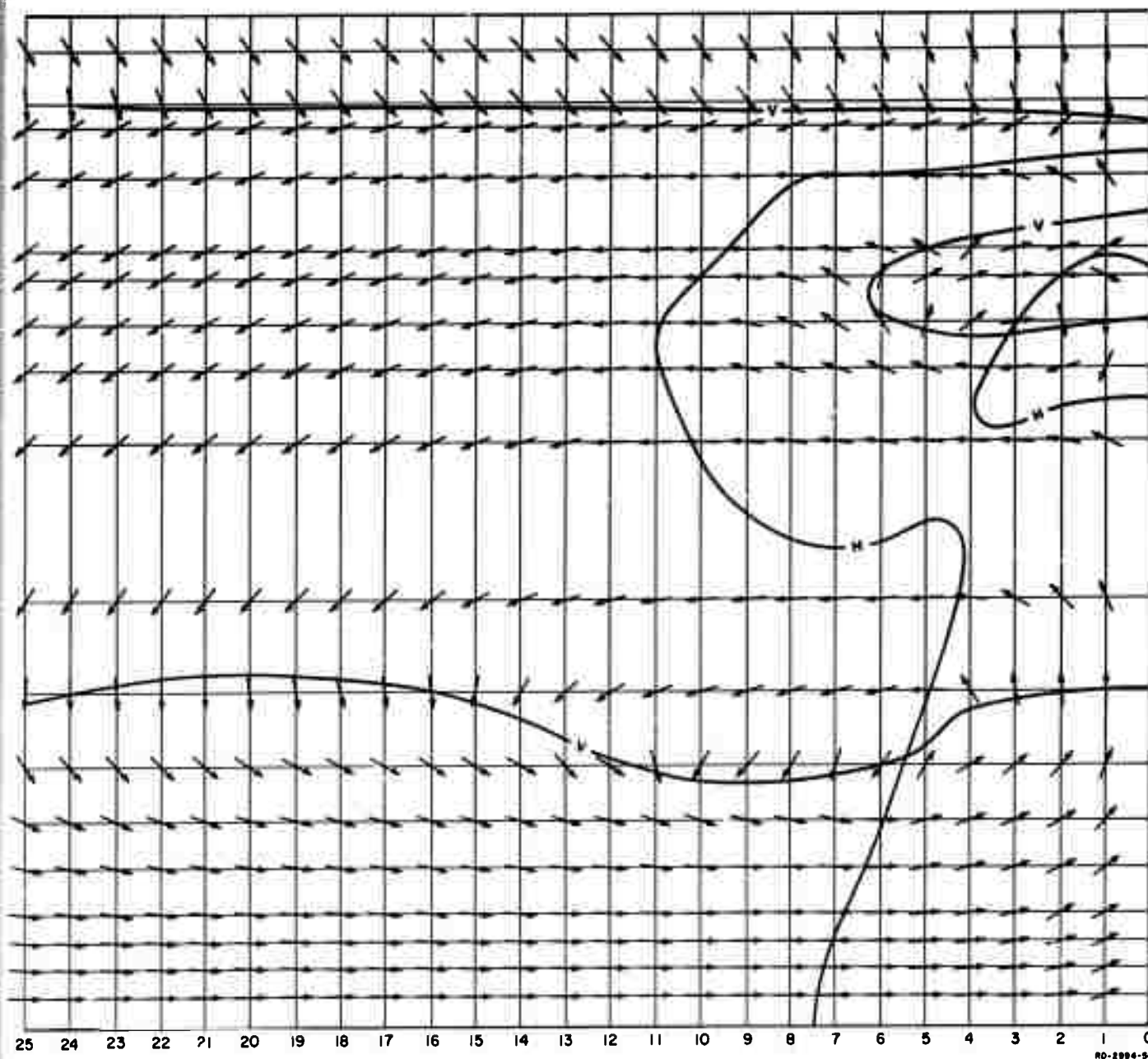


FIG. 27 WINTER HEATING, STREAMLINE SCHEMATIC AT  $\tau = 182$  (~9 hours)

intensifying. The predominant northward motion seems to reach a peak at about Hour 6; thereafter the southward flow begins to dominate. This observation suggests that a hemisphere compression-gravity oscillation with period of about 24 hours is superimposed on the meridional cellular circulation.

This major gravity oscillation occurs because of the relative abruptness of the winter heating applied to a Standard Atmosphere at relative rest. Its reversals are dictated by zero flow at the pole and across the equator. To avoid this oscillation, the heating would have to be introduced gradually over a period of a day or so.

Table I  
THE EVOLUTION OF SELECTED  $v$  COMPONENTS IN UNITS OF  $\text{CM SEC}^{-1}$   
(to five digits)

	1	2	3	4	5	9	7	6
	$\odot_{10, 2}$	$\odot_{15, 14}$	$\odot_{21, 7}$	$\odot_{28, 13}$	$\odot_{32, 1}$	$\odot_{42, 5}$	$\odot_{45, 13}$	$\odot_{47, 3}$
2								
3	$+ 0.51443 \times 10^{-1}$	$+ 0.61192 \times 10^{-3}$	$-0.98003 \times 10^{-4}$	$+ 0.83852 \times 10^{-4}$	$-0.57374 \times 10^{-1}$	$-0.30583 \times 10^{-1}$	$-0.92981 \times 10^{-3}$	$+0.15366 \times 10^{-3}$
22	$+ 0.13643 \times 10^{-1}$	$+ 0.73839$	$+0.16145$	$+ 0.53603$	$-0.59603 \times 10^{-1}$	$-0.32615 \times 10^{-1}$	$-0.44379$	$+0.16335$
23	$+ 0.15632 \times 10^{-1}$	$+ 0.79701$	$+0.17398$	$+ 0.57930$	$-0.31450$	$-0.24119$	$-0.46919$	$+0.16308$
42	$+ 0.75840 \times 10^{-1}$	$+ 3.0265$	$+0.74518$	$+ 2.1851$	$-0.31450$	$+0.28783$	$-1.1502$	$+1.0137$
43	$- 0.84219 \times 10^{-1}$	$+ 3.1286$	$+0.77176$	$+ 2.2374$	$-0.33179$	$+1.3277$	$-1.1743$	$+1.0468$
62	$- 0.61040$	$+ 6.2300$	$+1.5453$	$+ 4.4293$	$-0.73008$	$+1.3728$	$-1.4976$	$+2.2317$
63	$- 0.63892$	$+ 6.3451$	$+1.5665$	$+ 4.5186$	$-0.75152$	$+2.5766$	$-1.5041$	$+2.2628$
82	$- 1.9465$	$+ 9.4950$	$+2.0388$	$+ 8.9682$	$-1.0053$	$+2.8193$	$-1.5949$	$+3.2345$
83	$- 2.0061$	$+ 9.5942$	$+2.0484$	$+ 7.0570$	$-1.0182$	$+3.4100$	$-1.5176$	$+3.2471$
102	$- 4.3351$	$+11.983$	$+1.9434$	$+ 9.2245$	$-1.1240$	$+3.4240$	$-1.5019$	$+3.6716$
103	$- 4.4352$	$+12.047$	$+1.9301$	$+ 9.2938$	$-1.1399$	$+3.4645$	$-1.5816$	$+3.6097$
122	$- 7.8456$	$+13.326$	$+1.1496$	$+10.585$	$-1.4580$	$+3.6693$	$-1.1436$	$+3.5965$
123	$- 7.9831$	$+13.357$	$+1.1178$	$+10.607$	$-1.4903$	$+3.2414$	$-0.83038$	$+3.0645$
142	$-12.261$	$+13.600$	$-0.28910$	$+10.420$	$-2.0391$	$+3.2187$	$-0.61991$	$+3.0362$
143	$-12.426$	$+13.593$	$-0.34150$	$+10.389$	$-2.0941$	$+2.3175$	$-0.53719$	$+2.2883$
162	$-17.228$	$+13.063$	$-2.1762$	$+ 9.8337$	$-2.9729$	$+2.2877$	$-0.53653$	$+2.2215$
163	$-17.410$	$+13.031$	$-2.2306$	$+ 9.8165$	$-2.9087$	$+1.1865$	$-0.49068$	$+1.4006$
182	$-22.339$	$+12.003$	$-4.0206$	$- 6.8386$	$-3.6079$	$+1.1422$	$-0.48810$	$+1.2672$
183	$-22.516$	$+11.952$	$-4.0654$	$- 6.5636$	$-3.6219$			

## VII RECOMMENDATIONS

On appraising the model and the experimental findings, a number of modifications and improvements may be put into focus.

For the investigation of planetary circulations driven by seasonal heating, the most obvious and major improvement is to extend the model from pole to pole. This not only removes the artificial boundary influence on the hemisphere, but also allows us to investigate the important seasonal exchanges of mass, momentum, and energy between the northern and southern hemispheres.

Another major consideration is that the model be reprogrammed for a faster computer with greater storage. This would make experiments more economical on the one hand, and would allow the evolutions to be carried to great lengths on the other hand.

In planning to so extend the evolutions, additional physical processes should be included. Those to be considered are:

- (1) The surface layer should be frictionally coupled to the earth with a flow of angular momentum across the lower boundary.
- (2) There should be mixing in the vertical, attributed to convection. This may be handled by exchanges of mass, momentum, and energy between modules along the vertical. This can be done periodically and should be dependent on vertical structure and stability considerations.
- (3) A horizontally acting friction may also be necessary. A friction of the type

$$\frac{\partial}{\partial t} (\rho \mathbf{V}_H) = \dots + \left[ \mu_1 \nabla_H^2 (\rho \mathbf{V}_H) + \mu_2 \nabla_H \nabla_H \cdot (\rho \mathbf{V}_H) \right] \quad (116)$$



may be considered. This friction allows independent lower-scale control of horizontal mass divergence and momentum vorticity.\*

When allowing convectional mixing, the heating, particularly the sensible heating, should be modified accordingly.

The numerical analogue which we have developed is also, of course, not the last word. We have tried to rigorously couple the variables by physical relationship. In this we have not been completely successful, as evidenced by some double differences in the analogue. The selection of levels and the module dimensional constants may also be subjected to further statistical refinements. For lengthy evolutions, the "leap-frog" method may create some difficulties. The method may introduce extraneous behavior as shown by linear analysis. A non-linear numerical instability may also arise; however, the type discovered and analyzed by Phillips<sup>(8)</sup> in 1959 is due to interactions in two horizontal dimensions. The use of the centered single-difference analogue, Eq. (83), should also be considered.

With these modifications, it should be possible and profitable to carry the integration through a complete annual cycle. This should be possible on one of the larger available computers, in the order of a few seconds per time step. The evolution can again be started with a Standard Atmosphere at rest, or with balanced zonal motion. The heating should be introduced in steps over a period of several days, in order to avoid exciting a 48-hour pole-to-pole compression-gravity oscillation.

Such an experiment would yield an abundance of information on the primary scale (the planetary scale) in our atmosphere. It would indicate the circulation undisturbed by longitudinal variations and dynamic-instability breakdowns, and would allow a separate appreciation of these effects. It would yield more understanding of the cascade of energy downscale from the primary and dictating planetary scale.

---

\* This form of friction with experimental findings will be discussed in a forthcoming report by the author.

The model may also be used to investigate a number of geophysical influences and may be applied to arbitrary planetary atmospheres.

#### ACKNOWLEDGMENT

The capable assistance of Harmon Wildermuth in all data and diagram preparations is gratefully acknowledged. Leonard McCulley performed the difficult task of integrating the numerical analogue on SRI's Burroughs 220 Electronic Computer.

## REFERENCES

1. K. L. Coulson, "Atmospheric Radiative Heating and Cooling," Scientific Report 1, Contract AF 19(604)-5965, AFCRL TN-60-273, Stanford Research Institute, Menlo Park, California (1960).
2. K. L. Coulson and P. M. Furukawa, "Distributions of Atmospheric Radiative Heating and Cooling," Scientific Report 2, Contract AF 19(604)-5965, AFCRL-TN-60-835, Stanford Research Institute, Menlo Park, California (1960).
3. M. M. Holl, "On Meteorological Objective Analysis and Model Theory," Final Report, Contract AF 19(604)-5703, GRD-TR-60-293, Stanford Research Institute, Menlo Park, California (1960).
4. M. M. Holl (1960), op. cit., p. 27.
5. M. M. Holl (1960), op. cit., p. 28.
6. M. M. Holl, "A Numerical Investigation of the Barotropic Development of Eddies," Geophysics Research Papers, No. 61, USAF (1958).
7. M. M. Holl (1958), op. cit., Sec. 5.
8. N. A. Phillips, "An Example of Non-Linear Instability," The Atmosphere and The Sea in Motion, The Rossby Memorial Volume, (The Rockefeller Institute Press, New York City, 1959.)

**STANFORD  
RESEARCH  
INSTITUTE**

**MENLO PARK, CALIFORNIA**

## **Regional Offices and Laboratories**

**SOUTHERN CALIFORNIA LABORATORIES**  
820 Mission Street  
South Pasadena, California

**WASHINGTON OFFICE**  
808 17th Street, N.W.  
Washington 5, D.C.

**NEW YORK OFFICE**  
270 Park Avenue, Room 1770  
New York 17, New York

**DETROIT OFFICE**  
The Stevens Building  
1025 East Maple Road  
Birmingham, Michigan

**EUROPEAN OFFICE**  
Pelikanstrasse 37  
Zurich 1, Switzerland

## **Representatives**

**HONOLULU, HAWAII**  
Finance Factors Building  
195 South King Street  
Honolulu, Hawaii

**LONDON, ONTARIO, CANADA**  
85 Wychwood Park  
London, Ontario, Canada

**LONDON, ENGLAND**  
15 Abbotsbury Close  
London W. 14, England

**MILAN, ITALY**  
Via Macedonio Melloni 40  
Milano, Italy

**UNCLASSIFIED**

**UNCLASSIFIED**

- Line 1 - change the number 1 to 2 in Eq. (4) - change  $\frac{1}{2}$  to  $\frac{1}{4}$
- p. 9 Eq. (8) - change sign of  $\frac{1}{2}$  to minus
- p. 12 Eq. (12) - change sign of  $V_0(\text{or } V)$  to minus
- p. 25 Line 2 - Eq. (64) instead of Eq. (65)
- p. 29 Line 4 - (65) should be (64)
- p. 39 Line 7 - change  $\square_n$  to  $\square_n$
- p. 40 Line 20 - change P to p
- p. 41 Line 1 - change P to p
- p. 42 Line 4 - meriodical to meridional